

Dissertation zur Erlangung des Doktorgrades
der Fakultät für Chemie und Pharmazie
der Ludwig-Maximilians-Universität München

**Characterization of $\beta 1$ Integrin Cytoplasmic
Domain Binding Proteins**

Hao-Ven Wang

aus

Hsin-Chu, Taiwan

2008

Erklärung

Diese Dissertation wurde im Sinne von § 13 Abs. 3 bzw. 4 der Promotionsordnung vom 29. Januar 1998 von Herrn Prof. Dr. Reinhard Fässler betreut.

Ehrenwörtliche Versicherung

Diese Dissertation wurde selbständig, ohne unerlaubte Hilfe erarbeitet.

München, am 07.04.2008

(Hao-Ven Wang)

Dissertation eingereicht am 10.04.2008

1. Gutachter: Prof. Dr. Reinhard Fässler
2. Gutachter: PD. Dr. Stefan Weiss

Mündliche Prüfung am 11.06.2008

1 Table of Contents

1	Table of Contents	I
2	List of Publications	II
3	Abbreviations	III
4	Summary	1
5	Introduction	4
	5.1 Integrins	4
	5.1.1 Integrin activation	7
	5.1.1.1 The structure and regulation of integrin activity	7
	5.1.1.2 Integrin activation by Talin	10
	5.1.2 Integrin cytoplasmic binding proteins	13
	5.2 Integrin-linked kinase	15
	5.2.1 ILK and its binding partners	15
	5.2.2 Biochemical and genetic studies of ILK	17
	5.2.3 Analysis of the role of ILK in mammalian skeletal muscle	18
	5.2.3.1 Development and architecture of skeletal muscle	19
	5.2.3.2 Role of integrins in skeletal muscle development and function.....	22
	5.2.3.3 The role of ILK in skeletal muscle.....	23
	5.3 The Kindlin protein family	24
	5.3.1 Kindlin protein structure.....	24
	5.3.2 Kindlin gene expression	25
	5.3.3 <i>In vivo</i> function of Kindlins.....	26
	5.4 Palladin	27
	5.4.1 Palladin and its binding partners	27
	5.4.2 Biochemical and genetic studies of palladin	31
	5.4.3 The role of palladin in human disease	32
6	Aim of the thesis	34
7	Brief summaries of the publications	36
	7.1 Paper I: Integrin-linked kinase stabilizes myotendinous junctions and protect muscle from stress-induced damage	36
	7.2 Paper II: The Kindlins: subcellular localization and expression during murine development	37
	7.3 Paper III: Identification and embryonic expression of a new AP-2 transcription factor, AP-2 epsilon	37
	7.4 Manuscript I: Comparative expression analysis of the murine palladin isoforms	38
	7.5 Manuscript II: Characterization of striated muscle specific palladin 200kDa isoform and double myotilin/200kDa palladin deficient mice (manuscript in preparation)	39
8	Acknowledgements	41
9	Curriculum Vitae	42
10	References	44
11	Supplements	60

2 List of Publications

This thesis is based on the following publications, which are referred to the text by their Roman numerals (I-V):

- I. **Wang, H. V.**, L. W. Chang, K. Brixius, S. A. Wickström, E. Montanez, I. Thievensen, M. Schwander, U. Müller, W. Bloch, U. Mayer, and R. Fässler. (2008). Integrin-linked kinase stabilizes myotendinous junctions and protects muscle from stress-induced damage. *J Cell Biol.* 180: 1037-1049.
- II. Ussar, S., **H. V. Wang**, S. Linder, R. Fässler, and M. Moser. (2006). The Kindlins: Subcellular localization and expression during murine development. *Exp. Cell Res.* 312: 3142-3151.
- III. **Wang, H. V.**, K. Vaupel, R. Buettner, A. K. Bosserhoff, and M. Moser. (2004). Identification and embryonic expression of a new AP-2 transcription factor, AP-2ε. *Developmental Dynamics.* 231: 129-135.
- IV. **Wang, H. V.**, and M. Moser. (2008) Comparative expression analysis of the murine palladin isoforms. Manuscript in submission.
- V. Moza, M*., **H. V. Wang***, W. Bloch, R. Fässler, M. Moser, and O. Carpén. (2008) Characterization of striated muscle specific palladin 200kDa isoform and double myotilin/200kDa palladin deficient mice. Manuscript in preparation. (*:have contributed equally to this work)

Reprints were made with permission from the publishers.

3 Abbreviations

aa	amino acid
A	Alanine
ANK	ankyrin
ATP	adenosine-triphosphate
BM	basement membrane
bp	base pair
cDNA	complementary DNA
<i>C.elegans</i>	<i>Caenorhabditis elegans</i>
CH	calponin homology
CMV	Cytomegalovirus
D	aspartic acid / dermis
DNA	deoxyribonucleic acid
Dock180	180kDa protein downstream of Crk
E	embryonic day /Glutamic acid
ECM	extracellular matrix
EGF	epidermal growth factor
EGFP	enhanced green fluorescent protein
ELISA	Enzyme-linked Immunosorbent Assay
EMT	epithelial-to-mesenchymal transition
ES cells	embryonic stem cells
F-actin	filamentous actin
FA	focal adhesion
FAK	focal adhesion kinase
FC	focal complex
FERM	four-point-one, ezrin, radixin, moesin
FGFR	fibroblast growth factor receptor
FN	fibronectin
G-actin	globular actin
GSK-3	glycogen synthase kinase 3
GTP	guanosine triphosphate
h	hour

Abbreviations

H&E	Hematoxylin and Eosin
HeLa cells	cell line derived from cervical cancer taken from Henrietta Lacks
HRP	horseradish peroxidase
ILK	Integrin-linked kinase
ILKAP	ILK-associated phosphatase
ICAP	Integrin-cytoplasmic domain associated protein
IP	immunoprecipitation
JAB	jun-activating binding protein
K	lysine
kDa	kilo Dalton
LIM domain	Lin-11, Isl-1, Mec-3 domain
μl	micro litre
M/mM	molar/millimolar
MBP	myelin basic protein
mDia	mammalian diaphanous
MEF	murine embryonic fibroblast
Mg/MgCl ₂	Magnesium/Magnesiumchloride
Mn	Manganese
mg	milligram
Mig-2	mitogen-inducible gene 2
min	minutes
MLC	myosin light chain
N	number
NMR	nuclear magnetic resonance
o/n	overnight
nm	nanometer
PAT	paralyzed and arrested at twofold
PBS	phosphate buffered saline / paxillin binding site
PCR	polymerase chain reaction
PI3K	phosphoinositide 3- kinase
PH	pleckstrin homology
Pinch	particularly interesting new cysteine-histidine rich protein
PIP2	phosphatidylinositol (4,5) bisphosphate
PIP3	phosphatidylinositol (3,4,5) trisphosphate

Abbreviations

PIPKI γ	phosphatidylinositol-4-phosphate 5-kinase type I gamma
PIX	PAK-interacting exchange factor
PTP	protein tyrosine phosphatase
R	Arginine
Rac	Ras-related C3 botulinum substrate
RACK	receptor for activated C-kinase
RGD	Arginine-Glycine-Aspartic acid
RNA	ribonucleic acid
RT	reverse transcription/room temperature
siRNA	small interfering RNA
Ser	Serine
SH domain	src-homology domain
Thr	Threonine
Tyr	Tyrosine
U	Unit
VCAM	vascular cell adhesion molecule
VEGF	vascular endothelial growth factor
VN	vitronectin
wt	wild type

4 Summary

The extracellular matrix (ECM) provides the structural frame for the development of tissues and organs. The ECM is bound by numerous membranous matrix-adhesion molecules and thereby triggers intracellular signals that control various cellular functions such as survival, polarity, proliferation and differentiation. Integrins represent an important family of ECM adhesion molecules which link the ECM with the intracellular actin-cytoskeleton. Integrin mediated adhesion structures also serve as important signaling platforms, although the integrin itself does not harbor any catalytic domains. Therefore integrin signaling depends on the recruitment of a number of cytoplasmic proteins that directly or indirectly bind to the short cytoplasmic integrin tails. During my PhD thesis I worked on three of these molecules, ILK, Kindlins and Palladin, and used the mouse as a model system to address their *in vivo* function.

First, I investigated the role of integrin-linked kinase (ILK) in skeletal muscle. Loss of ILK expression in mice leads to peri-implantation lethality due to a cell polarization defect of the early embryo and abnormal actin accumulations. Studies in *Caenorhabditis elegans* and *Drosophila melanogaster* revealed an essential function for ILK in the attachment of actin filaments to the membrane of muscle cells and lack of ILK expression results in early lethality during embryogenesis. We generated mice with a skeletal muscle-restricted deletion of ILK that developed a mild, but progressive muscular dystrophy. This phenotype is predominantly restricted to myotendinous junctions (MTJs). Ultrastructural analyses showed muscle cell detachment from the basement membranes, and an accumulation of extracellular matrix. Endurance exercise training enhances the defect leading to disturbed subsarcolemmal myofiber architecture and an abrogation of the phosphorylation of Ser473 as well as Thr308 of protein kinase B (PKB)/Akt. The reduction in PKB/Akt activation is accompanied by an impaired insulin-like growth factor 1 receptor (IGF-1R) activation.

Summary

Second, I studied the expression and *in vivo* function of a further integrin- and actin- associated protein, palladin. Palladin belongs to the palladin/myotilin/myopalladin protein family. Palladin represents a phosphoprotein which plays an important role in cell adhesion and motility. Initially, I characterized the gene structure and the expression pattern of palladin. The palladin gene spans about 400 kb, with 25 exons and 3 alternative promoters resulting in at least three different isoforms (200 kDa, 140 kDa and 90-92 kDa) in mice. Using RT-PCR and *in situ* hybridizations of embryonic and adult tissues, I could show that the 200kDa isoform is predominantly expressed in heart and skeletal muscle. In contrast, the 140kDa isoform is expressed in various tissues and represents the major palladin isoform of the brain. The 90-92 kDa isoform is almost ubiquitously expressed with highest levels in tissues rich in smooth muscle, like bladder, uterus, small intestine and colon. The expression of the 200kDa isoform was characterized in more detail with a polyclonal antibody showing that this isoform localizes to the Z-discs of heart and skeletal muscle cells. *In vitro* differentiation experiments with a mouse myoblast cell line revealed an induction of the 200kDa isoform during myoblast fusion and differentiation suggesting that the biggest palladin isoform may serve as a molecular scaffold during myogenesis.

Third, I specifically inactivated the largest palladin isoform in mice. Lack of the 200 kDa palladin isoform has no impact on the development, viability and fertility of mice. However ultrastructural analyses by transmission electron microscopy (TEM) showed a mild cardiac myopathy due to disintegration of myofibrils.

In collaboration with the group of Olli Carpén, we generated palladin 200 kDa isoform/ myotilin double knockout mice. Myotilin is also expressed in heart and skeletal muscle. Ablation of both myotilin and palladin 200 kDa isoform in mouse revealed in addition to the mild cardiac myopathy a structural and functional impairment of skeletal muscle.

Finally, I was also involved in the characterization of the expression and subcellular localization of a novel family of integrin associated proteins: the Kindlins.

Summary

The Kindlin family consists of three members, Kindlin-1, -2 and -3. Mutations in Kindlin-1 cause a human disease, called Kindler Syndrome, which represents a skin blistering disease affecting the actin cytoskeleton of basal keratinocytes. Kindlin gene expression was first analyzed at the mRNA level by RT-PCR and Northern Blot studies. *In situ* hybridizations showed that Kindlin-1 is preferentially expressed in epithelia. Kindlin-2 is expressed in all tissues with highest levels in striated and smooth muscle cells. While both localize to integrin-mediated adhesion sites in cultured keratinocytes Kindlin-2, but not Kindlin-1, colocalizes with E-cadherin to cell-cell contacts in differentiated keratinocytes. In contrast, Kindlin-3 expression is restricted to hematopoietic cells. Using a Kindlin-3-specific antiserum and an EGFP-tagged Kindlin-3 construct, we could show that Kindlin-3 is present in podosomes, which are specialized adhesion structures of hematopoietic cells.

5 Introduction

5.1 Integrins

Integrins represent a major class of cell adhesion molecules, which are expressed in all types of cells and mediate adhesion to extracellular matrix (ECM) proteins and other cell surface proteins. Integrins are α/β heterodimeric type I transmembrane molecules, which associate with intracellular proteins upon extracellular ligand binding. The integrin mediated matrix-adhesion complex, which can be easily detected *in vitro*, is named focal adhesion (FA) (Figure 1.1A). Members of the integrin family have been identified in most metazoa from sponges, *Drosophila melanogaster*, *Caenorhabditis elegans* to vertebrates (Figure 1.1B). In mammalian, 18 different α and 8 different β subunits exist, which assemble into 24 different heterodimeric receptors (Hynes and Zhao, 2000; Brakebusch et al., 2002; Hynes, 2002).

Based on the recognition specificity, integrins interact with three different subsets of ECM components (Figure 1.1B). The first group recognizes fibronectin (FN) or vitronectin (VN); both proteins contain the amino acid sequence arginine-glycine-aspartic acid (or, in abbreviated amino acid nomenclature, RGD). Two related integrins ($\alpha4\beta1$, $\alpha9\beta1$) can bind FN and also interact with immunoglobulin (Ig)-superfamily counter receptors such as VCAM-1 (vascular cell adhesion molecule). The second group interacts with laminin and the third group binds to collagen. The $\beta2$ integrin family represents a separate group, which is restricted to leukocytes and recognizes Ig-superfamily containing cell surface proteins thereby mediating heterotypic cell-cell adhesion.

In principle, integrins fulfil two major tasks. They link the extracellular matrix via a number of adaptor proteins with the intracellular cytoskeleton and are therefore crucial for cell adhesion, cell spreading and migration of cells. In addition, integrin associated complexes are signalling relays which influence other signalling pathways directly or

Introduction

indirectly and thereby control a number of cellular processes like cell adhesion, cell polarity, cell motility, cell growth and survival (Brakebusch et al., 2002; Danen and Sonnenberg, 2003; Wiesner et al., 2005).

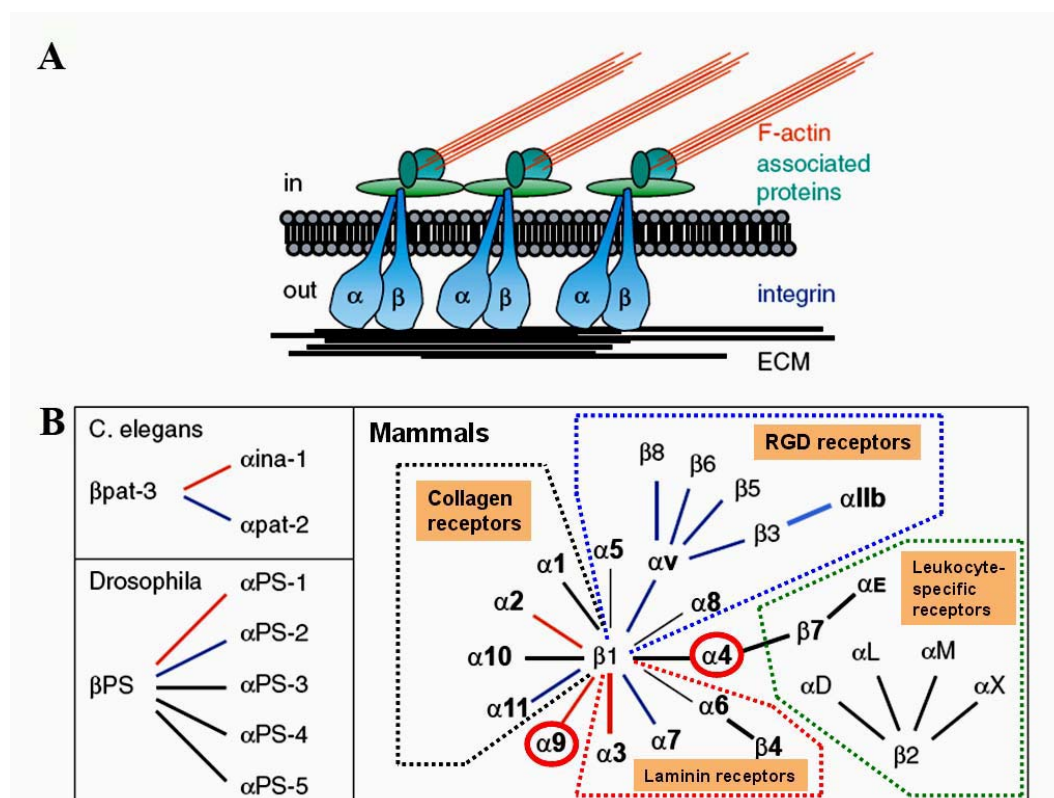


Figure 1.1 (A) Schematic representation of an integrin mediated cell-matrix adhesion site connecting the ECM with the actin cytoskeleton. (B) The integrin receptor family in *C.elegans*, *Drosophila* and mammals (Taken from Hynes, 2002; Danen and Sonnenberg, 2003 and modified)

With the advent of genetically modified mice the *in vivo* function of the individual α or β subunits could be addressed resulting in the observation of a diversity of phenotypes (Table 1.1). These phenotypes range from peri-implantation lethality (β 1), major developmental defects (α 4, α 5, α v and β 8), perinatal lethality (α 3, α 6, α 8, α v, β 4 and β 8), and defects in haematopoietic cell function (α 2, α IIb, α L, α M, α E, β 2, β 3 and

Introduction

$\alpha 1$	V, F	No immediately obvious developmental defects, reduced tumor vascularization	Gardner et al., 1996; Pozzi et al., 2000, 2002
$\alpha 2$	V, F	Few immediately obvious developmental defects, delayed platelet aggregation and reduced binding to monomeric collagen, reduced mammary gland branching	Holtkotter et al., 2002; Chen et al., 2002
$\alpha 3$	P	Kidney tubule defects, reduced branching morphogenesis in lungs, mild skin blistering, lamination defects in neocortex	Kriedberg et al., 1996; DiPersio et al., 1997; Anton et al., 1999
$\alpha 4$	E11/14	Defects in placenta (chorioallantoic fusion defect) and heart (epicardium, coronary vessels). Chimeras show defects in hematopoiesis.	Yang et al., 1995; Arroyo et al., 1996, 1999
$\alpha 5$	E10-11	Defects in mesoderm (posterior somites) and vascular development, neural crest apoptosis. Chimeras show muscular dystrophy	Yang et al., 1993; Goh et al., 1997; Taverna et al., 1998
$\alpha 6$	P	Severe skin blistering, other epithelial tissues also defective. Lamination defects in cortex and retina.	Georges-Labouesse et al., 1996, 1998
$\alpha 7$	V, F	Muscular dystrophy, defective myotendinous junctions	Mayer et al., 1997
$\alpha 8$	P	Small or absent kidneys, inner ear hair cell defects	Muller et al., 1997; Littlewood Evans et al., 2000
$\alpha 9$	V	Die within 10 days of birth, chylothorax due to lymphatic duct defect	Huang et al., 2000
αv	E10/P	Two classes: embryonic lethality due to placental defects, perinatal lethality with cerebral vascular defects probably due to neuroepithelial defects, cleft palate. Most blood vessels develop normally	Bader et al., 1998; McCarty et al., 2002
$\alpha 1b$	V, F	Hemorrhage, no platelet aggregation	Tronik-Le Roux et al., 2000
αL	V, F	Impaired leukocyte recruitment	Schmits et al., 1996
αM	V, F	Defective phagocytosis and apoptosis of neutrophils, mast cell development defects, adipose accumulation.	Coxon et al., 1996; Tang et al., 1997; Dong et al., 1997
αE	V, F	Greatly reduced numbers of intraepithelial lymphocytes.	Schon et al., 1999
$\beta 1$	E6.5	Peri-implantation lethality, ICM deteriorates, embryos fail to gastrulate. Extensive analyses of chimeras.	Fässler and Meyer, 1995; Stephens et al., 1995; Brakebusch et al., 1997
$\beta 2$	V, F	Leukocytosis, impaired inflammatory responses, skin infections, T cell proliferation defects	Scharffetter-Kochanek et al., 1998
$\beta 3$	V, F	Hemorrhage, no platelet aggregation, osteosclerosis, hypervascularisation of tumors	Hodivala-Dilke et al., 1999; McHugh et al., 2000; Reynolds et al., 2002
$\beta 4$	P	Severe skin blistering, other epithelial tissues also defective	van der Neut et al., 1996; Dowling et al., 1996
$\beta 5$	V, F	No immediately obvious developmental defects	Huang et al., 2000
$\beta 6$	V, F	Inflammation in skin and airways, impaired lung fibrosis—all probably due to failure to activate TGF β	Huang et al., 1996; Munger et al., 1999
$\beta 7$	V	Deficits in gut-associated lymphocytes—no Peyer's patches, reduced intraepithelial lymphocytes (IEL).	Wagner et al., 1996
$\beta 8$	E10/P	Two classes: embryonic lethality due to placental defects, perinatal lethality with cerebral vascular defects probably due to neuroepithelial defects. Most blood vessels develop normally.	Zhu et al., 2002

Abbreviations: E, embryonic lethal (day of lethality); P, perinatal lethal; V, viable; F, fertile.

Table 1.1 Integrin gene knockout phenotypes. (Taken from Hynes, 2002 and modified)

$\beta 7$), inflammation ($\beta 6$), angiogenesis ($\alpha 1$ and $\beta 3$) and muscular dystrophy ($\alpha 7$) (Hynes, 2002). In parallel, abnormal integrin function has also been described in human diseases

such as epidermolysis bullosa ($\alpha 6\beta 4$) and Glanzmann thrombosthenia ($\alpha IIb\beta 3$). Therefore, further extensive investigations of integrins are absolutely essential for a deeper understanding of the molecular processes controlling integrin functions. This will potentially open new therapeutic strategies.

5.1.1 Integrin activation

5.1.1.1 The structure and regulation of integrin activity

Integrins display allosteric regulation through binding of both extracellular and intracellular ligands which trigger the transition from a low-affinity state (the “inactive” state) towards a high-affinity state (the “active” state) (Liddington and Ginsberg, 2002; Calderwood, 2004).

The crystal structure of integrin $\alpha v\beta 3$, a receptor implicated in cardiovascular and bone function, provided unprecedented insights into the mechanism of integrin activation and ligand binding (Xiong et al., 2001). The length of integrins is approximately $\sim 280\text{\AA}$. Integrins consist of an α ($\sim 150\text{-}180\text{kDa}$) and a β ($\sim 100\text{kDa}$) subunit. Both subunits consist of a large extracellular domain, a transmembrane domain and a small cytoplasmic tail of around 20 to 50 amino acids (aa.). One exception is the $\beta 4$ integrin cytoplasmic tail consisting of more than 1000aa.

The $\alpha v\beta 3$ integrin is composed of an ovoid head region which is formed by the β propeller from the αv subunit and the βA domain from the $\beta 3$ subunit. The two parallel leg regions are formed by the two calf domains and the thigh domain of the α subunit and the three EGF-like repeats and the hybrid domain of the β subunit (Figure 1.2). The metal ion-dependent adhesion site (MIDAS), which binds activating divalent cations (e.g. Mn^{2+} or Mg^{2+}), is located in the βA domain adjacent to an inhibitory calcium binding site (ADMIDAS termed from ‘adjacent to MIDAS’) (Humphries et al., 2003). Since the first description of the integrin crystal structure in 2001 (Xiong et al., 2001), researchers tried to use electron microscopy (EM) and X-ray crystallization to investigate the shape

Introduction

and the atomic structure of integrins. It is still debated whether the bent integrin form represents the active or the inactive conformation (Figure 1.2A and B).

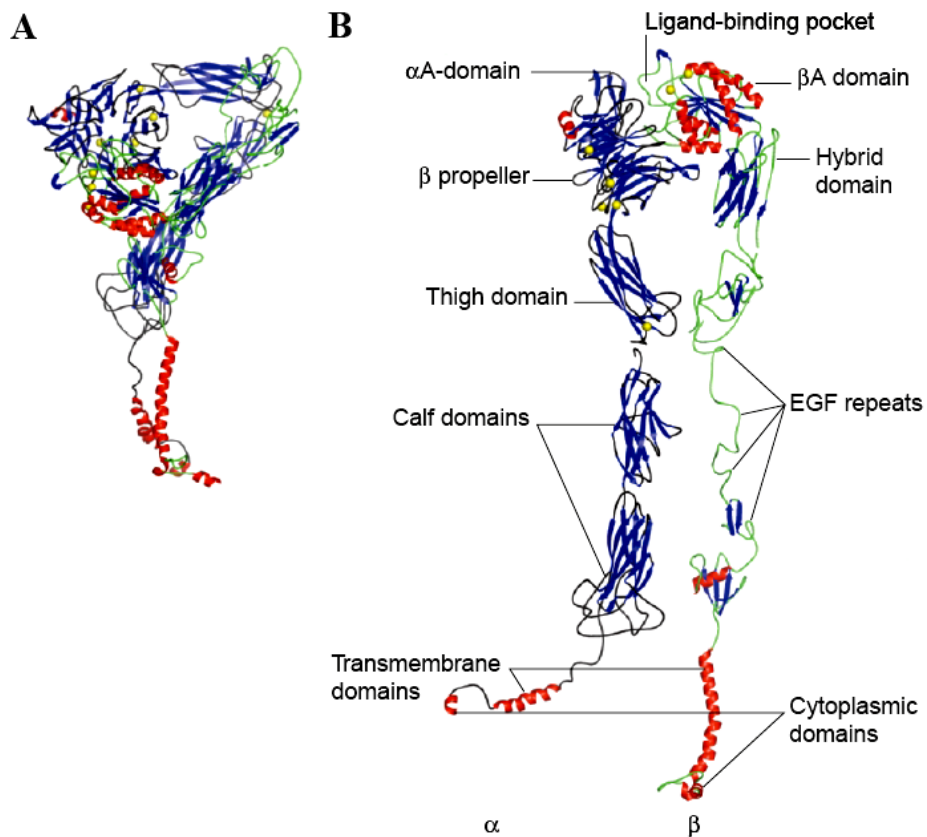


Figure 1.2 Schematic representation of the $\alpha\beta_3$ integrin crystal structure (A) bent-image ('inactive' or 'low-affinity ligand-binding') form. (B) Straightened image ('active' or 'high-affinity ligand-binding'). Left, α subunit and right, β subunit. The β subunit from N to C terminal comprises a βA domain, a hybrid domain, EGF repeats transmembrane domain and the cytoplasmic domain; the α subunit comprises an αA domain, a β propeller domain, a thigh domain, two calf domains, a transmembrane domain and the cytoplasmic domain.. The β strands are shown in blue and α helices in red. (Taken from Humphries et al., 2003 and modified)

Introduction

Arnaout and co-workers showed that the bent-form still can bind RGD peptides and FN (Xiong et al., 2002; Adair et al., 2005) in a Mn^{2+} -dependent manner and therefore concluded that the bent conformation indeed represents an active form. In parallel, Springer and co-workers showed with negative stain EM that a recombinant extracellular part of the $\alpha\beta3$ integrin drastically changed its conformation from a bent- to straightened-form upon Mn^{2+} - or RGD-dependent activation (Takagi et al., 2002) (Figure 1.3).

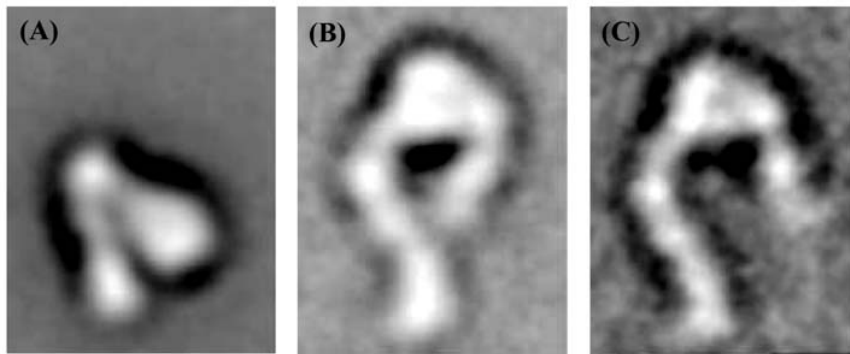


Figure 1.3 Switchblade model for global integrin conformation regulation defined by EM. (A) Bent conformation. (B) Extended conformation with closed headpiece seen in Mn^{2+} . (C) Extended conformation with opened headpiece seen with cyclic RGD peptide ligand. (Taken from Takagi et al., 2002 and modified)

This led to the conclusion that the individual integrin conformations bind their ligands with different affinities (Carman and Springer 2003). The conformational changes are mainly regulated through binding of intracellular proteins to the β integrin cytoplasmic tail. This event is called ‘inside-out signalling’ and is explained in the following chapters.

5.1.1.2 Integrin activation by Talin

A number of cytoskeletal proteins, including talin, α -actinin, filamin, tensin and ILK are implicated in linking members of the integrin family to filamentous actin (Brakebusch and Fässler, 2003). Talin represents one of the best studied integrin cytoplasmic binding proteins, and is also the key regulator of integrin activation. Talin is a large cytoplasmic protein (~270 kDa), composed of an N-terminal head domain of ~50 kDa, and a large C-terminal rod domain of ~220 kDa which is made up of a series of amphipathic helical bundles (Campbell and Ginsberg, 2004; Wegener et al., 2007). The head domain contains a band Four-point-one, Ezrin, Radixin, and Moesin (FERM) domain with three subdomains (F1, F2 and F3). The F3 subdomain harbours a binding site for the β integrin cytoplasmic domain and is sufficient to activate integrins (Calderwood et al., 2002).

Structural and biochemical studies from NMR, crystal structure, cell-based function assays and immunoprecipitations (IPs) revealed that the binding of talin to the integrin β cytoplasmic tail is the final common step in integrin activation (Figure 1.4) (Tadokoro et al., 2003; Wegener et al., 2007) (Figure 1.4). So far, binding of the talin head domain with β 1, β 2, β 3, and β 5 and weakly with β 7 has been shown. It also interacts with focal adhesion kinase (FAK), phosphatidylinositol-4,5-biphosphate (PIP_2), phosphatidylinositol-phosphate kinase type I gamma ($\text{PIPKI}\gamma$) and weakly to actin (Brakebusch and Fässler, 2003; Wiesner et al., 2005). The C-terminal rod domain contains binding sites for vinculin, a ubiquitous cytoskeletal protein found at cell-cell and cell-ECM contacts, for actin and also with a much lower affinity to the integrin β subunit (Hemmings et al., 1996; Yan et al., 2001).

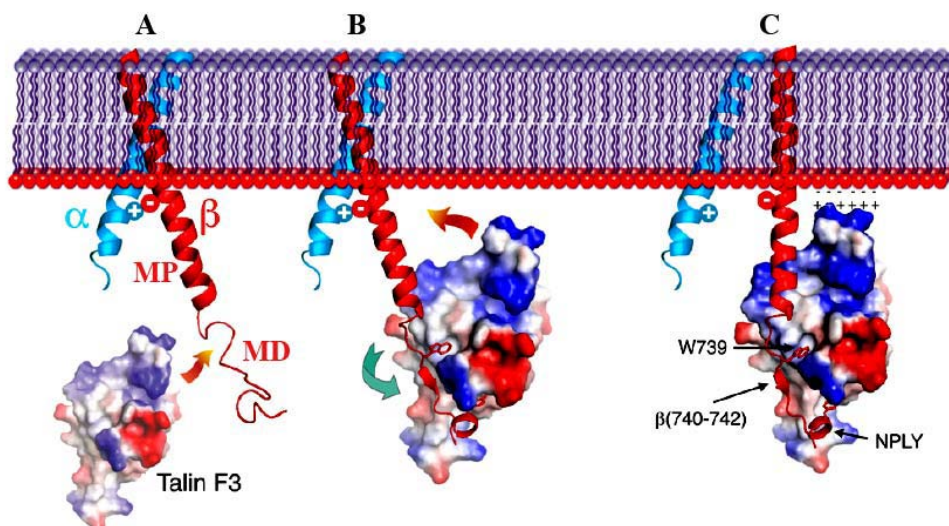


Figure 1.4 Schematic representation of talin-induced integrin activation. (A) The talin F3 domain binds to the cytoplasmic tail of β integrin. (B) F3 engages the membrane-distal (MD) part of the β 3-integrin tail (in red), which becomes ordered, but the α - β integrin interactions that hold the integrin in the low-affinity conformation remain intact. (C) In the subsequent step, F3 domain engages the membrane-proximal (MP) portion of β 3 tail while maintaining its MD interactions. Consequences of this additional interaction are (1) destabilization of the putative integrin salt-bridge; (2) stabilization of the helical structure of the MP region; and (3) electrostatic interactions between F3 and the acidic lipid head groups. The net result is a change in the position of the transmembrane helix, which is continuous with the MP- β -tail helix. (Taken from Wegener et al., 2007)

The interaction between talin and the β integrin subunit does not only promote integrin activation but in addition leads to recruitment and activation of the PIP₂-producing enzyme PIPKI γ (Di Paolo et al., 2002; Ling et al., 2002). This leads to an increased local concentration of PIP₂, which on one hand, further increases the affinity of the talin FERM domain to bind the integrin cytoplasmic tail, and on the other hand attracts other PIP₂ binding proteins like vinculin to the integrin adhesion sites. Upon

Introduction

binding to PIP₂, vinculin changes its conformation and exposes binding sites for talin and α -actinin (Gilmore and Burridge, 1996; Hüttelmaier et al., 1998, 1999). Finally, the interaction between talin and vinculin increases the affinity of vinculin for filamentous (F)-actin leading to the recruitment of F-actin to FAs (Figure 1.5).

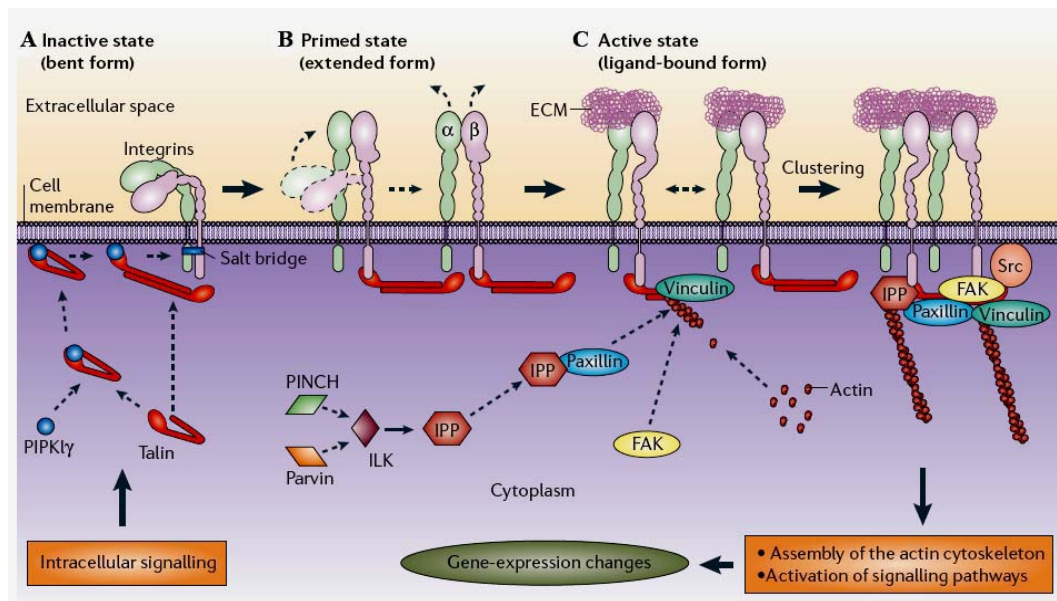


Figure 1.5 Talin-mediated integrin activation and integrin associated protein recruitment to focal adhesions. (A) Many integrins that are not bound to the extracellular matrix (ECM) are present on the cell surface in an inactive conformation, which is characterized by 'bent' extracellular domains that mask the ECM-binding pocket. (B) When talin is recruited to the plasma membrane and activated in association with PIPK1 γ , it binds to the cytoplasmic tail of β integrins. This interaction separates the cytoplasmic domains and induces the integrins to adopt the 'primed' conformation. (C) The integrin extracellular domains extend and unmask the ligand-binding site, allowing the integrin to bind specific ECM molecules. Finally, the integrin cytoplasmic domains recruit other focal-adhesion proteins, like vinculin, focal adhesion kinase, paxillin and integrin-linked-kinase, leading to the activation of some signalling pathways. (Taken from Legate et al., 2006 and modified)

5.1.2 Integrin cytoplasmic binding proteins

Increased ligand binding affinity of the integrin's extracellular domain is controlled by the interaction between cytoplasmic proteins and the integrin cytoplasmic tails. Although the integrin cytoplasmic tails are short and do not harbour any functional domains, they serve as docking sites for proteins that link integrins to the cytoskeleton or for a number of signalling proteins like kinases (Figure 1.1A). Genetic deletion or mutation studies showed that the integrin cytoplasmic tails control integrin activity (O'Toole et al., 1991, 1994; Ginsberg et al., 2001). Since the integrin cytoplasmic tails lack enzymatic activity, the signal transduction from outside into the cell critically depends on the recruitment of cytoplasmic tail binding proteins. This event is called 'outside-in signalling'.

Focal adhesions (FA) are well studied integrin mediated cell-adhesion structures that connect the extracellular matrix with the cytoskeleton. However, these structures can only be observed *in vitro* and have a size of ~ 1µm. They form from more immature structures which are named focal complexes (FCs; 100-200 nm in size). More than 50 proteins have been localized in FAs including tyrosine kinases (e.g. c-src, FAK), Ser/Thr kinases (e.g. PKC, PAK), proteases (calpain II) or GTPase modulators (e.g. Pix, Dock180) (Zamir and Geiger, 2001). This indicates that FAs also serve as important signalling relays. In the past 20 years, interactions of the integrin cytoplasmic tails with more than 20 proteins have been shown (Table 1.2).

Introduction

Binding partner	Integrin tail	Detection	Reference
Actin-binding protein			
Talin	$\beta_{1A}, \beta_{1D}, \beta_2, \beta_3$	COIP, PEP, EQ, INT, SLS	Horwitz et al., 1986; Knezevic et al., 1996; Pfaff et al., 1998; Goldmann, 2000
Filamin	$\beta_{1A}, \beta_2, \beta_3, \beta_7$	COIP, PEP, 2HYB, SLS	Pavalko et al., 1989; Loo et al., 1998; Pfaff et al., 1998; Goldmann, 2000
α -actinin	β_{1A}, β_2	PEP, INT, COIP, SLS	Otev et al., 1990; Pavalko et al., 1991; Cattelino et al., 1999
F-actin	α_2	PEP	Kieffer et al., 1995
Myosin	β_3	PEP, COIP	Jenkins et al., 1998; Sajid et al., 2000
Skelemin	β_1, β_3	2HYB, PEP	Reddy et al., 1998
Signaling protein			
ILK	β_1, β_3	2HYB, COIP	Hannigan et al., 1996
FAK	$\beta_1, \beta_2, \beta_3$	PEP, COIP	Schaller et al., 1995; Chen et al., 2000
Cytohesin-1	β_2	2HYB, COIP, PEP	Kolanus et al., 1996
Cytohesin-3	β_2	2HYB	Hmama et al., 1999
Other protein			
Paxillin	$\beta_1, \beta_3, \alpha_4$	PEP, COIP	Schaller et al., 1995; Chen et al., 2000; Liu et al., 1999
Grb2	β_3	PEP	Law et al., 1996
Shc	β_3	PEP	Law et al., 1996
β_3 -endonexin	β_3	2HYB, INT, PEP	Shattil et al., 1995; Eigenthaler et al., 1997
TAP-20	β_5	PEP	Tang et al., 1999
CIB	α_{ITb}	2HYB, PEP, COIP	Naik et al., 1997; Shock et al., 1999; Valler et al., 1999
Calreticulin	α	PEP, COIP	Rojiani et al., 1991; Leung-Hagesteijn et al., 1994; Coppolino et al., 1995
Caveolin-1	α	COIP	Wary et al., 1998
Rack1	$\beta_1, \beta_2, \beta_3$	2HYB, PEP, COIP	Liliental et al., 1998
WAI1-1	β_7	2HYB, PEP	Rietzler et al., 1998
JAB1	β_2	2HYB, PEP, COIP	Bianchi et al., 1998
Melusin	$\beta_{1A}, \beta_{1B}, \beta_{1D}$	2HYB, INT	Brancaccio et al., 1999
MIBP	β_{1A}, β_{1D}	2HYB, PEP, COIP	Li et al., 1999
ICAP-1	β_{1A}	2HYB, PEP, INT	Chang et al., 1997; Zhang and Hemler, 1999
CD98	β_{1A}, β_3	PEP	Zent et al., 2000
DRAL/FHL2	$\alpha_{3A}, \alpha_{3B}, \alpha_{7A}, \beta$	2HYB, PEP	Wixler et al., 2000
Kindlin/Unc-112/Mig-2	β_1, β_3	PEP	Kloeker et al., 2004

COIP—Coimmunoprecipitation; PEP—Synthetic/recombinant peptide studies; 2HYB—Yeast two-hybrid screen; INT—Binding to purified integrins; SLS—Static light scattering; EQ—Equilibrium gel filtration

Table 1.2 Integrin cytoplasmic domain binding proteins. Integrins interact with a number of proteins which are connected to the actin cytoskeleton or to different signalling pathways. (Taken from Liu et al., 2000 and modified)

These integrin cytoplasmic tail binding proteins include actin-binding proteins (e.g. α -actinin, talin and filamin), adaptor or kinase proteins (e.g. integrin-linked-kinase, ILK; focal adhesion kinase, FAK; paxillin and Grb2), guanine nucleotide exchange factors

(e.g. cytohesin-1,-3), transcriptional co-activators (e.g. JAB1), transmembrane protein (e.g. CD98) and a novel FERM domain protein family (e.g. Kindlin-1, -2 and -3) (Liu et al., 2000; Kloeker et al., 2004; Ussar et al., 2006).

Taken together, the integrin family plays a central role in the transduction of cell-matrix adhesion signals. Integrin signalling is indispensable not only for cell adhesion, cell migration, cell proliferation, cell survival and cell differentiation but also for the assembly of ECMs. Since integrins lack actin-binding sites and enzymatic activities, they recruit a number of intracellular proteins, which bind to the integrin cytoplasmic tails and serve as signalling platforms and docking sites for the actin cytoskeleton. Three integrin- and actin-associated proteins, integrin-linked kinase (ILK), kindlin and plectin, will be introduced in the following section.

5.2 Integrin-linked kinase

5.2.1 ILK and its binding partners

Integrin-linked kinase (ILK) was initially described as a non-receptor serine/threonine (Ser/Thr) kinase and was identified in a yeast-two hybrid (Y2H) screen as a protein which binds to the cytoplasmic tails of $\beta 1$ and $\beta 3$ integrin (Hannigan et al., 1996). The molecular function of ILK at the integrin adhesion site is not fully understood. ILK was believed to act as a kinase phosphorylating target proteins including PKB/Akt and GSK-3 β (Delcommenne et al., 1998; Persad et al., 2000). Moreover, ILK expression and activity were upregulated in several cancers suggesting that it plays a role in tumorigenesis and cancer invasion. (Persad and Dedhar, 2003).

ILK consists of 452 aa and has a molecular weight of ~52 kDa. The protein is composed of three distinct domains. The N-terminal domain contains four ankyrin

Introduction

repeats, which mediate protein-protein interactions. The N-terminus binds to PINCH-1 and PINCH-2 (particularly interesting Cys-His-rich protein, also known as LIMS1 and LIMS2) (Tu et al., 1999; Zhang et al., 2002; Braun et al., 2003). The C-terminal domain shares significant homology to Ser/Thr protein kinases, however a number of biochemical and cell biological assays demonstrated that the C-terminus also serves as an interaction domain for $\beta 1$ and $\beta 3$ integrins (Hannigan et al., 1996; Wu and Dedhar, 2001), paxillin, α -parvin (Nikolopoulos and Turner, 2000; Olski et al., 2001; Tu et al., 2001), β -parvin (Olski et al., 2001; Yamaji et al., 2001) and kindlin-2 (Mig-2 or UNC-112) (Mackinnon et al., 2002; Ussar et al., 2006). A putative pleckstrin homology (PH) domain is located between these two domains and partially overlaps with the C-terminal kinase domain. ILK, PINCH and parvin form a heterotrimeric complex, called IPP complex (Figure 1.6).

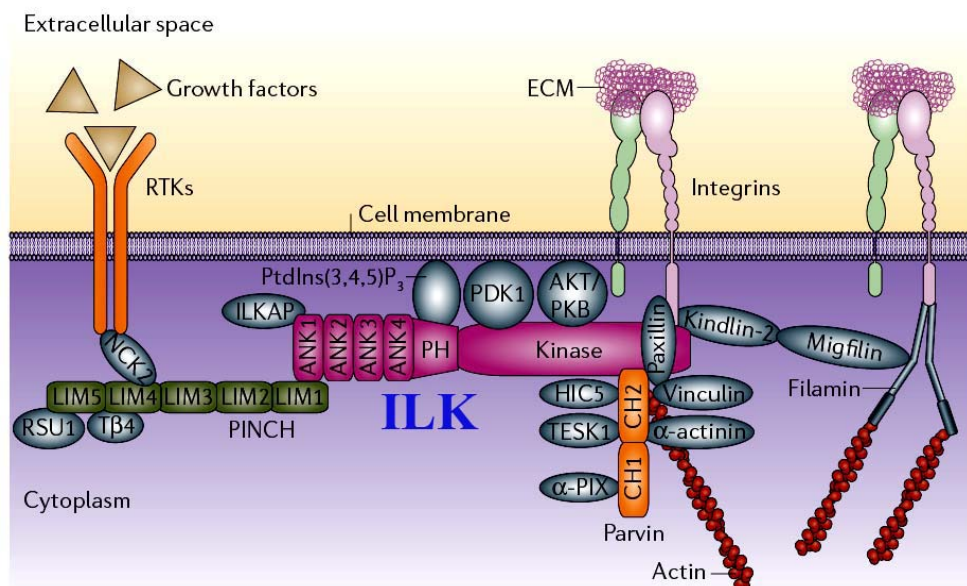


Figure 1.6 Schematic picture of ILK and its associated partners. ILK represents an adaptor protein at integrin adhesion sites and links integrins to the actin cytoskeleton. (Taken from Legate et al., 2006)

5.2.2 Biochemical and genetic studies of ILK

ILK plays an important role in integrin signalling. Although the C-terminal kinase domain lacks certain amino acids, which are usually highly conserved in other Ser/Thr kinases, a kinase activity has been shown in ILK overexpressing cells. Putative phosphorylation targets are e.g. PKB/Akt (at Ser473), GSK-3 β (at Ser9), myosin light chain, myosin phosphatase, parvins and the integrin cytoplasmic tails (Delcommenne et al., 1998; Janji et al., 2000; Deng et al., 2001; Deng et al., 2002; Kiss et al., 2002) (Table 1.3).

Target	Phosphorylation site	Reference
ILK	Ser343	Persad et al., 2001
β 1 integrin	Ser785	Hannigan et al., 1996
β 3 integrin	—————	Pasquet et al., 2002
Akt/PKB	Ser473	Delcommenne et al., 1998
GSK-3 β	Ser9	Delcommenne et al., 1998
β -parvin	—————	Yamaji et al., 2001
Myosin light chain	Thr18/ Thr19	Deng et al., 2001
Myelin basic protein	—————	Hannigan et al., 1996
MYPT1	Thr695/ Thr495	Kiss et al., 2002
CPI-17	Thr38	Deng et al., 2002
PHI-1	Thr57	Deng et al., 2002
α -NAC	Ser43	Quelo et al., 2004

Table 1.3 ILK substrates. List of proteins which were shown to be phosphorylated by ILK.

Genetic ablation of ILK in *Caenorhabditis elegans* and *Drosophila melanogaster* led to actin filament detachment in muscle resulting in early lethality during embryogenesis. Interestingly, the severe phenotypes in nematodes as well as in flies can be fully rescued by an ILK protein harboring an inactive kinase domain. These experimental results indicate that ILK kinase activity is dispensable for the development and physiology of invertebrates (Zervas et al., 2001; Mackinnon et al., 2002). In mice conditional ablation of ILK in fibroblasts, chondrocytes, hepatocytes or keratinocytes showed that PKB/Akt or GSK-3 β phosphorylation levels were not diminished (Grashoff et al., 2003; Sakai et al., 2003; Terpstra et al., 2003; Gkretsi et al., 2007; Lorenz et al., 2007). However, studies in other cell types such as endothelial cells, neurons, or macrophages show that ILK loss leads to reduced PKB/Akt or GSK-3 β activity (Gary et al., 2003; Troussard et al., 2003; Friedrich et al., 2004). Sequence alignments of the ILK kinase domains from different organisms revealed a lack of essential motifs (e.g. the catalytic base and Mg²⁺ chelating residues) which are highly conserved in other Ser/Thr kinases (Legate et al., 2006; Hanks, 2003). Therefore, it is still obscure whether ILK possesses kinase activity *in vivo*.

5.2.3 Analysis of the role of ILK in mammalian skeletal muscle

Loss of ILK expression in mice leads to peri-implantation lethality with impaired actin dynamics at integrin attachment points and abnormal epiblast polarity (Sakai et al., 2003). β 1 integrins regulate myoblast fusion and maintenance the muscle sarcomeres in mammals (Fässler et al., 1996; Hirsch et al., 1998; Schwander et al., 2003). Similar in *C. elegans* and *Drosophila*, mammalian, ILK is also highly expressed in myofibers and myoblasts.

5.2.3.1 Development and architecture of skeletal muscle

Skeletal muscle consists of highly specialized contractile cells, which enable locomotion of an organism but it fulfils also important functions for other physiological processes such as breathing. Mammalian skeletal muscle is derived from progenitor cells that originate from somites. During the split of the somites into dermomyotome and sclerotome, the mononucleated embryonic myogenic progenitor cells (e.g. myoblasts) invade the myotome and fuse and form myotubes at around embryonic day 11 (e.g. E11.0). Probably at the same time, a phase that is referred as primary myogenesis, myoblasts start migrating from the dermomyotome towards the limb and differentiate into multinucleated muscle fibers, known as primary fibers. A second wave of myogenesis takes place between E14.5 and E17.5. This phase is called secondary myogenesis and involves fusion of fetal myoblasts either with each other to give rise to secondary fibers or they fuse with the previously formed primary fibers (Duxson et al., 1989; Evans et al., 1994; Doberstein et al., 1997) (Figure 1.7). Certain cell surface receptors are particularly involved in the cross-talk between cells and the extracellular matrix (Henry and Campbell., 1998; Sasaki et al., 1998). In skeletal muscle, two major matrix adhesion complexes exist: dystrophin-glycoprotein complex (DGC) and integrins (Henry and Campbell, 1998, 1999; Mayer, 2003).

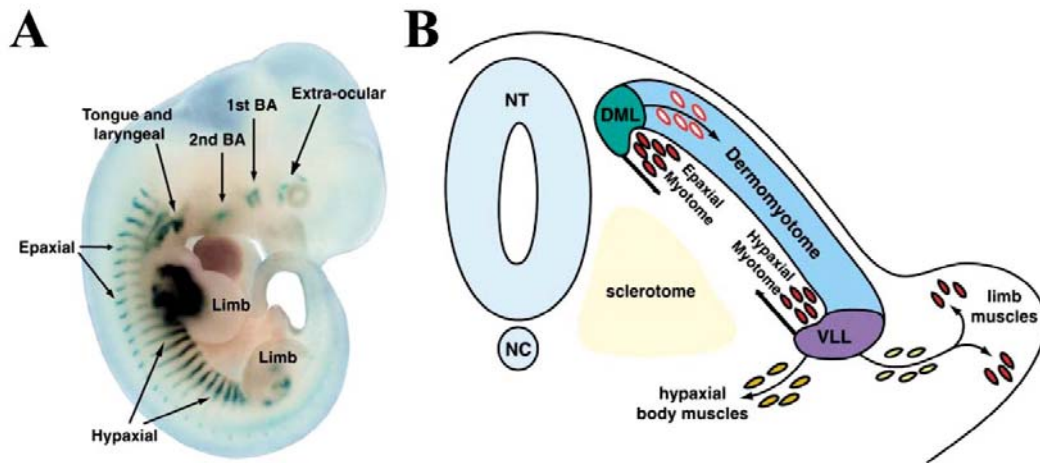


Figure 1.7 (A) Myogenic progenitors in mouse embryo E11.5 days, as visualized through expression of the MyoD LacZ reporter. MyoD expression is localized to the trunk somite progenitors at the sites of epaxial, hypaxial and limb muscle differentiation, and the head mesoderm progenitors, including the first and the second branchial arches (BA), the tongue and larynx and the extra-ocular muscles. (B) Somite origins of myogenic progenitors originate in the dorsal-medial and ventral-lateral lips (DML and VLL) of the dermomyotome. Cells of DML migrate ventrolaterally, differentiate and form the myotomal muscles, which will give rise to the epaxial deep back muscles. The VLL provides progenitors that migrate ventrally to form the ventral body wall muscles; that migrate dorsolaterally to form the hypaxial myotome and that delaminate from the VLL and migrate to the dorsal and ventral muscle-forming regions of the limb where they differentiate to form the limb muscles (Taken from Elizabeth Pownall et al. 2002).

A skeletal muscle cell (also called muscle fiber) has a highly unorthodox structure. A single, cylindrically shaped muscle cell is 10 to 100 μm thick, up to 100 mm long, and contains hundreds of nuclei. Skeletal muscle cells have a highly ordered internal architecture. A longitudinal section through the muscle fiber reveals a cable-like structure with hundreds of thinner, cylindrical strands, called myofibrils (Figure 1.8A). Each myofibril consists of several contractile units, called sarcomeres. Each sarcomere

Introduction

in turn shows a distinctive banding pattern, which gives the muscle fiber a striated appearance. An ultra-structural analysis reveals that the banding pattern is due to two distinct types of filaments, thin filaments and thick filaments (Figure 1.8B). Each sarcomere is flanked by a Z-disc (or Z-line) and contains a central dark band (called A bands) and light zones adjacent to the Z-disc (called I band) (Figure 1.8B, C). In relaxed sarcomeres, a H zone is visible in the center of an A band (Figure 1.8C).

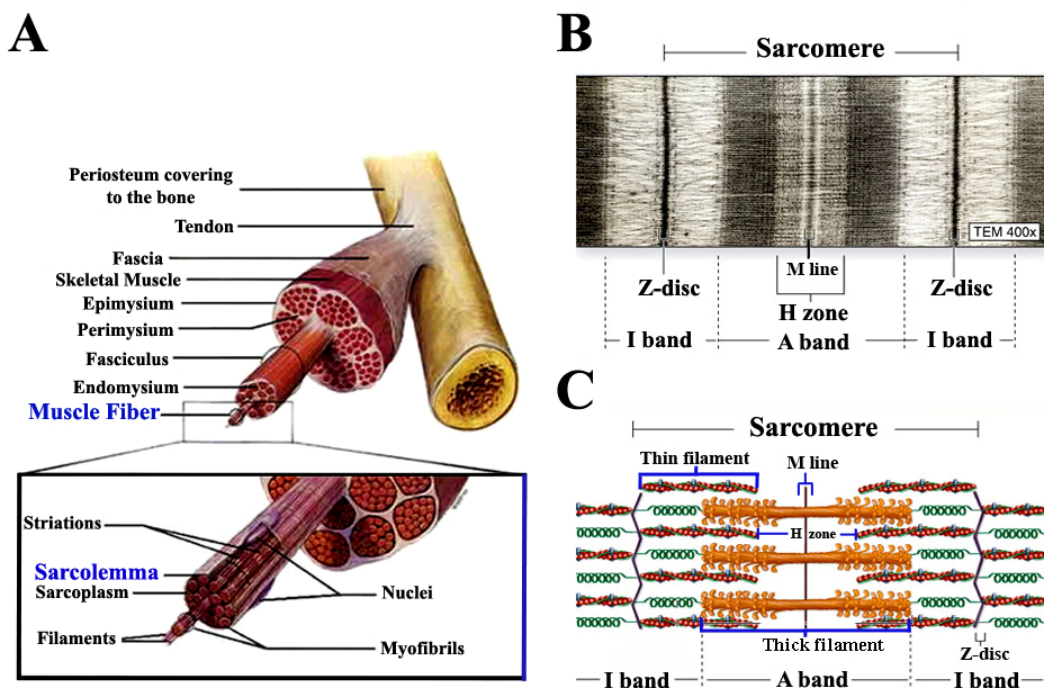


Figure 1.8 The structure of skeletal muscle. (A) Schematic diagram of skeletal muscle organization from an entire body muscle to a muscle fiber. A longitudinal section through the muscle fiber reveals a cable-like structure with hundreds of thinner, cylindrical strands, called myofibrils. (B) Electron micrograph of a longitudinal section through a single sarcomere shows the typical banding pattern. (C) Schematic diagram of the contractile unit, called sarcomere, with overlapping arrays of thin and thick filaments. Each sarcomere extends from one Z-disc (or

Z-line) to the other Z-disc and contains dark bands (called A bands) and light zones (called I band).. (Taken from the website: <http://Dayton.fsci.umn.edu/~bill>)

5.2.3.2 Role of integrins in skeletal muscle development and function

Integrins play an essential role during murine myogenesis and muscle homeostasis (Mayer, 2003). A whole set of different $\beta 1$ integrins (e.g. $\alpha 1$, $\alpha 3$, $\alpha 4$, $\alpha 5$, $\alpha 6$, $\alpha 7$ and αv) is expressed in muscle progenitor cells (Gullberg et al., 1998). It has been shown that these integrins localize to costameres (FA-like structure connecting the sarcomeric Z-discs with the sarcolemma), to the neuromuscular junctions (NMJs), the myotendinous junctions (MTJs) and the sarcolemma. During myogenesis, the $\beta 1$ integrin switches from the $\beta 1A$ to the $\beta 1D$ variant (van der Flier et al., 1997; Zhidkova et al., 1995; Belkin et al., 1996). In parallel, $\alpha 5\beta 1$ (FN receptor) and $\alpha 6\beta 1$ (laminin receptor) are highly expressed in early muscle development and become downregulated after myotube formation, whereas $\alpha 7\beta 1$ (laminin receptor) is mainly restricted to skeletal and cardiac muscle and becomes strongly upregulated upon myoblast fusion. These data suggests that during terminal muscle differentiation, the muscle cell environment switches from a fibronectin-rich matrix to a laminin-containing basement membrane (Bronner-Fraser et al., 1992, Blaschuk and Holland, 1994; Boettiger et al., 1995; Yao et al., 1996; Blaschuk et al., 1997).

Due to the early lethality of $\beta 1$, $\alpha 4$ and $\alpha 5$ integrin knockout mice, an analysis of their roles in muscle development was not possible. On the other hand, no obvious muscle defects have been described for $\alpha 1$ -, $\alpha 3$ -, $\alpha 6$ - and αv -deficient mice (Table 1.1). Analysis of $\alpha 5$ integrin-knockout chimeras and $\alpha 7$ -deficient mice showed muscular dystrophy, suggesting that $\alpha 5$ - and $\alpha 7$ integrins regulate muscle fibre integrity (Mayer et al., 1997; Taverna et al., 1998). Mice lacking $\beta 1$ integrin specifically in skeletal muscle die immediately after birth strongly suggesting that $\beta 1$ integrins regulate myoblast fusion and sarcomere assembly (Schwander et al., 2003).

5.2.3.3 The role of ILK in skeletal muscle

ILK is highly expressed in the skeletal muscle (Hannigan et al., 1996). There it predominantly localizes to myotendinous junctions (MTJs) and costameres. Costameres are composed of proteins typically found in FAs, such as integrins, vinculin, talin, and α -actinin, and provide structural linkage to sarcomeric actin filaments. Thus, costameres transmit contractile forces from the sarcomere across the sarcolemma to the extracellular matrix.

It has been recently shown that knockdown of ILK in zebrafish (*z-ilk*) results in lethal heart failure (Bendig et al., 2006). Conditional deletion of ILK in mouse cardiomyocytes by using *muscle creatine kinase-Cre* (*mck-Cre*) leads to heart dilation, fibrosis and disaggregation of cardiomyocytes. These animals die at an age of 6 to 12 weeks (White et al., 2006), similar to cardiac-specific $\beta 1$ integrin and FAK knockout mice (Shai et al., 2002; Peng et al., 2006). Interestingly, the loss of cardiac ILK is accompanied by a reduction in Akt phosphorylation (at Ser473). Based on the reduced Ser473-phosphorylation of ILK deficient cardiomyocytes, the ability of ILK to phosphorylate Ser473 of PKB/Akt *in vitro* (Persad et al., 2000; Delcomenne et al., 1998) and the observation that PKB/Akt activity is crucial for cardiomyocyte growth and contractility (DeBosch et al., 2006; Condorelli et al., 2002), it was concluded that mechanical stress-mediated activation of ILK supports cardiomyocyte homeostasis via PKB/Akt activation.

However, the role of ILK in skeletal muscle is still unclear. *In vitro* overexpression of ILK in mouse C2C12 myoblasts abrogates myotube formation by inactivating p44/p42 MAP kinase, thus preventing cell cycle exit and inhibiting the expression of myogenic determination genes (MyoD and myogenin) (Huang et al., 2000). In contrast, Miller et al. (2003a) showed that overexpression of ILK increases the expression of myogenin and promotes the formation of myotubes in rat L6 myoblast cells. However, *mck-Cre* driven conditional deletion of ILK in murine cardiac and skeletal muscle revealed no obvious skeletal muscle defect indicating that ILK is dispensable for the

development and homeostasis of skeletal muscle (White et al., 2006). This unexpected finding might be explained by the severe heart abnormalities and the early death of the mice, or alternatively could result from incomplete Cre-mediated (*mck-Cre*) ILK gene deletion in skeletal muscle.

5.3 The Kindlin protein family

5.3.1 Kindlin protein structure

The Kindlin gene family is named after the gene mutated in Kindler syndrome, an autosomal recessive genodermatosis in human (Jobard et al., 2003). The family consists of three members in mice and men: Kindlin-1 (URP1), Kindlin-2 (Mig-2) and Kindlin-3 (URP2/Mig2B). The first member was identified in a differential cDNA library screen as mitogen inducible gene-2 (Mig-2) (Wick et al., 1994). The other two members were initially named URP1 (Unc-112 Related Protein 1) and URP2 due to their sequence homology to the kindlin orthologue in *Caenorhabditis elegans*: Unc-112 (Rogalski et al., 2000; Weinstein et al., 2003).

Murine Kindlin-1, 2 and 3 are composed of 677, 680 and 665 amino acids and have a molecular size of ~77.4 kDa, ~78 kDa and ~76 kDa, respectively. An amino acid sequence alignment revealed a 60% identity and 74% similarity between murine Kindlin-1 and -2, 53% identity and 69% similarity between Kindlin-1 and -3, and 49% identity and 67% similarity between Kindlin-2 and -3.

Kindlins harbor a FERM domain, which consists of three subdomains: F1 to 3. The hallmark of Kindlin proteins is a PH (Pleckstrin Homology) domain, which is inserted into the F2 subdomain (Weinstein et al., 2003; Kloeker et al., 2004) (Figure 1.9). A nuclear localization signal (NLS) is exclusively present in Kindlin-2. A comparison of

FERM domain proteins revealed highest homology between the F3 subdomain of Kindlins and Talin. Furthermore, like talin, all Kindlin proteins bind to the cytoplasmic tails of $\beta 1$ and $\beta 3$ integrins through its FERM domain *in vitro* (Weinstein et al., 2003; Shi et al., 2007; Moser et al., 2008).

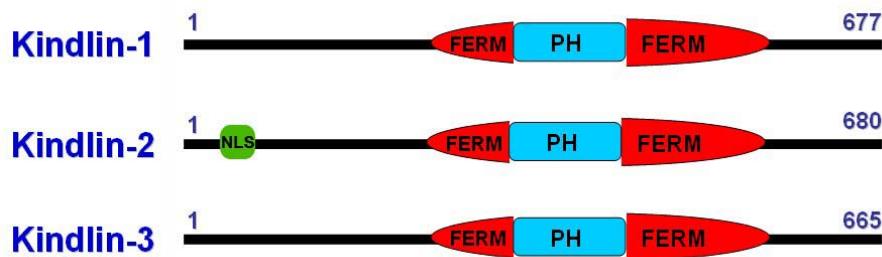


Figure 1.9 Domain structure of Kindlin-1, -2 and -3 proteins. Schematic representation of the FERM (red color), PH (blue color) and NLS (green color) domains of Kindlins.

5.3.2 Kindlin gene expression

In humans, Northern blots and RT-PCR analyses from different tissues showed high Kindlin-1 expression in keratinocytes, colon, kidney and placenta and at lower levels in heart, skeletal muscle, liver and small intestine. Kindlin-2 was moderately expressed in spleen, prostate, testis, ovary, small intestine, colon, heart, placenta, lung, liver, kidney and pancreas, and weakly expressed in thymus, brain, skeletal muscle and keratinocytes. Kindlin-3 was highly expressed in spleen, thymus and peripheral blood leukocytes (Siegel et al., 2003; Weinstein et al., 2003). Subcellular localization of Kindlin proteins was studied by transfection experiments with EGFP-tagged Kindlin cDNA constructs showing that Kindlin-1 colocalizes to actin stress fibers in fibroblasts (Tu et al., 2003) and Kindlin-2 is present in FAs of epithelial cells (Siegel et al., 2003).

Microarray analyses of different tumor tissues showed upregulated Kindlin-1 expression in colon and lung tumors (Weinstein et al., 2003). Furthermore, increased Kindlin-2 levels have been reported in leiomyomas. Interestingly, in this study Kindlin-2 was mainly localized to the nucleus of normal and neoplastic smooth muscle cells (Kato et al., 2004).

5.3.3 *In vivo* function of Kindlins

Loss of Kindlin-1 in humans gives rise to Kindler syndrome, a rare genodermatosis, which is characterized by atrophy, trauma-induced blistering at early life, sun sensitivity, abnormal pigmentation and fragility of the skin (Siegel et al., 2003). Kindler syndrome is the first skin blistering disease resulting from defects in the linkage of the actin skeleton to cell matrix adhesions (Kindler, 1954; Siegel et al., 2003; Ashton et al., 2004; White et al., 2005). Genetic studies in *C. elegans* showed a requirement of the Kindlin orthologue, Unc-112, for the attachment of body-wall muscle cells to the hypodermis. Therefore, loss of Unc-112 in nematodes results in an embryonic lethal PAT (paralyzed, arrested elongation at twofold) phenotype (Rogalski et al., 2000).

Biochemical studies with recombinant integrin tails revealed differences in the binding mode between kindlin and talin. A point-mutant of the proximal NPxY-motif within the $\beta 3$ integrin cytoplasmic tail (Y₇₄₇A) which abrogates talin binding was still bound by Kindlin-2 *in vitro* (Shi et al., 2007). However, a mutation of the distal NxxY-motif prevented Kindlin-3 binding to $\beta 1$ and $\beta 3$ integrin tails (Moser et al., 2008).

Cell biological studies showed that the FERM domain is necessary for the correct targeting of Kindlin proteins to FAs. Interestingly, Kindlin-2 promotes $\alpha IIb\beta 3$ integrin activation and fibrinogen binding in a chinese hamster ovary (CHO) cell reporter system, however integrin activation was less efficient than talin (Shi et al., 2007) indicating that Kindlin-2 is involved in integrin activation.

Recently, a critical role of Kindlin-2 for cardiogenesis in zebrafish has been reported. Downregulation of the Kindlin-2 homologue in zebrafish (z-kindlin-2) by using the morpholino knockdown technique showed a severe disruption of cardiac structure and function affecting ventricle morphology, size and contractility. Ultrastructural analysis of these hearts revealed abnormalities of intercalated discs and a failure in the attachment of myofibrils to membrane complexes (Dowling et al., 2008). Inactivation of Kindlin-3 in mice results in a postnatal lethal phenotype, which is characterized by severe bleedings and anemia. *In vitro* and *in vivo* analyses of Kindlin-3 deficient platelets revealed that Kindlin-3 is required for platelet integrin activation. Lack of Kindlin-3 causes a defect in platelet aggregation and resistance to arterial thrombosis. Thus, Kindlin-3, like Talin, is an essential regulator of integrin activation (Moser et al., 2008).

Taken together, Kindlins are important integrin binding proteins that regulate integrin activation in all different cell types.

5.4 Palladin

5.4.1 Palladin and its binding partners

Palladin represents a member of the recently characterized palladin/myotilin/myopalladin protein family in human and mice. They are all characterized by highly conserved Ig-like domains (called IgCAM, a member of the immunoglobulin domain Cell Adhesion Molecule subfamily) in the C-terminus of each protein (Figure 1.10) (Otey et al., 2005).

Palladin colocalizes to actin-based structures such as stress fibers, cell-cell junctions, embryonic Z-lines and FAs (Parast and Otey, 2000; Mykkänen et al., 2001). Palladin was reported to be ubiquitously expressed in embryonic tissues and

downregulated in certain tissues of adult mice (Parast and Otey, 2000). In contrast, the expression of the two other family members, myotilin and myopalladin, are highly restricted to striated muscle tissue (Bang et al., 2001; Mykkänen et al., 2001).

Murine Palladin/Myotilin/Myopalladin Gene Family

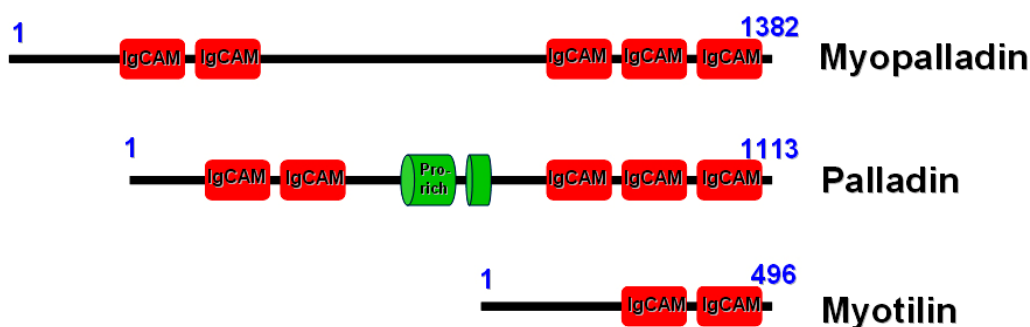


Figure 1.10 The structural homologies between palladin (largest isoform), myotilin and myopalladin suggest that they belong to the same family. The homologies are strongest in the IgCAM (immunoglobulin domain Cell Adhesion Molecule subfamily) domains (red color). Only palladin contains two Proline-rich regions (green color).

Northern and Western blot analyses of palladin revealed a complex expression pattern with multiple isoforms (Parast and Otey, 2000; Mykkänen et al., 2001). The palladin gene spans about 400 kb, with at least 24 exons and 3 alternative promoters in human and mice (Otey et al., 2005). Immunoblots from different tissues showed that at least 3 different variants are expressed: a 200 kDa isoform, a 140 kDa isoform and a 90-92 kDa isoform (Figure 1.11A).

The 200 kDa isoform is composed of five Ig-CAM domains, two of them are localized in the N-terminus and three are located in the common C-terminus. A cluster of proline-rich/serine-rich regions are found in the center of the protein. The 140 kDa isoform lacks the first N-terminal Ig-CAM domain. Expression of the 90-92 kDa isoform

Introduction

is controlled by a promoter in the middle of the gene resulting in a protein with the proline-rich/serine-rich region at the N-terminus followed by the three Ig-CAM domains in the C-terminus (Figure 1.11A).

The 200 kDa isoform has been detected in embryonic and adult heart as well as in skeletal muscle. The 140 kDa isoform is widely expressed in many embryonic tissues and is downregulated in most adult tissues. An exception is stomach and uterus which are tissues rich in smooth muscle cells. The 90-92 kDa isoform is ubiquitously expressed in embryonic tissues and downregulated in certain adult tissues of mice (Figure 1.11B).

Various biochemical assays identified a large number of palladin interaction partners, most of them are actin-binding proteins: α -actinin, VASP, profilin, ezrin, Esp8, Lasp-1 and even F-actin itself (Mykkänen et al., 2001; Boukhelifa et al., 2004; Rönty et al., 2004; Goicoechea et al., 2006; Boukhelifa et al., 2006; Rachlin and Otey, 2006; Dixon et al., 2008). In addition, palladin binds to a number of proteins that influence actin organization: Abl/Arg kinase binding protein (ArgBP2), lipoma preferred partner (LPP) and SPIN90 (also known as DIP, mDia interacting protein) (Figure 1.12) (Rönty et al., 2005; Jin et al., 2007; Rönty et al., 2007). Taken together, the cellular localization of palladin and its binding partners suggests that it fulfils an important function as an actin-associated scaffolding molecule.

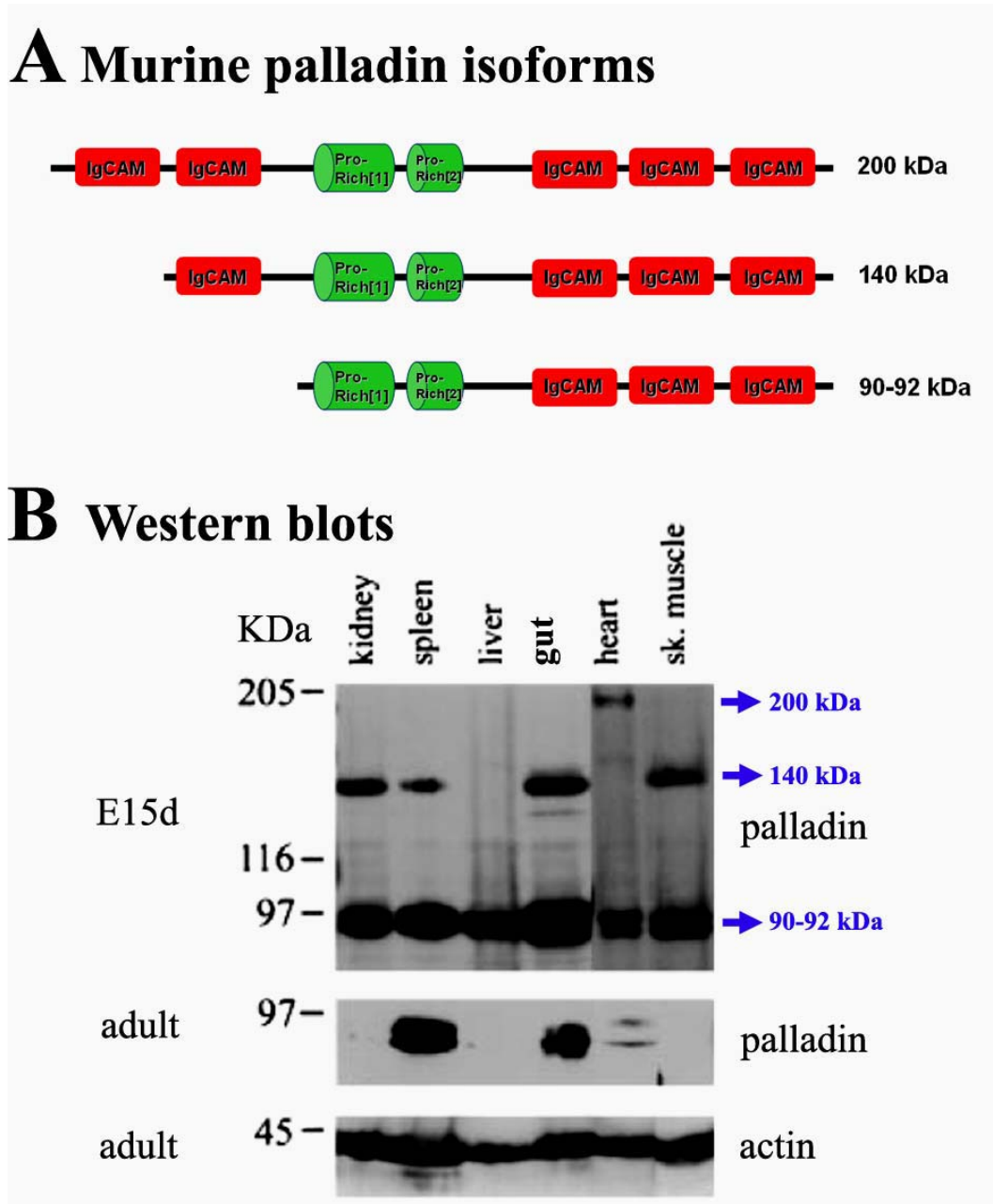


Figure 1.11 Palladin isoforms. (A) Schematic representation of palladin isoforms. (B) Western blot analyses show a ubiquitous palladin expression at embryonic day 15 (E15), and become

restricted to a few tissues such as spleen and gut in the adult tissues. (Taken from Parast and Otey, 2000)

Palladin Interactive Partners

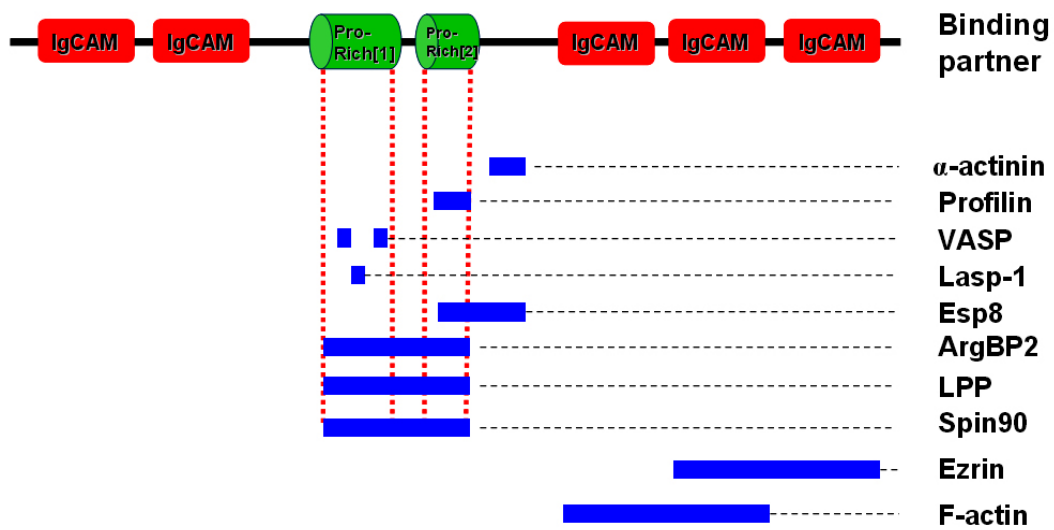


Figure 1.12 Palladin interacting proteins. Blue bars indicate their interaction sites within the palladin protein.

5.4.2 Biochemical and genetic studies of palladin

The IgCAM domains are the hallmark of the palladin/myotilin/myopalladin protein family. Ig-like domains are thought to mediate protein-protein interactions (Williams and Barclay, 1988). Actin co-sedimentation and differential sedimentation assays showed that the third IgCAM domain of palladin directly binds to F-actin *in vitro*.

Furthermore, the tandem third and fourth IgCAM domains are required to bundle F-actin (Dixon et al., 2008).

Overexpression of the 140 kDa and 90-92 kDa palladin isoforms resulted in changes in cell morphology and actin distribution (Rachlin and Otey, 2006). Reduced palladin expression by antisense or siRNA approaches caused dramatic reduction of stress fibers, FAs, dorsal ruffles and podosomes (Parast and Otey, 2000; Goicoechea et al., 2006). Complete inactivation of all palladin isoforms in mice results in embryonic lethal phenotype at ~E15.5 due to cranial neural tube closure defects (Luo et al., 2005). Fibroblasts isolated from these embryos showed defects in cell migration, adhesion and stress fiber assembly (Luo et al., 2005; Liu et al., 2007a). In addition, analyses of the palladin deficient fetal liver showed a defective erythropoiesis and erythroblastic island formation (Liu et al., 2007b). Taken together, these data suggest again that palladin plays an essential role in the assembly and remodeling of the actin cytoskeleton.

5.4.3 The role of palladin in human disease

Biochemical and genetic studies showed that palladin interacts with various actin-binding proteins. Palladin is important for cell migration, adhesion and the assembly of the actin cytoskeleton *in vitro* and inactivation of palladin in mouse results in neural tube closure and fetal erythropoietic defects.

Recently, Shiffman and co-workers have shown a single nucleotide polymorphisms (SNPs) in the palladin gene which is linked to myocardial infarction (MI) (Shiffman et al., 2005). In addition, a point mutation within the human *palladin* gene (P₂₃₉S at the α -actinin binding site of the 90-92 kDa isoform) was found in familial pancreatic cancer and overexpression of palladin correlates to sporadic pancreatic cancer (Pogue-Geile et al., 2006; Zogopoulos et al., 2007). These observations suggest that abnormal or high levels of palladin cause cytoskeletal changes in pancreatic cancer and may be responsible for or contribute to the tumor's invasive and migratory abilities. However,

Introduction

the role of palladin in the onset and progression of these diseases is still unclear. Thus, a detailed examination of the molecular function of palladin could lead to a better understanding of the pathophysiology of these human diseases.

6 Aim of the thesis

The aim of my thesis was to study the role of integrin associated proteins in mouse by analyzing their expression patterns and by generating specific mouse mutants to address their *in vivo* functions.

The main project addresses the role of ILK in skeletal muscle. Inactivation of ILK in mice, nematodes and flies revealed an essential function for the early development of these organisms making it impossible to study ILK function in skeletal muscle. *In vitro* studies in murine C2C12 myoblasts showed that ILK overexpression inhibits the formation of multinucleated myotubes by activating p44/p42 MAP kinase and thereby preventing cell cycle exit. In contrast, a conflictive observation in rat L6 myoblasts showed that overexpression of ILK stimulates myotube formation and induces muscle differentiation without affecting MAP kinase activity. To investigate the role of ILK for myogenesis *in vivo*, the ILK gene was conditionally deleted in skeletal muscle by transgenic expression of the Cre-recombinase under the control of the *human skeletal α -actin (HSA)* promoter. The results are presented in paper I: “Integrin-linked kinase stabilizes myotendinous junctions and protects muscle from stress-induced damage”.

As a second aim I functionally characterized palladin, an F-actin associated protein that also localizes to integrin-mediated adhesion sites. At the beginning I characterized the complex genomic organization of the gene and analyzed the expression pattern of the different splice variants during mouse development and in adult tissues. I became particularly interested in the largest palladin isoform, which is mainly expressed in heart and skeletal muscle. A deeper characterization of this isoform was achieved with the help of a specific antiserum and the generation of an isoform specific knockout mouse (manuscript I and II, in preparation).

Finally, I was involved in an initial characterization of a novel integrin interacting family, the Kindlins. Kindlins localize to integrin-mediated adhesion structures and directly interact with the β integrin subunit and ILK. We analyzed the mRNA expression

Aim of the thesis

pattern of all three Kindlin genes during embryonic development and in adult tissues. EGFP-tagged Kindlin-1 to 3 cDNA constructs were used to determine their subcellular localization in various cell types. The results are presented in paper II: “The Kindlins: subcellular localization and expression during murine development”.

7 Brief summaries of the publications

7.1 Paper I: Integrin-linked kinase stabilizes myotendinous junctions and protect muscle from stress-induced damage

Integrin-mediated cell-matrix interactions play crucial roles for development, tissue homeostasis, and maintenance. Upon ligand binding, integrins recruit a number of different proteins to their cytoplasmic tails. An important binding partner of integrins represents integrin-linked kinase (ILK). ILK is highly expressed in skeletal muscle predominantly at costameres, which are the focal adhesion-like structures and myotendinous junctions (MTJs). To investigate the function of ILK in skeletal muscle, we conditionally ablated the ILK gene by using the human skeletal α -actin (HSA) promoter-driven Cre transgene.

In this paper, we show that loss of ILK triggers a mild, progressive muscular dystrophy, which is mainly restricted to MTJ areas and characterized by detachment of basement membranes and accumulation of extracellular matrix. Interestingly, endurance exercise training enhances the defects at MTJs, leads to disturbed subsarcolemmal myofiber architecture and abrogates phosphorylation of Ser473 as well as Thr308 of PKB/Akt. The reduction in PKB/Akt activation is accompanied by an impaired insulin-like growth factor 1 receptor (IGF-1R) activation. Co-immunoprecipitation experiments revealed that the β 1 integrin subunit is associated with the IGF-1R in muscle cells. Our data identify the β 1 integrin-ILK complex as an important component of IGF-1R/insulin receptor substrate signaling to PKB/Akt during mechanical stress in skeletal muscle.

7.2 Paper II: The Kindlins: subcellular localization and expression during murine development

The Kindlin gene family represents a new family of focal adhesion (FA) proteins and is named after the gene mutated in Kindler syndrome, an autosomal recessive genodermatosis in human. It consists of three members in mice and men: Kindlin-1 (URP1, Unc-112 Related Protein 1), Kindlin-2 (Mig-2) and Kindlin-3 (URP2/Mig2B). Their modular structure consists of a centrally located FERM (Band Four point one/Ezrin/Radixin/Moesin) domain whose F2 subdomain is split by a pleckstrin homology (PH) domain. *In vitro* studies have shown that Kindlin-1 can bind to the cytoplasmic tails of $\beta 1$ and $\beta 3$ integrins and Kindlin-2 binds to ILK.

In this paper, we describe the genomic organization, gene expression and subcellular localization of murine Kindlins-1, -2 and -3. *In situ* hybridization data show that Kindlin-1 is preferentially expressed in epithelia, and Kindlin-2 in striated and smooth muscle cells. Kindlins-1 and -2 are both expressed in the epidermis. While both localize to integrin-mediated adhesion sites in cultured keratinocytes. Kindlin-2, but not Kindlin-1, colocalizes with E-cadherin to cell-cell contacts in differentiated keratinocytes. Using a Kindlin-3-specific antiserum and an EGFP-tagged Kindlin-3 construct, we could show that Kindlin-3 is present in the F-actin surrounding ring structure of podosomes, which are specialized adhesion structures of hematopoietic cells

7.3 Paper III: Identification and embryonic expression of a new AP-2 transcription factor, AP-2 epsilon

AP-2 (activator protein-2) represents a family of four closely related and evolutionarily conserved sequence-specific transcription factors: AP-2 α , - β , - γ and - δ . AP-2 α was first identified in 1991 due to its ability to bind to the SV40 and the human metallothionein IIa gene promoters and was initially considered as a unique transcription

factor without any homology to other transcriptional regulators. A second homologous gene, AP-2 β , was identified in 1995 and subsequently two further genes, AP-2 γ and AP-2 δ , were cloned. AP-2 proteins consists of an N-terminal proline- and glutamine-rich transactivation domain, followed by a positively charged α -helical DNA binding region and a helix-span-helix motif, which mediates homo- and heterodimerization of AP-2 proteins.

In this paper, we describe the identification of a fifth, previously unknown AP-2 gene, AP-2 ϵ . AP-2 ϵ consists of 434 amino acids with an almost identical C-terminal DNA-binding and dimerization domain compared to the other AP-2 family members. Although the N-terminal localized activation domain is less homologous, the position and identity of certain amino acids known to be essential for transcriptional transactivation are conserved. Reverse transcriptase-polymerase chain reaction analyses from total RNA of murine embryos revealed AP-2 ϵ expression from embryonic day E7.until birth. Whole-mount *in situ* hybridizations with a specific AP-2 ϵ cDNA fragment on mouse embryos demonstrated that AP-2 ϵ expression is mainly restricted to neural tissue, particularly to the midbrain, hindbrain, and olfactory bulb. This expression pattern was confirmed by immunohistochemical stainings with an AP-2 ϵ -specific antiserum. Furthermore, AP-2 ϵ is specifically expressed in a hypothalamic nucleus and the neuroepithelium of the vomeronasal organ suggesting that AP-2 ϵ may play an important role during the development of the olfactory system.

7.4 Manuscript I: Comparative expression analysis of the murine palladin isoforms

Palladin is a recently identified phosphoprotein and colocalizes to actin-based structures such as stress fibers, cell-cell junctions, embryonic Z-lines and FAs. Multiple palladin isoforms exist due to different promoter usage and alternative splicing giving

rise to at least three major products: a 200kDa isoform, a 140kDa isoform and a doublet of 90-92 kDa.

In this manuscript, we describe the expression of the different palladin isoforms during mouse development and adult tissues by RT-PCR and *in situ* hybridizations. The 200kDa isoform is predominantly expressed in developing heart and skeletal muscle and remains the dominant isoform in both tissues after birth. The 140kDa isoform is expressed in various tissues and represents the major isoform of the brain. The 90-92 kDa isoforms are almost ubiquitously expressed with highest levels in smooth muscle rich tissues. We generated a specific antiserum against the 200kDa isoform which localizes it to the Z-discs of cardiac and skeletal muscle cells. Interestingly, the expression of this isoform increases during *in vitro* differentiation and fusion of C2C12 myoblasts, which is concordant with the expression of this isoform in more differentiated myoblasts *in vivo*. Therefore our data suggest that the large palladin isoform is an important molecular scaffold during sarcomeric organization.

7.5 Manuscript II: Characterization of striated muscle specific palladin 200kDa isoform and double myotilin/200kDa palladin deficient mice (manuscript in preparation)

Palladin, Myopalladin and Myotilin form a small subfamily of cytoskeletal proteins that contain Ig (immunoglobulin) domains. They all bind actin and actin-associated proteins and are thought to play important roles in actin cytoskeleton organization. Myotilin and myopalladin are predominantly expressed in cardiac and skeletal muscle, whereas palladin displays a ubiquitous expression pattern in vertebrate tissues. We could recently show that the 200 kDa palladin isoform, one of the palladin's multiple isoforms, is mainly expressed in heart and skeletal muscle and might play a role in the organization of the sarcomere.

Brief summaries of the publications

Missense mutations in the human myotilin gene cause muscle disorders, like dominant limb girdle muscular dystrophy type 1A causing a myofibrillar myopathy. Surprisingly, inactivation of myotilin in mice had no consequences on muscle integrity suggesting that palladin or myopalladin functionally compensate for the absence of myotilin in these animals.

In this paper, we describe the generation of a palladin mouse mutant that lacks specifically the 200kDa isoform. These mice develop a mild cardiomyopathy with ultrastructural modification of the cardiac myofibrils. In contrast, skeletal muscles do not show this phenotype.

In order to address the question whether palladin and myotilin can functionally compensate each other, we generated palladin 200kDa isoform/myotilin double knockout mice. Double knockout animals show the same cardiac ultrastructural alterations like in palladin single knockout mice. Interestingly, double mutants develop a skeletal muscle phenotype consisting of late-onset skeletal muscle myofibrillar disorganization. Grip force tests confirmed that only the double knockout mice show a significant decrease in muscle force. These data suggest that the 200kDa palladin isoform and myotilin can compensate for each other in skeletal muscle and that the absence of both causes a skeletal muscle architectural and contractile phenotype. In contrast to that, myotilin does not seem to play a crucial role in the organization of cardiac myofibrils.

8 Acknowledgements

First of all, I would like to express my deepest gratitude to Prof. Dr. Reinhard Fässler for giving me the opportunity to study the extremely interesting subject in his laboratory. I would like to thank him for the encouragement and the continual support throughout the entire period of my study.

I would like to thank PD Dr. Stefan Weiss for his kindly help for being the co-referee of my thesis committee and also thank to Prof. Dr. Martin Biel, Prof. Dr. Karl-Peter Hopfner, Prof. Dr. Angelika Vollmar and Prof. Dr. Christian Wahl-Schott for being the members of my thesis committee.

Uncountable thanks go to Dr. Markus Moser for his invaluable advice and constant support. I also have to thank Prof. Dr. Ulrike Mayer, Prof. Dr. Wilhelm Bloch, Prof. Dr. Olli Carpén, PD Dr. Klara Brixius and Dr. Monica Moza for the fruitful and exciting collaboration.

I thank the current and the former members in the department of Molecular Medicine for providing accommodative environment to a foreigner like me and many helps. In particular, I would like to Anika, Claudia, Daniel, Eloi, Fabio, Ingo, Martina, Ralph, Sara, Siegfried and Tina for generously sharing their specialty opinions and many insightful discussions. Their friendships and the good working atmosphere became the main basis for the success of this work.

I thank Dr. Walter Göhring and Sylvia Zehner for providing all the helps in the laboratory.

The deepest thanks go to my wife, Ling-Wei Chang, not only for her enormous support and patience, but also beneficial discussions with her. The same deep thanks belong to my parents and my family in Taiwan for their understanding and support.

9 Curriculum Vitae

Hao-Ven Wang

ADDRESS

Am Kirchplatz 6a, D-82152 Martinsried

DATE AND PLACE OF BIRTH

24. April.1972, Hsin-Chu, Taiwan

EDUCATION

08/2002 – present	Max Planck Institute of Biochemistry	Munich, Germany
	Ph.D. student in the Department of Molecular Medicine headed by Prof. Dr. Reinhard Fässler	
08/1994 – 01/1997	National Taiwan University Institute of Botany	Taipei, Taiwan
	Master thesis in the group of Prof. Dr. Tsong-Teh Kuo in the Institute of Molecular Biology, Academia Sinica “Characterization of non-pathogenesis mutant of <i>Xanthomonas campestris</i> pv. <i>citri</i> induced by transposon, Tn5 <i>tac1</i> ”	
08/1990 – 06/1994	National Cheng Kung University Department of Biology	Tainan Taiwan
09/1987 – 06/1990	Provincial Hsin-Chu Senior High School	Hsin-Chu Taiwan

PROFESSIONAL AND WORKING EXPERIENCE

08/2002 – present	Max Planck Institute of Biochemistry	Munich, Germany
	Ph.D. student in the Department of Molecular Medicine headed by Prof. Dr. Reinhard Fässler	
05/2001 – 07/2002	National Taiwan University Hospital, Dep. Of Obstetrics and Gynecology	Taipei Taiwan
	Research Assistant in the lab. of Prof.Dr. Hong-Nerg Ho “Study on the relationship between Nitric Oxide Synthase and Sex Steroid System on Endometriosis”	
07/1999 – 08/2000	Academia Sinica Institute of Biochemistry	Taipei Taiwan
	Research Assistant in the lab of Dr. Shu-Mei Liang and Dr. Chi-Ming Liang “Purification and Proliferation Assay of a Protein, Pneumolysin”	

Curriculum Vitae

07/1997 – 06/1999	Ministry of Defence	Taipei Taiwan
02/1997 – 06/1997	Second Lieutenant in the Air Force Academia Sinica Institute of Molecular Biology	Taipei Taiwan
09/1994 – 01/1997	Research Assistant in the lab of Prof. Dr. Jenn Tu and Prof. Dr. Tsong-Teh Kuo “Promoter analysis of <i>Xanthomonas campestris</i> pv. <i>citri</i> ”	Taipei Taiwan
09/1994 – 06/1996	Part-time Research Assistant National Taiwan University Institute of Botany Teaching Instructor	Taipei Taiwan

10 References

- Adair, B. D., J. P. Xiong, C. Maddock, S. L. Goodman, M. A. Arnaout, and M. Yeager. 2005. Three-dimensional EM structure of the ectodomain of integrin α V β 3 in a complex with fibronectin. *J. Cell Biol.* 168: 1109-1118.
- Ashton, G. H., W. H. McLean, A. P. South, N. Oyama, F. J. Smith, R. Al-Suwaid, A. Al-Ismaily, D. J. Atherton, C. A. Harwood, I. M. Leigh, C. Moss, B. Didona, G. Zambruno, A. Patrizi, R. A. Eady, and J. A. McGrath. 2004. Recurrent mutations in kindlin-1, a novel keratinocyte focal contact protein, in the autosomal recessive skin fragility and photosensitivity disorder, Kindler syndrome. *J. Invest. Dermatol.* 122: 78–83.
- Attwell, S., C. Roskelley, and S. Dedhar. 2000. The integrin-linked kinase (ILK) suppresses anoikis. *Oncogene* 19: 3811-3815.
- Bang, M. L., R. E. Mudry, A. S. McElhinny, K. Trombitás, A. J. Geach, R. Yamasaki, H. Sorimachi, H. Granzier, C.C. Gregorio, and S. Labeit. 2001. Myopalladin, a novel 145-kilodalton sarcomeric protein with multiple roles in Z-disc and I-band protein assemblies. *J. Cell Biol.* 153: 413-427.
- Belkin, A. M., N. I. Zhidkova, F. Balzac, F. Altruda, D. Tomatis, A. Maier, G. Tarone, V. E. Kotliansky, and K. Burridge. 1996. β 1D integrin displaces the β 1A isoform in striated muscles: localization at junctional structures and signaling potential in nonmuscle cells. *J. Cell Biol.* 132: 211-226.
- Bendig, G., M. Grimmer, I. G. Huttner, G. Wessels, T. Dahme, S. Just, N. Trano, H. A. Katus, M. C. Fishman, and W. Rottbauer. 2006. Integrin-linked kinase, a novel component of the cardiac mechanical stretch sensor, controls contractility in the zebrafish heart. *Genes Dev.* 20: 2361-2372.
- Blaschuk, K. L., and P. C. Holland. 1994. The regulation of alpha 5 beta 1 integrin expression in human muscle cells. *Dev. Biol.* 164: 475-483.
- Blaschuk, K. L., C. Guérin, and P. C. Holland. 1997. Myoblast alpha v beta3 integrin levels are controlled by transcriptional regulation of expression of the beta3 subunit and down-regulation of beta3 subunit expression is required for skeletal muscle cell differentiation. *Dev. Biol.* 184: 266-277.

References

- Bodine, S. C., T. N. Stitt, M. Gonzalez, W. O. Kline, G. L. Stover, R. Bauerlein, E. Zlotchenko, A. Scrimgeour, J. C. Lawrence, D. J. Glass, and G. D. Yancopoulos. 2001. Akt/mTOR pathway is a crucial regulator of skeletal muscle hypertrophy and can prevent muscle atrophy in vivo. *Nat. Cell. Biol.* 3: 1014-1019.
- Boettiger, D., M. Enomoto-Iwamoto, H. Y. Yoon, U. Hofer, A. S. Menko, and R. Chiquet-Ehrismann. 1995. Regulation of integrin alpha 5 beta 1 affinity during myogenic differentiation. *Dev. Biol.* 169: 261-272.
- Boukhelifa, M., M. M. Parast, J. G. Valtschanoff, A. S. LaMantia, R. B. Meeker, and C. A. Otey. 2001. A role for the cytoskeleton-associated protein palladin in neurite outgrowth. *Mol. Biol. Cell.* 12: 2721-2729.
- Boukhelifa, M., S. J. Hwang, J. G. Valtschanoff, R. B. Meeker, A. Rustioni, and C. A. Otey. 2003. A critical role for palladin in astrocyte morphology and response to injury. *Mol. Cell. Neurosci.* 23: 661-668.
- Boukhelifa, M., M. M. Parast, J. E. Bear, F. B. Gertler, and C. A. Otey. 2004. Palladin is a novel binding partner for Ena/VASP family members. *Cell Motil. Cytoskeleton.* 58: 17-29.
- Boukhelifa, M., M. Moza, T. Johansson, A. Rachlin, M. Parast, S. Huttelmaier, P. Roy, B. M. Jockusch, O. Carpen, R. Karlsson, and C.A. Otey. 2006. The proline-rich protein palladin is a binding partner for profilin. *FEBS J.* 273: 26-33.
- Bouvard, D., C. Brakebusch, E. Gustafsson, A. Aszodi, T. Bengtsson, A. Berna, and R. Fässler. 2001. Functional consequences of integrin gene mutations in mice. *Circ. Res.* 89: 211-223.
- Brakebusch, C., D. Bouvard, F. Stanchi, T. Sakai, and R. Fässler. 2002. Integrins in invasive growth. *J. Clin. Invest.* 109: 999-1006.
- Brakebusch, C., and R. Fässler. 2003. The integrin-actin connection, an eternal love affair. *EMBO J.* 22: 2324-2333.
- Braun, A., R. Bordoy, F. Stanchi, M. Moser, G. G. Kostka, E. Ehler, O. Brandau, and R. Fässler. 2003. PINCH2 is a new five LIM domain protein, homologous to PINCH and localized to focal adhesions. *Exp. Cell Res.* 284: 239-250.
- Bronner-Fraser, M., M. Artinger, J. Muschler, and A. F. Horwitz. 1992. Developmentally regulated expression of alpha 6 integrin in avian embryos. *Development.* 115: 197-211.

References

- Calderwood, D. A., B. Yan, J. M. de Pereda, B. G. Alvarez, Y. Fujioka, R. C. Liddington, and M. H. Ginsberg. 2002. The phosphotyrosine binding-like domain of talin activates integrins. *J. Biol. Chem.* 277: 21749–21758.
- Calderwood, D.A. 2004. Talin controls integrin activation. *Biochem. Soc. Trans.* 32: 434-437.
- Campbell, I. D., and M. H. Ginsberg. 2004. The talin-tail interaction places integrin activation on FERM ground. *Trends Biochem. Sci.* 29: 429-435.
- Carman, C. V., and T. A. Springer. 2003. Integrin avidity regulation: are changes in affinity and conformation underemphasized? *Curr. Opin. Cell Biol.* 15: 547-556.
- Chishti, A. H., A. C. Kim, S. M. Marfatia, M. Lutchman, M. Hanspal, H. Jindal, S. C. Liu, P. S. Low, G. A. Rouleau, N. Mohandas, J. A. Chasis, J. G. Conboy, P. Gascard, Y. Takakuwa, S. C. Huang, E. J. Benz Jr., A. Bretscher, R.G. Fehon, J. F. Gusella, V. Ramesh, F. Solomon, V. T. Marchesi, S. Tsukita, S. Tsukita, M. Arpin, D. Louvard, N. K. Tonks, J. M. Anderson, A. S. Fanning, P. J. Bryant, D. F. Woods, and K. B. Hoover. 1998. The FERM domain: a unique module involved in the linkage of cytoplasmic proteins to the membrane. *Trends Biochem. Sci.* 23: 281–282.
- Chu, H., I. Thievessen, M. Sixt, T. Lammermann, A. Waisman, A. Braun, A. A. Noegel, and R. Fässler. 2006. γ -Parvin is dispensable for hematopoiesis, leukocyte trafficking, and T-cell-dependent antibody response. *Mol. Cell. Biol.* 26: 1817-1825.
- Condorelli, G., A. Drusco, G. Stassi, A. Bellacosa, R. Roncarati, G. Iaccarino, M. A. Russo, Y. Gu, N. Dalton, C. Chung, M. V. Latronico, C. Napoli, J. Sadoshima, C. M. Croce, and J. Ross. Jr. 2002. Akt induces enhanced myocardial contractility and cell size *in vivo* in transgenic mice. *Proc. Natl. Acad. Sci. USA.* 99: 12333-12338.
- Danen, E. H., and A. Sonnenberg. 2003. Integrins in regulation of tissue development and function. *J. Pathol.* 200: 471-480.
- DeBosch, B., I. Treskov, T.S. Lupu, C. Weinheimer, A. Kovacs, M. Courtois, and A.J. Muslin. 2006. Akt1 is required for physiological cardiac growth. *Circulation* 113: 2097-2104.
- Delcommenne, M., C. Tan, V. Gray, L. Rue, J. Woodgett, and S. Dedhar. 1998. Phosphoinositide-3-OH kinase-dependent regulation of glycogen synthase kinase 3 and protein kinase B/AKT by the integrin-linked kinase. *Proc. Natl. Acad. Sci. USA.* 95: 11211-11216.

References

- Deng, J. T., J. E. Van Lierop, C. Sutherland, and M. P. Walsh. 2001. Ca²⁺-independent smooth muscle contraction. A novel function for integrin-linked kinase. *J. Biol. Chem.* 276: 16365-16373.
- Deng, J. T., C. Sutherland, D. L. Brautigan, M. Eto, and M. P. Walsh. 2002. Phosphorylation of the myosin phosphatase inhibitors, CPI-17 and PHI-1, by integrin-linked kinase. *Biochem. J.* 367: 517-524.
- Di, Paolo G., L. Pellegrini, K. Letinic, G. Cestra, R. Zoncu, S. Voronov, S. Chang, J. Guo, M. R. Wenk, and P. De Camilli. 2002. Recruitment and regulation of phosphatidylinositol phosphate kinase type 1 gamma by the FERM domain of talin. *Nature.* 420: 85-89.
- Dixon, R.D.S., D.K. Arneman, A.S. Rachlin, N. Sundaresan, M. Joseph Costello, S.L. Campbell, and C.A. Otey. 2008. Palladin is an actin crosslinking protein that uses immunoglobulin-like domains to bind filamentous actin. *J. Biol. Chem.* In press.
- Doberstein, S. K., R. D. Fetter, A. Y. Mehta, and C. S. Goodman. 1997. Genetic analysis of myoblast fusion: blown fuse is required for progression beyond the prefusion complex. *J. Cell Biol.* 136: 1249-1261.
- Dowling, J. J., Q. C. Yu, and E. Fuchs. 1996. Beta4 integrin is required for hemidesmosome formation, cell adhesion and cell survival. *J. Cell Biol.* 134: 559-572.
- Dowling, J. J., E. Gibbs, M. Russell, D. Goldman, J. Minarcik, J. A. Golden, and E. L. Feldman. 2008. Kindlin-2 Is an Essential Component of Intercalated Discs and Is Required for Vertebrate Cardiac Structure and Function. *Circ. Res.* In press.
- Duxson, M., Y. Usson, and A. Harris. 1989. The origin of secondary myotubes in mammalian skeletal muscles: ultrastructural studies. *Development* 107: 743-750.
- Endlich, N., C. A. Otey, W. Kriz, and K. Endlich. 2007. Movement of stress fibers away from focal adhesions identifies focal adhesions as sites of stress fiber assembly in stationary cells. *Cell. Motil. Cytoskeleton.* 64: 966-976.
- Evans, D., H. Baillie, A. Caswell, and P. Wigmore. 1994. During fetal muscle development, clones of cells contribute to both primary and secondary fibers. *Dev. Biol.* 162: 348-353.
- Frias, M. A., C. C. Thoreen, J. D. Jaffe, W. Schroder, T. Sculley, S. A. Carr, and D. M. Sabatini. 2006. mSin1 is necessary for Akt/PKB phosphorylation, and its isoforms define three distinct mTORC2s. *Curr. Biol.* 16: 1865-1870.

References

- Friedrich, E. B., S. Sinha, L. Li, S. Dedhar, and T. Force, A. Rosenzweig and R. E. Gerszten. 2002. Role of integrin-linked kinase in leukocyte recruitment. *J. Biol. Chem.* 277: 16371-16375.
- Friedrich, E. B., E. Liu, S. Sinha, S. Cook, D. S. Milstone, C. A. MacRae, M. Mariotti, P. J. Kuhlencordt, T. Force, A. Rosenzweig, R. St-Arnaud, S. Dedhar, and R. E. Gerszten. 2004. Integrin-linked kinase regulates endothelial cell survival and vascular development. *Mol. Cell Biol.* 24: 8134-8144.
- Garcia-Alvarez, B., J. M. de Pereda, D. A. Calderwood, T. S. Ulmer, D. Critchley, I. D. Campbell, M. H. Ginsberg, and R. C. Liddington. 2003. Structural determinants of integrin recognition by talin. *Mol. Cell.* 11: 49–58.
- Gary, D. S., O. Milhavet, S. Camandola, and M. P. Mattson. 2003. Essential role for integrin linked kinase in Akt-mediated integrin survival signaling in hippocampal neurons. *J. Neurochem.* 84: 878-890.
- Gilmore, A. P., and K. Burridge. 1996. Regulation of vinculin binding to talin and actin by phosphatidyl-inositol-4-5-bisphosphate. *Nature.* 381: 531-535.
- Ginsberg, M. H., B. Yaspan, J. Forsyth, T. S. Ulmer, I. D. Campbell, and M. Slepak. 2001. A membrane-distal segment of the integrin alpha IIb cytoplasmic domain regulates integrin activation. *J. Biol. Chem.* 276: 22514-22521.
- Gkretsi, V., Y. Zhang, Y. Tu, K. Chen, D.B. Stolz, Y. Yang, S.C. Watkins, and C. Wu. 2005. Physical and functional association of migfilin with cell–cell adhesions. *J. Cell Sci.* 118: 697–710.
- Gkretsi, V., W. M. Mars, W. C. Bowen, L. Barua, Y. Yang, L. Guo, R. St-Arnaud, S. Dedhar, C. Wu, and G. K. Michalopoulos. 2007. Loss of integrin linked kinase from mouse hepatocytes in vitro and in vivo results in apoptosis and hepatitis. *Hepatology.* 45: 1025-1034.
- Glass, D. J. 2003. Signalling pathways that mediate skeletal muscle hypertrophy and atrophy. *Nat. Cell Biol.* 5: 87-90.
- Goicoechea, S., D. Arneman, A. Disanza, R. Garcia-Mata, G. Scita, and C.A. Otey. 2006. Palladin binds to Eps8 and enhances the formation of dorsal ruffles and podosomes in vascular smooth muscle cells. *J. Cell Sci.* 119: 3316-3324.

References

- Goel, H. L., M. Fornaro, L. Moro, N. Teider, J. S. Rhim, M. King, and L. R. Languino. 2004. Selective modulation of type 1 insulin-like growth factor receptor signaling and functions by beta1 integrins. *J. Cell Biol.* 166: 407-418.
- Goel, H. L., L. Moro, M. King, N. Teider, M. Centrella, T. L. McCarthy, M. Holgado-Madruga, A. J. Wong, E. Marra, and L. R. Languino. 2006. Beta1 integrins modulate cell adhesion by regulating insulin-like growth factor-II levels in the microenvironment. *Cancer Res.* 66: 331-342.
- Grashoff, C., A. Aszodi, T. Sakai, E. B. Hunziker, and R. Fässler. 2003. Integrin-linked kinase regulates chondrocyte shape and proliferation. *EMBO Rep.* 4: 432-438.
- Grashoff, C., I. Thievensen, K. Lorenz, S. Ussar, and R. Fässler. 2004. Integrin-linked kinase: integrin's mysterious partner. *Curr. Opin. Cell. Biol.* 16: 565-571.
- Gullberg, D., T. Velling, L. Lohikangas, and C. F. Tiger. 1998. Integrins during muscle development and in muscular dystrophies. *Front Biosci.* 3: D1039-1050.
- Guo, C., M. Willem, A. Werner, G. Raivich, M. Emerson, L. Neyses, and U. Mayer. 2006. Absence of $\alpha 7$ integrin in dystrophin-deficient mice causes a myopathy similar to Duchenne muscular dystrophy. *Hum. Mol. Genet.* 15: 989-98.
- Fässler, R., and M. Meyer. 1995. Consequences of lack of beta 1 integrin gene expression in mice. *Genes Dev.* 9: 1896-1908.
- Hemmings, L., D. J. Rees, V. Ohanian, S. J. Bolton, A. P. Gilmore, B. Patel, H. Priddle, J. E. Trevithick, R. O. Hynes, and D. R. Critchley. 1996. Talin contains three actin-binding sites each of which is adjacent to a vinculin-binding site. *J. Cell Sci.* 109: 2715-2726.
- Hanks, S. K. 2003. Genomic analysis of the eukaryotic kinase superfamily: a perspective. *Genome Biol.* 4: 111.
- Hannigan, G. E., C. Leung-Hagesteijn, L. Fitz-Gibbon, M. G. Coppelino, G. Radeva, J. Filmus, J. C. Bell, and S. Dedhar. 1996. Regulation of cell adhesion and anchorage-dependent growth by a new beta 1-integrin-linked protein kinase. *Nature* 379: 91-96.
- Henry, M. D., and K. P. Campbell. 1998. A role for dystroglycan in basement membrane assembly. *Cell.* 95: 859-870.
- Henry, M. D., and K. P. Campbell. 1999. Dystroglycan inside and out. *Curr. Opin. Cell Biol.* 11: 602-607.

References

- Hentzen, E. R., M. Lahey, D. Peters, L. Mathew, I. A. Barash, J. Fridén, and R. L. Lieber. 2006. Stress-dependent and -independent expression of the myogenic regulatory factors and the MARP genes after eccentric contractions in rats. *J. Physiol.* 570: 157-167.
- Hirsch, E., L. Lohikangas, D. Gullberg, S. Johansson, and R. Fässler. 1998. Mouse myoblasts can fuse and form a normal sarcomere in the absence of $\beta 1$ integrin expression. *J. Cell Sci.* 111: 2397-2409.
- Horne, B. D., J. F. Carlquist, J. B. Muhlestein, Z. P. Nicholas, and J. L. Anderson. 2007. Associations with myocardial infarction of six polymorphisms selected from a three-stage genome-wide association study. *Am. Heart. J.* 154: 969-975.
- Hoffman, E. P., and G. A. Nader. 2004. Balancing muscle hypertrophy and atrophy. *Nat. Med.* 10: 584-585.
- Huang, Y., J. Li, Y. Zhang, and C. Wu. 2000. The roles of integrin-linked kinase in the regulation of myogenic differentiation. *J. Cell Biol.* 150: 861-872.
- Humphries, M. J., P. A. McEwan, S. J. Barton, P. A. Buckley, J. Bella, and A. P. Mould. 2003. Integrin structure: heady advances in ligand binding, but activation still makes the knees wobble. *Trends Biochem. Sci.* 28: 313-320.
- Hüttelmaier, S., O. Mayboroda, B. Harbeck, T. Jarchau, B. M. Jockusch, and M. Rüdiger. 1998. The interaction of the cell-contact proteins VASP and vinculin is regulated by phosphatidylinositol-4,5-bisphosphate. *Curr. Biol.* 8: 479-488.
- Hwang, S. J., S. Pagliardini, M. Boukhelifa, M. M. Parast, C. A. Otey, A. Rustioni, and J.G. Valtschanoff. 2001. Palladin is expressed preferentially in excitatory terminals in the rat central nervous system. *J. Comp. Neurol.* 436: 211-224.
- Hynes, R. O., and Q. Zhao. 2000. The evolution of cell adhesion. *J. Cell Biol.* 150: 89-96.
- Hynes, RO., 2002. Integrins: bidirectional, allosteric signaling machines. *Cell* 110: 673-687.
- Janji, B., C. Melchior, L. Vallar, and N. Kieffer. 1000. Cloning of an isoform of integrin-linked kinase (ILK) that is upregulated in HT-144 melanoma cells following TGF-beta1 stimulation. *Oncogene.* 19: 3069-3077.
- Jin, L., M. J. Kern, C. A. Otey, B. R. Wamhoff, and A. V. Somlyo. 2007. Angiotensin II, focal adhesion kinase, and PRX1 enhance smooth muscle expression of lipoma preferred partner (LPP) and its newly identified binding partner palladin to promote cell migration. *Circ. Res.* 100: 817-825.

References

- Jobard, F., B. Bouadjar, F. Caux, S. Hadj-Rabia, C. Has, F. Matsuda, J. Weissenbach, M. Lathrop, J. F. Prud'homme, and J. Fischer. 2003. Identification of mutations in a new gene encoding a FERM family protein with a pleckstrin homology domain in Kindler syndrome. *Hum. Mol. Genet.* 12: 925–935.
- Kato, K., T. Shiozawa, J. Mitsushita, A. Toda, A. Horiuchi, T. Nikaido, S. Fujii, and I. Konishi. 2004. Expression of the mitogen-inducible gene-2 (mig-2) is elevated in human uterine leiomyomas but not in leiomyosarcomas. *Hum. Pathol.* 35: 55–60.
- Kindler, T. 1954. Congenital poikiloderma with traumatic bulla formation and progressive cutaneous atrophy. *Br. J. Dermatol.* 66: 104–111.
- Kiss, E., A. Muranyi, C. Csontos, P. Gergely, M. Ito, D. J. Hartshorne, and F. Erdodi. 2002. Integrin-linked kinase phosphorylates the myosin phosphatase target subunit at the inhibitory site in platelet cytoskeleton. *Biochem. J.* 365: 79–87.
- Kloeker, S., M.B. Major, D.A. Calderwood, M.H. Ginsberg, D.A. Jones, and M.C. Beckerle. 2004. The Kindler syndrome protein is regulated by transforming growth factor-beta and involved in integrin-mediated adhesion. *J. Biol. Chem.* 279: 6824–6833.
- Legate, K. R., E. Montanez, O. Kudlacek, and R. Fässler. 2006. ILK, PINCH and parvin: the tIPP of integrin signalling. *Nat. Rev. Mol. Cell Biol.* 7: 20–31.
- Lemmon, M. A., and K. M. Ferguson. 2000. Signal-dependent membrane targeting by pleckstrin homology (PH) domains. *Biochem. J.* 350: 1–18.
- Leung-Hagesteijn, C., A. Mahendra, I. Naruszewicz, and G. E. Hannigan. 2001. Modulation of integrin signal transduction by ILKAP, a protein phosphatase 2C associating with the integrin-linked kinase, ILK1. *EMBO J.* 20: 2160–2170.
- Liang, W., H. Yang, X. Xue, Q. Huang, M. Bartlam, and S. Chen. 2006. Expression, crystallization and preliminary X-ray studies of the immunoglobulin-like domain 3 of human palladin. *Acta Crystallogr. Sect. F Struct. Biol. Cryst. Commun.* 62: 556–558.
- Liddington, R. C., and M. H. Ginsberg. 2002. Integrin activation takes shape. *J. Cell Biol.* 158: 833–839.
- Linder, S. and M. Aepfelbacher. 2003. Podosomes: adhesion hot-spots of invasive cells. *Trends Cell Biol.* 13: 376–385.
- Linder, S. and P. Kopp. 2005. Podosomes at a glance. *J. Cell Sci.* 118: 2079–2082.

References

- Ling, K., R. L. Doughman, A. J. Firestone, M. W. Bunce, and R. A. Anderson. 2002. Type I gamma phosphatidylinositol phosphate kinase targets and regulates focal adhesions. *Nature*. 420: 89-93.
- Liu, S., D. A. Calderwood, and M. H. Ginsberg. 2000. Integrin cytoplasmic domain-binding proteins. *J. Cell Sci.* 113: 3563-3571.
- Liu, X.S., H.J. Luo, H. Yang, L. Wang, H. Kong, Y.E. Jin, F. Wang, M.M. Gu, Z. Chen, Z.Y. Lu, and Z.G. Wang. 2007a. Palladin regulates cell and extracellular matrix interaction through maintaining normal actin cytoskeleton architecture and stabilizing beta1-integrin. *J. Cell. Biochem.* 100: 1288-1300.
- Liu, X.S., X.H. Li, Y. Wang, R.Z. Shu, L. Wang, S.Y. Lu, H. Kong, Y.E. Jin, L.J. Zhang, J. Fei, S.J. Chen, Z. Chen, M.M. Gu, Z.Y. Lu, and Z.G. Wang. 2007b. Disruption of palladin leads to defects in definitive erythropoiesis by interfering with erythroblastic island formation in mouse fetal liver. *Blood* 110: 870-876.
- Lorenz, K., C. Grashoff, R. Torka, T. Sakai, L. Langbein, W. Bloch, M. Aumailley, and R. Fässler. 2007. Integrin-linked kinase is required for epidermal and hair follicle morphogenesis. *J. Cell Biol.* 177: 501-513.
- Lotem, M., M. Raben, R. Zeltser, M. Landau, M. Sela, M. Wygoda, and Z.A. Tochner. 2001. Kindler syndrome complicated by squamous cell carcinoma of the hard palate: successful treatment with high-dose radiation therapy and granulocyte-macrophage colony-stimulating factor. *Br. J. Dermatol.* 144: 1284-1286.
- Luo, H., X. Liu, F. Wang, Q. Huang, S. Shen, L. Wang, G. Xu, X. Sun, H. Kong, M. Gu, S. Chen, Z. Chen, and Z. Wang. 2005. Disruption of palladin results in neural tube closure defects in mice. *Mol. Cell. Neurosci.* 29: 507-515.
- Lynch, H.T., R.M. Fusaro, J.F. Lynch, and R. Brand. 2008. Pancreatic cancer and the FAMMM syndrome. *Fam. Cancer.* 7: 103-112.
- Mackinnon, A.C., H. Qadota, K.R. Norman, D.G. Moerman, and B.D. Williams. 2002. C. elegans PAT-4/ILK functions as an adaptor protein within integrin adhesion complexes. *Curr. Biol.* 12: 787-797.
- Mayer, U., G. Saher, R. Fässler, A. Bornemann, F. Echtermeyer, H. von der Mark, N. Miosge, E. Poschl, and K. von der Mark. 1997. Absence of integrin $\alpha 7$ causes a novel form of muscular dystrophy. *Nat. Genet.* 17: 318-323.

References

- Mayer, U. 2003. Integrins: redundant or important players in skeletal muscle? *J. Biol. Chem.* 278: 14587-14590.
- Menko, A. S., and D. Boettiger. 1987. Occupation of the extracellular matrix receptor, integrin, is a control point for myogenic differentiation. *Cell* 51: 51-57.
- Michele, D. E., and K. P. Campbell 2003. Dystrophin-glycoprotein complex: post-translational processing and dystroglycan function. *J. Biol. Chem.* 278: 15457-15460.
- Miller, M. G., I. Naruszewicz, A. S. Kumar, T. Ramlal, and G. E. Hannigan. 2003a. Integrin-linked kinase is a positive mediator of L6 myoblast differentiation. *Biochem. Biophys. Res. Commun.* 310: 796-803.
- Miller, M. K., M. L. Bang, C. C. Witt, D. Labeit, C. Trombitas, K. Watanabe, H. Granzier, A. S. McElhinny, C. C. Gregorio, and S. Labeit. 2003b. The muscle ankyrin repeat proteins: CARP, ankrd2/Arpp and DARP as a family of titin filament-based stress response molecules. *J. Mol. Biol.* 333: 951-964.
- Miosge, N., C. Klenczar, R. Herken, M. Willem, and U. Mayer. 1999. Organization of the myotendinous junction is dependent on the presence of $\alpha7\beta1$ integrin. *Lab. Invest.* 79: 1591-1599.
- Moser, M., B. Nieswandt, S. Ussar, M. Pozgajova, and R. Fässler. 2008. Kindlin-3 is essential for integrin activation and platelet aggregation. *Nat. Med.* In press.
- Moza, M., L. Mologni, R. Trokovic, G. Faulkner, J. Partanen, and O. Carpén. 2007. Targeted deletion of the muscular dystrophy gene myotilin does not perturb muscle structure or function in mice. *Mol. Cell. Biol.* 27: 244-252.
- Mourkioti, F., and N. Rosenthal. 2005. IGF-1, inflammation and stem cells. Interactions during muscle regeneration. *Trends Immunol.* 26: 535-542.
- Musaro, A., K. McCullagh, A. Paul, L. Houghton, G. Dobrowolny, M. Molinaro, E.R. Barton, H.L. Sweeney, and N. Rosenthal. 2001. Localized Igf-1 transgene expression sustains hypertrophy and regeneration in senescent skeletal muscle. *Nat. Genet.* 27: 195-200.
- Mykkänen, O. M., M. Grönholm, M. Rönty, M. Lalowski, P. Salmikangas, H. Suila, and O. Carpén. 2001. Characterization of human palladin, a microfilament-associated protein. *Mol. Biol. Cell.* 12: 3060-3073.

References

- Nawrotzki, R., M. Willem, N. Miosge, H. Brinkmeier, and U. Mayer. 2003. Defective integrin switch and matrix composition at $\alpha 7$ -deficient myotendinous junctions precede the onset of muscular dystrophy in mice. *Hum. Mol. Genet.* 12: 483-495.
- Nikolopoulos, S. N. and C. E. Turner. 2000. Actopaxin, a new focal adhesion protein that binds paxillin LD motifs and actin and regulates cell adhesion. *J. Cell Biol.* 151: 1435-1448.
- Nikolopoulos, S. N. and C. E. Turner. 2001. Integrin-linked kinase (ILK) binding to paxillin LD1 motif regulates ILK localization to focal adhesions. *J. Biol. Chem.* 276: 23499-23505.
- Nikolopoulos, S. N. and C. E. Turner. 2002. Molecular dissection of actopaxin-integrin-linked kinase-Paxillin interactions and their role in subcellular localization. *J. Biol. Chem.* 277: 1568-1575.
- Olski, T. M., A. A. Noegel, and E. Korenbaum. 2001. Parvin, a 42 kDa focal adhesion protein, related to the alpha-actinin superfamily. *J. Cell Sci.* 114: 525-538.
- Otey, C. A., F. M. Pavalko, and K. Burridge. 1990. An interaction between alpha-actinin and the beta 1 integrin subunit in vitro. *J. Cell Biol.* 111: 721-729.
- Otey, C. A., A. Rachlin, M. Moza, D. Arneman, and O. Carpen. 2005. The palladin/myotilin/myopalladin family of actin-associated scaffolds. *Int. Rev. Cytol.* 246: 31-58.
- O'Toole, T. E., Y. Katagiri, R. J. Faull, K. Peter, R. Tamura, V. Quaranta, J. C. Loftus, S. J. Shattil and M. H. Ginsberg. 1994. Integrin cytoplasmic domains mediate inside-out signal transduction. *J. Cell Biol.* 124: 1047-1059.
- Parast, M. M. and C.A. Otey. 2000. Characterization of palladin, a novel protein localized to stress fibers and cell adhesions. *J. Cell Biol.* 150: 643-656.
- Pasquet, J. M., M. Noury, and A. T. Nurden. 2002. Evidence that the platelet integrin alphaIIb beta3 is regulated by the integrin-linked kinase, ILK, in a PI3-kinase dependent pathway. *Thromb. Haemost.* 88: 115-122.
- Peng, X., M. S. Kraus, H. Wei, T. L. Shen, R. Pariaut, A. Alcaraz, G. Ji, L. Cheng, Q. Yang, M. I. Kotlikoff, J. Chen, K. Chien, H. Gu, and J. L. Guan. 2006. Inactivation of focal adhesion kinase in cardiomyocytes promotes eccentric cardiac hypertrophy and fibrosis in mice. *J. Clin. Invest.* 116: 217-227.
- Persad, S., S. Attwell, V. Gray, M. Delcommenne, A. Troussard, J. Sanghera, and S. Dedhar. 2000. Inhibition of integrin-linked kinase (ILK) suppresses activation of protein kinase

References

- B/Akt and induces cell cycle arrest and apoptosis of PTEN-mutant prostate cancer cells. *Proc. Natl. Acad. Sci. USA.* 97: 3207-3212.
- Persad, S., S. Attwell, V. Gray, N. Mawji, J. T. Deng, D. Leung, J. Yan, J. Sanghera, M. P. Walsh, and S. Dedhar. 2001. Regulation of protein kinase B/Akt-serine 473 phosphorylation by integrin-linked kinase: critical roles for kinase activity and amino acids arginine 211 and serine 343. *J. Biol. Chem.* 276: 27462-27469.
- Persad, S. and S. Dedhar. 2003. The role of integrin-linked kinase (ILK) in cancer progression. *Cancer Metastasis Rev.* 22: 375-384.
- Pogue-Geile, K. L., R. Chen, M. P. Bronner, T. Crnogorac-Jurcevic, K. W. Moyes, S. Downen, C. A. Otey, D. A. Crispin, R. D. George, D. C. Whitcomb, and T. A. Brentnall. 2006. Palladin mutation causes familial pancreatic cancer and suggests a new cancer mechanism. *PLoS Med.* 3: 516.
- Pownall, M. E., M. K. Gustafsson, and C. P. Emerson Jr. 2002. Myogenic regulatory factors and the specification of muscle progenitors in vertebrate embryos. *Annu. Rev. Cell Dev. Biol.* 18: 747-783.
- Quelo, I., C. Gauthier, G. E. Hannigan, S. Dedhar, and R. St-Arnaud. 2004. Integrin-linked kinase regulates the nuclear entry of the c-Jun co-activator alpha-NAC and its co-activation potency. *J. Biol. Chem.* 279: 43893-43899.
- Rachlin, A. S. and C. A. Otey. 2006. Identification of palladin isoforms and characterization of an isoform-specific interaction between Lasp-1 and palladin. *J. Cell Sci.* 119: 995-1004.
- Rando, T. A., and H. M. Blau. 1994. Primary mouse myoblast purification, characterization, and transplantation for cell-mediated gene therapy. *J. Cell Biol.* 125: 1275-1287.
- Rogalski, T. M., G. P. Mullen, M. M. Gilbert, B. D. Williams, and D. G. Moerman. 2000. The UNC-112 gene in *Caenorhabditis elegans* encodes a novel component of cell-matrix adhesion structures required for integrin localization in the muscle cell membrane. *J. Cell Biol.* 150: 253-264.
- Rönty, M., A. Taivainen, M. Moza, C. A. Otey, and O. Carpen. 2004. Molecular analysis of the interaction between palladin and alpha-actinin. *FEBS Lett.* 566: 30-34.
- Rönty, M., A. Taivainen, M. Moza, G. D. Kruh, E. Ehler, and O. Carpen. 2005. Involvement of palladin and alpha-actinin in targeting of the Abl/Arg kinase adaptor ArgBP2 to the actin cytoskeleton. *Exp. Cell Res.* 310: 88-98.

References

- Rönty, M. J., S. K. Leivonen, B. Hinz, A. Rachlin, C. A. Otey, V. M. Kähäri, and O. Carpen. 2006. Isoform-specific regulation of the actin-organizing protein palladin during TGF-beta1-induced myofibroblast differentiation. *J. Invest. Dermatol.* 126:2387-2396.
- Rönty, M., A. Taivainen, L. Heiska, C. A. Otey, E. Ehler, W. K. Song, and O. Carpen. 2007. Palladin interacts with SH3 domains of SPIN90 and Src and is required for Src-induced cytoskeletal remodeling. *Exp. Cell. Res.* 313: 257525-85
- Rooney, J. E., J. V. Welser, M. A. Dechert, N. L. Flintoff-Dye, S. J. Kaufman, and D. J. Burkin. 2006. Severe muscular dystrophy in mice that lack dystrophin and $\alpha 7$ integrin. *J. Cell Sci.* 119: 2185-2195.
- Sakai, T., S. Li, D. Docheva, C. Grashoff, K. Sakai, G. Kostka, A. Braun, A. Pfeifer, P.D. Yurchenco, and R. Fässler. 2003. Integrin-linked kinase (ILK) is required for polarizing the epiblast, cell adhesion, and controlling actin accumulation. *Genes Dev.* 17: 926-940.
- Salaria, S. N., P. Illei, R. Sharma, K. M. Walter, A. P. Klein, J. R. Eshleman, A. Maitra, R. Schulick, J. Winter, M. M. Ouellette, M. Goggins, and R. Hruban. 2007. Palladin is overexpressed in the non-neoplastic stroma of infiltrating ductal adenocarcinomas of the pancreas, but is only rarely overexpressed in neoplastic cells. *Cancer Biol. Ther.* 6: 324-328.
- Sasaki, T., C. Brakebusch, J. Engel, and R. Timpl. 1998. Mac-2 binding protein is a cell-adhesive protein of the extracellular matrix which self-assembles into ring-like structures and binds beta1 integrins, collagens and fibronectin. *EMBO J.* 17: 1606-1613.
- Sastry, S. K., M. Lakonishok, D. A. Thomas, J. Muschler, and A. F. Horwitz. 1996. Integrin alpha subunit ratios, cytoplasmic domains, and growth factor synergy regulate muscle proliferation and differentiation. *J. Cell Biol.* 133: 169-184.
- Schwander, M., M. Leu, M. Stumm, O. M. Dorchies, U. T. Rugg, J. Schittny, and U. Muller. 2003. $\beta 1$ integrins regulate myoblast fusion and sarcomere assembly. *Dev. Cell* 4: 673-685.
- Shai, S. Y., A. E. Harpf, C. J. Babbitt, M. C. Jordan, M. C. Fishbein, J. Chen, M. Omura, T. A. Leil, K. D. Becker, M. Jiang, D. J. Smith, S. R. Cherry, J. C. Loftus, and R. S. Ross. Cardiac myocyte-specific excision of the beta1 integrin gene results in myocardial fibrosis and cardiac failure. *Circ. Res.* 90: 458-464.
- Shi, X., Y. Q. Ma, Y. Tu, K. Chen, S. Wu, K. Fukuda, J. Qin, E. F. Plow, and C. Wu. 2007. The MIG-2/integrin interaction strengthens cell-matrix adhesion and modulates cell motility. *J. Biol. Chem.* 282: 20455-20466.

References

- Shiffman, D., S.G. Ellis, C.M. Rowland, M.J. Malloy, M.M. Luke, O.A. Iakoubova, C.R. Pullinger, J. Cassano, B.E. Aouizerat, R.G. Fenwick, R.E. Reitz, J.J. Catanese, D.U. Leong, C. Zellner, J.J. Sninsky, E.J. Topol, J.J. Devlin, and J.P. Kane. 2005. Identification of four gene variants associated with myocardial infarction. *Am. J. Hum. Genet.* 77: 596-605.
- Siegel, D.H., G.H. Ashton, H.G. Penagos, J.V. Lee, H.S. Feiler, K.C. Wilhelmssen, A.P. South, F.J. Smith, A.R. Prescott, V. Wessagowit, N. Oyama, M. Akiyama, D. Al Aboud, K. Al Aboud, A. Al Githami, K. Al Hawsawi, A. Al Ismaily, R. Al-Suwaid, D.J. Atherton, R. Caputo, J.D. Fine, I.J. Frieden, E. Fuchs, R.M. Haber, T. Harada, Y. Kitajima, S.B. Mallory, H. Ogawa, S. Sahin, H. Shimizu, Y. Suga, G. Tadini, K. Tsuchiya, C.B. Wiebe, F. Wojnarowska, A.B. Zaghoul, T. Hamada, R. Mallipeddi, R.A. Eady, W.H. McLean, J.A. McGrath, and E.H. Epstein. 2003. Loss of kindlin-1, a human homolog of the *Caenorhabditis elegans* actin-extracellular-matrix linker protein UNC-112, causes Kindler syndrome. *Am. J. Hum. Genet.* 73: 174-187.
- Takagi, J., B. M. Petre, T. Walz, and T. A. Springer. 2002. Global conformational rearrangements in integrin extracellular domains in outside-in and inside-out signaling. *Cell* 110: 599-511.
- Taverna, D., M.H. Disatnik, H. Rayburn, R.T. Bronson, J. Yang, T.A. Rando, and R.O. Hynes. 1998. Dystrophic muscle in mice chimeric for expression of $\alpha 5$ integrin. *J. Cell Biol.* 143: 849-59.
- Tadokoro, S., S. J. Shattil, K. Eto, V. Tai, R. C. Liddington, J. M. de Pereda, M. H. Ginsberg, and D. A. Calderwood. 2003. Talin binding to integrin beta tails: a final common step in integrin activation. *Science* 302, 103-106
- Terpstra, L., J. Prud'homme, A. Arabian, S. Takeda, G. Karsenty, S. Dedhar, and R. St-Arnaud. 2003. Reduced chondrocyte proliferation and chondrodysplasia in mice lacking the integrin-linked kinase in chondrocytes. *J. Cell Biol.* 162: 139-148.
- Tu, Y., F. Li, and C. Wu. 1998. Nck-2, a novel Src homology2/3-containing adaptor protein that interacts with the LIM-only protein PINCH and components of growth factor receptor kinase-signaling pathways. *Mol. Biol. Cell.* 9: 3367-3382.
- Tu, Y., F. Li, S. Goicoechea, and C. Wu. 1999. The LIM-only protein PINCH directly interacts with integrin-linked kinase and is recruited to integrin-rich sites in spreading cells. *Mol. Cell Biol.* 19: 2425-2434.

References

- Tu, Y., Y. Huang, Y. Zhang, Y. Hua, and C. Wu. 2001. A new focal adhesion protein that interacts with integrin-linked kinase and regulates cell adhesion and spreading. *J. Cell Biol.* 153: 585-598.
- Tu, Y., S. Wu, X. Shi, K. Chen, and C. Wu. 2003. Migfilin and Mig-2 link focal adhesions to filamin and the actin cytoskeleton and function in cell shape modulation. *Cell* 113: 37-47.
- Troussard, A. A., N. M. Mawji, C. Ong, A. Mui, R. St Arnaud and S. Dedhar S. 2003. Conditional knock-out of integrin-linked kinase demonstrates an essential role in protein kinase B/Akt activation. *J. Biol. Chem.* 278: 22374-22378.
- Ussar, S., HV Wang, S. Linder, R. Fässler, and M. Moser. 2006. The Kindlins: subcellular localization and expression during murine development. *Exp. Cell Res.* 312: 3142-51.
- van der Flier, A., A.C. Gaspar, S. Thorsteinsdottir, C. Baudoin, E. Groeneveld, C.L. Mummery, and A. Sonnenberg. 1997. Spatial and temporal expression of the beta1D integrin during mouse development. *Dev. Dyn.* 210: 472-486.
- Wegener, K. L., A. W. Partridge, J. Han, A. R. Pickford, R. C. Liddington, M. H. Ginsberg, and I. D. Campbell. 2007. Structural basis of integrin activation by talin. *Cell.* 128: 171-182.
- Weinstein, E.J., M. Bourner, R. Head, H. Zakeri, C. Bauer, and R. Mazarrella. 2003. URP1: a member of a novel family of PH and FERM domain-containing membrane-associated proteins is significantly over-expressed in lung and colon carcinomas. *Biochim. Biophys. Acta* 1637: 207-216.
- White, D.E., P. Coutu, Y.F. Shi, J.C. Tardif, S. Nattel, R. St Arnaud, S. Dedhar, and W.J. Muller. 2006. Targeted ablation of ILK from the murine heart results in dilated cardiomyopathy and spontaneous heart failure. *Genes Dev.* 20: 2355-2360.
- White, S.J. and W.H. McLean. 2005. Kindler surprise: mutations in a novel actin-associated protein cause Kindler syndrome. *J. Dermatol. Sci.* 38: 169-175.
- Wiesner, S., A. Lange, and R. Fässler. 2006. Local call: from integrins to actin assembly. *Trends Cell Biol.* 16: 327-329.
- Williams, A. F. and A. N. Barclay. 1988. The immunoglobulin superfamily--domains for cell surface recognition. *Annu. Rev. Immunol.* 6: 381-405.
- Xiong, J. P., T. Stehle, B. Diefenbach, R. Zhang, R. Dunker, D. L. Scott, A. Joachimiak, S. L. Goodman, and M. A. Arnaout. 2001. Crystal structure of the extracellular segment of integrin alphaVbeta3. *Science* 294: 339-345.

References

- Xiong, J. P., T. Stehle, R. Zhang, A. Joachimiak, M. Frech, S. L. Goodman, and M. A. Arnaout. 2002. Crystal structure of the extracellular segment of integrin alpha Vbeta3 in complex with an Arg-Gly-Asp ligand. *Science* 296: 151-155.
- Yamaji, S., A. Suzuki, Y. Sugiyama, Y. Koide, M. Yoshida, H. Kanamori, H. Mohri, S. Ohno, and Y. Ishigatsubo. 2001. A novel integrin-linked kinase-binding protein, affixin, is involved in the early stage of cell-substrate interaction. *J. Cell Biol.* 153: 1251-1264.
- Yan, B., D. A. Calderwood, B. Yaspan, and M. H. Ginsberg. 2001. Calpain cleavage promotes talin binding to the beta 3 integrin cytoplasmic domain. *J. Biol. Chem.* 276: 28164-28170.
- Yao, C. C., B. L. Ziober, A. E. Sutherland, D. L. Mendrick, and R. H. Kramer. 1996. Laminins promote the locomotion of skeletal myoblasts via the alpha 7 integrin receptor. *J. Cell Sci.* 109: 3139-3150.
- Zamir, E. and B. Geiger. 2001. Molecular complexity and dynamics of cell-matrix adhesions. *J. Cell Sci.* 114: 3583-3590.
- Zervas, C.G., S.L. Gregory, and N.H. Brown. 2001. Drosophila integrin-linked kinase is required at sites of integrin adhesion to link the cytoskeleton to the plasma membrane. *J. Cell Biol.* 152: 1007-1018.
- Zhang, Y., K. Chen, L. Guo, and C. Wu. 2002. Characterization of PINCH-2, a new focal adhesion protein that regulates the PINCH-1-ILK interaction, cell spreading, and migration. *J. Biol. Chem.* 277: 38328-38338.
- Zhidkova, N. I., A. M. Belkin, and R. Mayne. 1995. Novel isoform of beta 1 integrin expressed in skeletal and cardiac muscle. *Biochem. Biophys. Res. Commun.* 214: 279-285.
- Zogopoulos, G., H. Rothenmund, A. Eppel, C. Ash, M.R. Akbari, D. Hedley, S.A. Narod, and S. Gallinger. 2007. The P239S palladin variant does not account for a significant fraction of hereditary or early onset pancreas cancer. *Hum. Genet.* 121: 635-637.

11 Supplements

In the following, paper I to III and manuscript I are printed.

Paper I

Integrin-linked kinase stabilizes myotendinous junctions and protects muscle from stress-induced damage

Hao-Ven Wang,¹ Ling-Wei Chang,^{1,2} Klara Brixius,³ Sara A. Wickström,¹ Eloi Montanez,¹ Ingo Thievensen,¹ Martin Schwander,⁴ Ulrich Müller,⁴ Wilhelm Bloch,³ Ulrike Mayer,⁵ and Reinhard Fässler¹

¹Department of Molecular Medicine, Max Planck Institute of Biochemistry, 82152 Martinsried, Germany

²Department of Obstetrics and Gynecology, National Cheng Kung University Medical College and Hospital, 70428 Tainan, Taiwan

³Department of Molecular and Cellular Sport Medicine, 50933 Cologne, Germany

⁴Department of Cell Biology, The Scripps Research Institute, La Jolla, CA 92037

⁵Biomedical Research Centre, School of Biological Sciences, University of East Anglia, Norwich NR4 7TJ, England, UK

Skeletal muscle expresses high levels of integrin-linked kinase (ILK), predominantly at myotendinous junctions (MTJs) and costameres. ILK binds the cytoplasmic domain of $\beta 1$ integrin and mediates phosphorylation of protein kinase B (PKB)/Akt, which in turn plays a central role during skeletal muscle regeneration. We show that mice with a skeletal muscle-restricted deletion of ILK develop a mild progressive muscular dystrophy mainly restricted to the MTJs with detachment of basement membranes and accumulation of extracellular matrix. Endurance exercise training enhances the defects at

MTJs, leads to disturbed subsarcolemmal myofiber architecture, and abrogates phosphorylation of Ser473 as well as phosphorylation of Thr308 of PKB/Akt. The reduction in PKB/Akt activation is accompanied by an impaired insulin-like growth factor 1 receptor (IGF-1R) activation. Coimmunoprecipitation experiments reveal that the $\beta 1$ integrin subunit is associated with the IGF-1R in muscle cells. Our data identify the $\beta 1$ integrin–ILK complex as an important component of IGF-1R/insulin receptor substrate signaling to PKB/Akt during mechanical stress in skeletal muscle.

Introduction

ECM of skeletal muscle consists of a basement membrane (BM) surrounding each myofiber and interstitial connective tissue (endomysium) between the myofibers. The attachment of myofibers to the BM is mainly mediated by integrins and the dystrophin–glycoprotein complex (DGC; Mayer, 2003; Michele and Campbell, 2003). Integrins are expressed throughout the sarcolemma of myofibers but are highly enriched at two force-transducing and force-regulating structures, the myotendinous junctions (MTJs), which connect myofibers to tendons, and the costameres, which are focal adhesion–like structures that connect the sarcomeric z bands with the sarcolemma.

Integrins are a large family of α/β heterodimeric adhesion receptors (Bouvard et al., 2001; Hynes, 2002). Several $\beta 1$ integrins were shown to play essential roles during myogenesis and

muscle homeostasis (Mayer, 2003). Antibody perturbation studies and $\beta 1$ integrin gene ablations in flies and mice demonstrated that $\beta 1$ integrins regulate proliferation and fusion of myoblasts and the assembly and maintenance of sarcomeres (Menko and Boettiger, 1987; Volk et al., 1990; Sastry et al., 1996; Hirsch et al., 1998; Schwander et al., 2003). The $\alpha 7\beta 1$ and, until the first postnatal days, the $\alpha 5\beta 1$ integrins are expressed at the MTJs, where they implement and maintain the linkage of the myofiber to the tendon matrix. $\alpha 5$ Integrin–deficient chimeric mice develop a muscle dystrophy associated with reduced adhesion and proliferation of myoblasts (Taverna et al., 1998). $\alpha 7$ Integrin–deficient mice suffer from a progressive muscular dystrophy with disrupted MTJs (Mayer et al., 1997; Miosge et al., 1999).

Integrins transduce important signals. They control actin dynamic and link the actin cytoskeleton with the ECM, and they transduce biochemical signals in cooperation with growth factor receptors, including receptors for insulin-like growth factor (IGF; Goel et al., 2004), PDGF (Schneller et al., 1997; Baron et al., 2002), VEGF (Soldi et al., 1999), and epithelial growth factor (EGF; Moro et al., 1998; Moro et al., 2002). An important and still largely unanswered question is how integrins execute their

Correspondence to Reinhard Fässler: Faessler@biochem.mpg.de

Abbreviations used in this paper: BM, basement membrane; ddH₂O, double-distilled H₂O; DGC, dystrophin–glycoprotein complex; DM, differentiation medium; E, embryonic day; EGF, epithelial growth factor; GC, gastrocnemius; GM, growth medium; HSA, human skeletal α -actin; IGF, insulin-like growth factor; IGF-1R, IGF receptor 1; ILK, integrin-linked kinase; MTJ, myotendinous junction.

The online version of this paper contains supplemental material.

functions in myoblasts and adult skeletal muscle. Integrin cytoplasmic domains lack actin binding sites and enzymatic activities. Therefore, integrin signals are transduced through accessory molecules such as talin, α -actinin, and integrin-linked kinase (ILK; Brakebusch and Fassler, 2003).

ILK is composed of ankyrin repeats at the N terminus, a pleckstrin homology-like domain, and a putative kinase domain at the C terminus, which binds the cytoplasmic tail of $\beta 1$ and 3 integrins (Grashoff et al., 2004; Legate et al., 2006). A major function of ILK is to organize the actin cytoskeleton by recruiting actin binding and actin-regulatory proteins, such as PINCH, parvin, paxillin, and kindlin (Legate et al., 2006), and to phosphorylate several proteins, including GSK-3 β and PKB/Akt (Delcomenne et al., 1998; Novak et al., 1998; Persad et al., 2000), both of which are important for homeostasis and regeneration of muscle (Glass, 2003; Hoffman and Nader, 2004).

ILK is ubiquitously expressed and essential for the development of vertebrates and invertebrates. Mice lacking ILK die during the periimplantation stage because of abnormal F-actin reorganization and polarity of the epiblast (Sakai et al., 2003). In *Drosophila melanogaster* and *Caenorhabditis elegans*, the deletion of ILK leads to muscle detachment resembling the β integrin loss-of-function phenotype (Zervas et al., 2001; Mackinnon et al., 2002). Interestingly, the severe phenotypes both in flies and nematodes can be fully rescued with kinase-dead versions of ILK, suggesting that in invertebrates the kinase activity is dispensable for development and physiology (Zervas et al., 2001; Mackinnon et al., 2002).

Similarly, as in flies and nematodes, mammalian myoblasts and myofibers express high levels of ILK. In myofibers ILK is found at MTJs and costameres. The costameric location makes ILK perfectly suited to transduce contractile forces from the sarcomeres across the sarcolemma to the ECM. Consistent with such a function, mice and zebrafish that lack ILK function in cardiomyocytes exhibit severe defects in mechanotransduction resulting in lethal heart dilation, fibrosis, and disaggregation of cardiomyocytes (Bendig et al., 2006; White et al., 2006). The defects in mouse cardiomyocytes are associated with reduced Ser473 phosphorylation of PKB/Akt. Because PKB/Akt activity is crucial for cardiomyocyte growth and contractility (Condorelli et al., 2002; DeBosch et al., 2006) and ILK phosphorylates Ser473 of PKB/Akt (Delcomenne et al., 1998; Persad et al., 2000), it was concluded that mechanical stress-mediated activation of ILK supports cardiomyocyte homeostasis via PKB/Akt activation.

The role of ILK functions in skeletal muscle is obscure. Overexpression of ILK in C2C12 myoblasts was shown to inhibit myoblast fusion by sustained phosphorylated Erk1/2 activation, thus preventing cell cycle exit and myogenic determination (Huang et al., 2000). However, ILK overexpression in L6 myoblasts was shown to promote fusion and myogenin expression (Miller et al., 2003a). Finally, genetic studies in mice showed that ILK is dispensable for the development and homeostasis of skeletal muscle (White et al., 2006). The latter finding was unexpected and could potentially be because of the severe heart abnormalities and the early death of the mice, or it could alternatively result from incomplete Cre-mediated ILK gene deletion in skeletal muscle.

To test ILK functions in the skeletal muscle of mice without affecting cardiac function, we conditionally ablated the ILK gene using human skeletal α -actin (HSA) promoter-driven Cre expression. We found that loss of ILK triggered a mild, progressive muscular dystrophy, mainly restricted to MTJ areas, which was dramatically aggravated after exercise and accompanied by an impaired phosphorylation of IGF-1 receptor (IGF-1R) and PKB/Akt at the Thr308 and Ser473 residues, respectively.

Results

Skeletal muscle-specific deletion of the ILK gene

Because ILK-null (*ILK^{lacZ/lacZ}*) mice die shortly after implantation (Sakai et al., 2003), we used the Cre/loxP system to disrupt the *ILK* gene specifically in skeletal muscle. To obtain mice with the genotype *HSACre⁺/ILK^{lox/lox}* (called HSACre-ILK), *ILK^{lox/lox}* mice (Grashoff et al., 2003) were intercrossed with a transgenic mouse strain expressing the Cre recombinase under the control of the *HSA* promoter (Schwander et al., 2003).

The efficiency of the Cre-mediated deletion of the ILK gene in vivo was tested by Southern blotting using genomic DNA and Western blotting using protein extracts from gastrocnemius (GC) muscle of 3-mo-old control and HSACre-ILK mice. The Southern blots revealed a recombination efficiency of $\sim 80\%$ (Fig. 1 A) and the Western blots an $\sim 70\%$ reduction of ILK protein level (Fig. 1 B). Similar experiments with muscle tissue from 4-wk-, 3-mo-, and 1-yr-old HSACre-ILK mice revealed that the ILK gene deletion and ILK protein reduction remained stable (Fig. 1 C and not depicted).

It has been reported that the HSA-Cre transgene induces DNA recombination as early as embryonic day (E) 9.5 (Schwander et al., 2003). Despite this early Cre activity, we observed robust ILK immunostaining in all hindlimb muscle of E14.5 and 16.5 HSACre-ILK embryos (Fig. 1 D and not depicted). The intensity and the distribution of ILK immunostaining were comparable to muscle tissue from control mice with a strong signal at the MTJs and a weaker sarcolemmal staining (Fig. 1 D). Peri- and postnatally, ILK was not detected in HSACre-ILK muscle by immunostaining (Fig. 1 D). Quantification of Western blots from muscle tissue lysates showed a 60–70% reduction in ILK protein levels at this stage (Fig. 1 C). These results show that the ILK gene is efficiently deleted by the HSA-Cre transgene and that the ILK mRNA and/or protein have a long half-life in skeletal muscle cell precursors and muscle fibers.

HSACre-ILK mice develop a muscular dystrophy

Intercrosses of *HSACre⁺/ILK^{+/-}* males with *ILK^{fl/fl}* females revealed a normal Mendelian distribution of the four possible genotypes among 231 offspring tested: *HSACre⁺/ILK^{fl/+}*; *HSACre⁺/ILK^{fl/+}*; *HSACre⁻/ILK^{fl/+}*; and *HSACre⁻/ILK^{fl/+}* = 24.4; 23.7; 25.2; and 26.8%. HSACre-ILK mice did not show an overt phenotype at birth. They were viable, fertile, and showed normal growth rates with normal weight and body length. At 3 wk of age, when control mice began to securely walk, HSACre-ILK mice still shambled and showed an abnormal walking pattern.

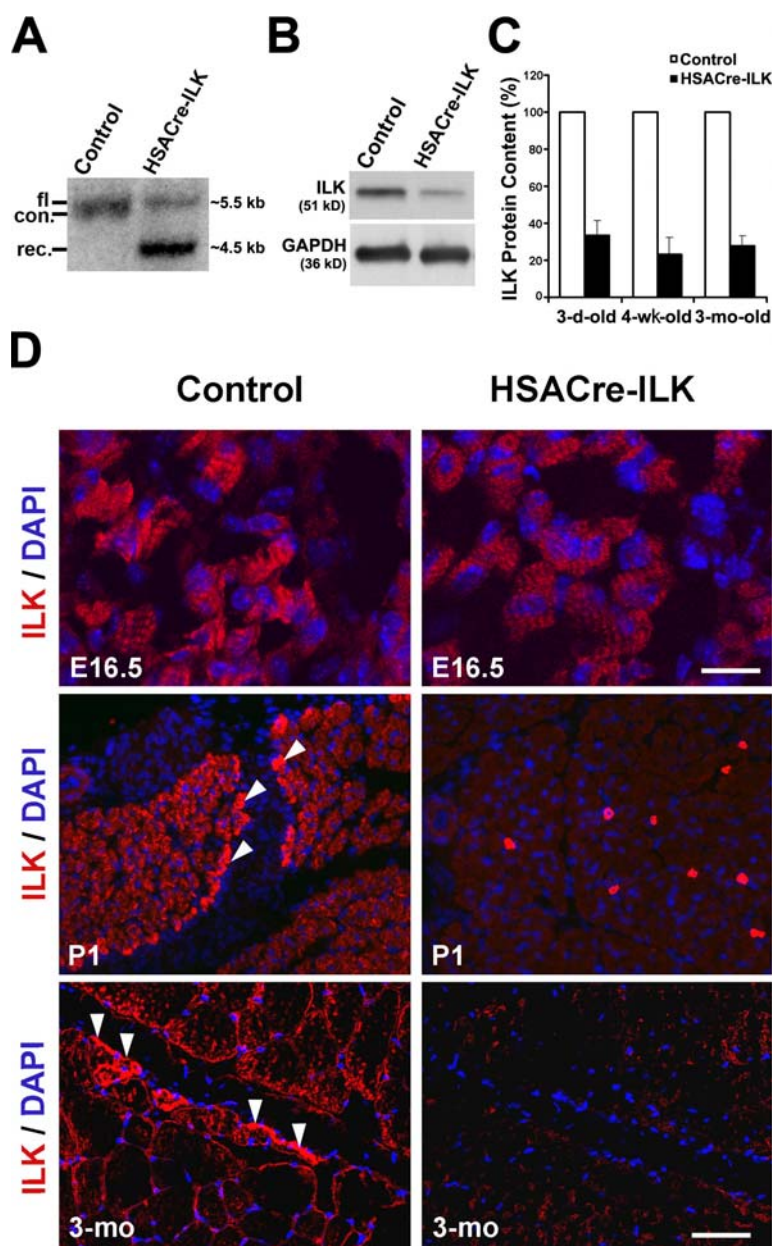


Figure 1. ILK expression in HSACre-ILK mice. (A) Southern blot analysis of ILK in control (HSACre⁻/ILK^{fl/+}) and HSACre-ILK (HSACre⁺/ILK^{fl/-}) GC muscles from two 4-wk-old mice. fl, floxed; con, control; rec., recombined allele. (B) Western blot analysis of ILK expression in muscle used for Southern blot assay. GAPDH was used as a loading control. (C) Quantification of the ILK protein content of control and HSACre-ILK muscle by densitometric measurement of the Western blot signals. Data are expressed as the mean \pm SD. (D) Immunofluorescence of ILK (red) in control and HSACre-ILK in E16.5 forelimbs, postnatal day 1 (P1) forelimbs, and 3-mo-old GC muscles. ILK is highly expressed at the MTJ (arrowheads). Lower levels of ILK are detected at the sarcolemma. No ILK signal is detected at the MTJ of HSACre-ILK mice. Nuclei are stained with DAPI (blue). Bars: (E16.5) 4 μ m; (P1 and 3-mo) 50 μ m.

To visualize the defect, we painted the front pad of control and HSACre-ILK mice with red ink and the hind pad with blue ink and let them walk on blotting paper. HSACre-ILK mice had an abnormal footprint pattern (Fig. 2 A) with a significantly shorter stride length, and this abnormality was maintained with age (Fig. 2 B).

Adult mammalian skeletal muscle is differentiated into distinct fiber types, which are characterized by a unique combination of functional, biochemical, and metabolic properties. To exclude the possibility that loss of ILK affected only specific muscle fiber types, we analyzed the histology of muscles with predominantly fast fibers (tibialis anterior muscle), slow fibers (soleus muscle), and a mixture of slow and fast fibers (GC muscle) from control and HSACre-ILK mice. Samples of all three mus-

cle groups derived from control mice exhibited myofibers with regular diameter and peripherally located nuclei. In contrast, all three muscle types analyzed from HSACre-ILK mice contained myofibers with variable fiber size and centralized nuclei (Fig. 3, A and B; Fig. S1 A; and Fig. S2, A and B, available at <http://www.jcb.org/cgi/content/full/jcb.200707175/DC1>). Staining of tissue sections for ATPase and NADH activity revealed that both fast and slow fiber types showed centralized nuclei (Fig. 3 B). The irregular fiber size with centralized nuclei could be observed as early as 10 d after birth and were aggravated with age (Fig. 3 A and Fig. S1 B). The number of myofibers with central nuclei increased from $11.6 \pm 2.9\%$ in 3-mo-old mice to $22.2 \pm 5.1\%$ in 12-mo-old mice, whereas the number in control mice was $\sim 2\%$ at all ages analyzed. Furthermore, we frequently

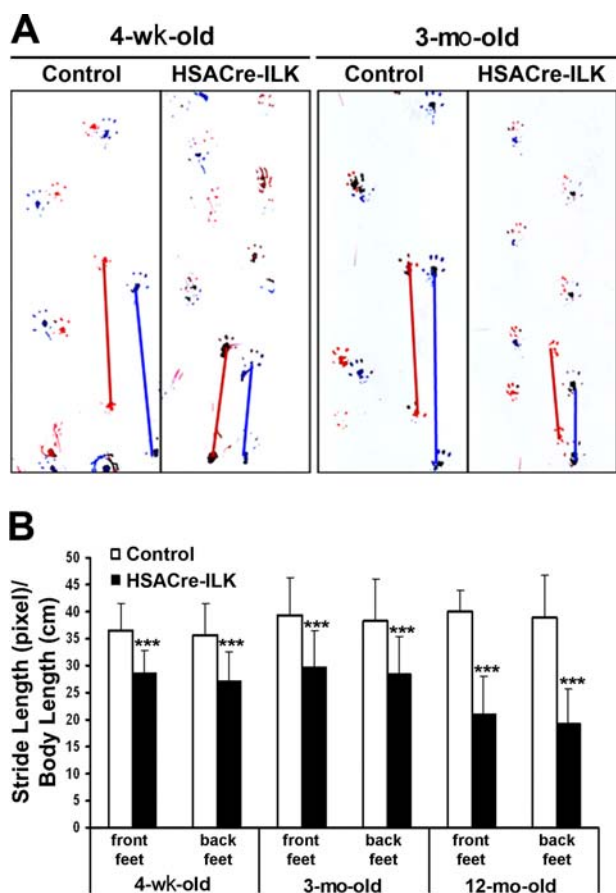


Figure 2. **Footprint analysis.** Footprints of 4-wk-, 3-mo-, and 12-mo-old control and HSACre-ILK mice. (A) Front and back pads were inked in red and blue colors, respectively. (B) The distances between each two footprints were measured by pixel, and to diminish the influence of body length, the distances were divided by body length. The stride length of front and back feet of 4-wk-, 3-mo-, and 12-mo-old mutant mice are significantly shorter in HSACre-ILK mice. Data are expressed as mean \pm SD ($n = 3$; ***, $P < 0.001$).

observed loosened intercellular space filled with fibrotic material and mononuclear cell infiltrates, which were particularly prominent at MTJs and in regions near tendons (Fig. 3 A).

The extent of the fibrosis was assessed in more detail by analyzing collagen deposition using trichrome staining. In the GC of 4-wk-old mice, no obvious difference between control and HSACre-ILK was observed. However, at the age of 5 mo, fibrotic regions were observed in the endomysial space around myofibers and at the MTJs of HSACre-ILK mice. The fibrosis became more pronounced in 12-mo-old muscle (Fig. 4).

Because ILK-deficient MTJs displayed abnormalities, we further analyzed them at the ultrastructural level. The MTJs from control mice were extensively folded, forming digit-like protuberances of regular size and width that were covered with a well-structured BM and extended from the muscle cells into the collagen-rich tendon matrix (Fig. 5, A and C). The MTJs of 5-mo-old HSACre-ILK mice had folds with irregular size and width (Fig. 5, B and D). We frequently observed that the BM was detached from the sarcolemma at the base of the digit-like pro-

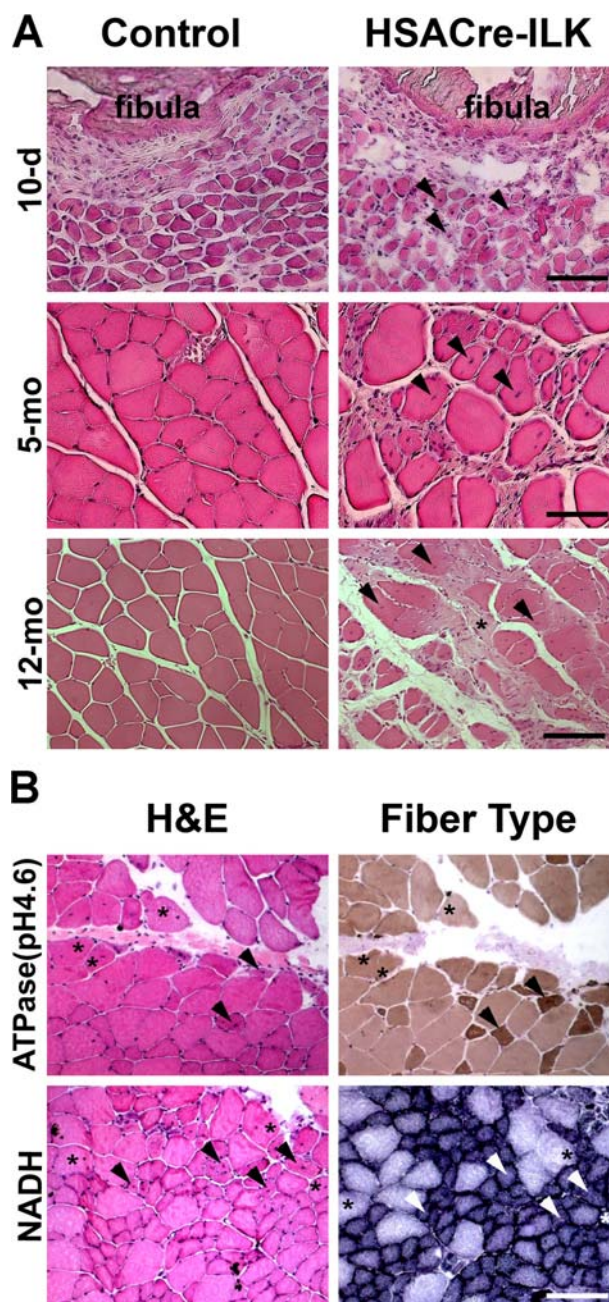


Figure 3. **HSACre-ILK muscle displays signs of a mild dystrophy.** (A) Hematoxylin/eosin-stained paraffin sections of the GC muscle of 10-d-, 5-mo-, and 12-mo-old control and HSACre-ILK mice. Note that the myofibers of HSACre-ILK mice show irregular diameter, centrally located nuclei (arrowheads), mononuclear cell infiltrates (asterisk), and fibrosis in 12-mo-old mutant muscle. Bars: (10-d) 40 μ m; (5-mo) 50 μ m; (12-mo) 60 μ m. (B) Myosin ATPase, pH 4.6, and NADH-stained cryosections of the GC muscle of 3-mo-old HSACre-ILK muscles. Myofiber with asterisks indicate type II fibers with centralized nuclei. Arrowheads indicate type I fibers with centralized nuclei. Bar, 80 μ m.

trusions (Fig. 5 D, arrowheads). Interestingly, sarcomeres of HSACre-ILK myofibrils that contained central nuclei and, hence, had regenerated, appeared similar to control mice (Fig. 5, E and F), indicating that regeneration occurs normally in the absence of ILK expression.

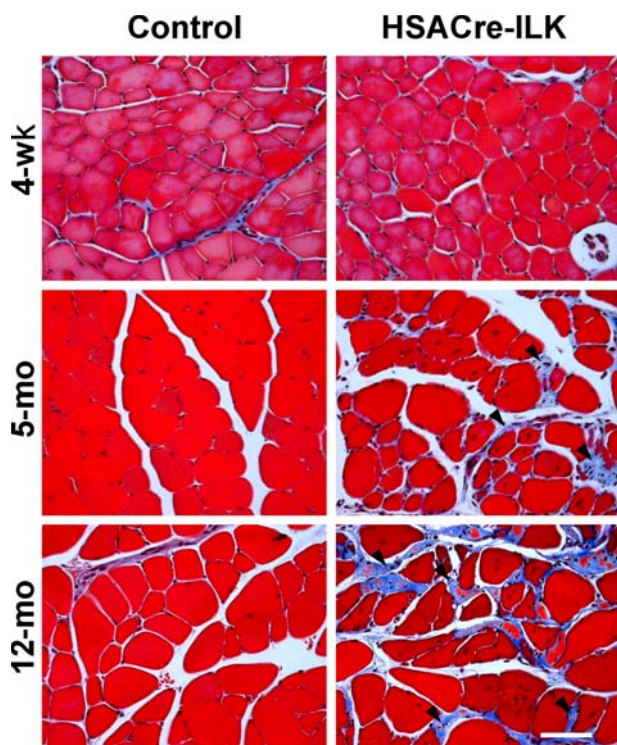


Figure 4. **Altered collagen deposition in HSACre-ILK muscles.** Trichrome staining of paraffin sections of GC muscle of 4-wk-, 5-mo-, and 12-mo-old control and HSACre-ILK mice. Collagen-containing fibrotic regions display blue color signals (arrowheads). Bar, 50 μ m.

Collectively, these results suggest that the deletion of the ILK gene from skeletal muscles leads to a mild muscular dystrophy characterized by abnormalities at MTJs, variation of myofiber size, and increased fibrosis.

Loss of ILK affects integrin localization at MTJs

ILK forms a ternary complex with PINCH and parvin that is important for the stability of the individual components and the recruitment of the complex into focal adhesions. Similarly, as reported for other cell types and tissues, HSACre-mediated loss of ILK was associated with reduced PINCH1 and β -parvin levels, which are both highly expressed in skeletal muscle (Fig. 6 A). The ILK–PINCH–parvin complex is thought to regulate integrin function and actin reorganization. Interestingly, however, ultrastructural analysis revealed no signs of F-actin detachment from the sarcolemma both at the MTJs and in central areas of the muscle tissue (Fig. S3, available at <http://www.jcb.org/cgi/content/full/jcb.200707175/DC1>). This indicates that, in contrast with flies and nematodes, ILK is not essential for anchoring actin filaments to the muscle cell membrane.

The predominant integrin of skeletal muscle is the α 7 β 1D integrin. The α 7 integrin gene is alternatively spliced, producing the α 7B splice variant (α 7B β 1), which is the predominant form in skeletal muscle found at the sarcolemma and the MTJ, and the α 7A splice variant (α 7A β 1), which is expressed at MTJs (Nawrotzki et al., 2003). Both α 7 subunits associate with a splice

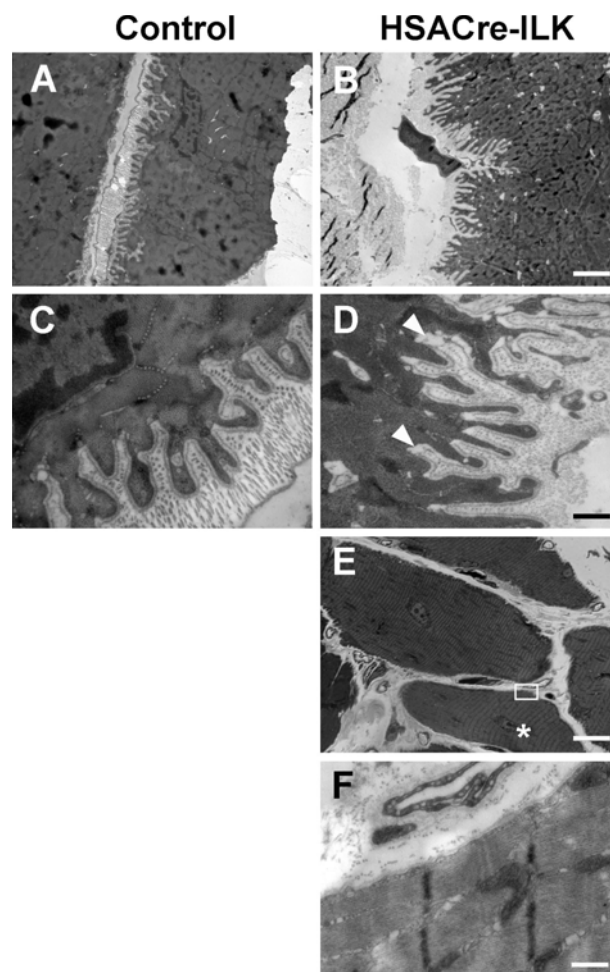
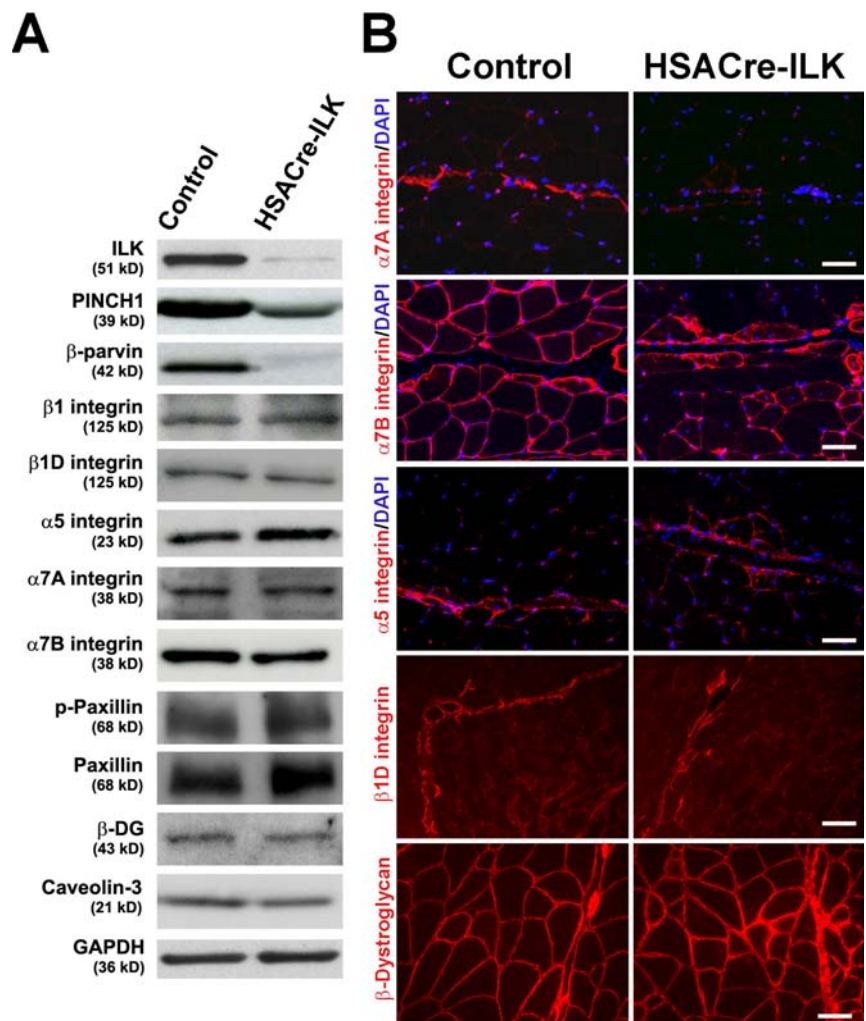


Figure 5. **Abnormalities at the MTJs of HSACre-ILK mice.** Alteration of MTJs in HSACre-ILK mice. Electron micrographs of the MTJ of 5-mo-old control (A and C) and HSACre-ILK (B and D) mice. (A and B) MTJs with multiple finger-like interdigitations of regular organization and length are observed in control (A) and HSACre-ILK (B) mice. (C) The finger-like folds are covered by a well-organized and closely attached BM interdigitating with collagen fibrils in control mice. (D) HSACre-ILK mice showed folds of slightly different length and width with a partial detachment of the BM (arrowheads). (E and F) The sarcomeric structure was normal in fibers of HSACre-ILK containing centralized nuclei (asterisk). The open white rectangle in E indicates the region shown in F. Bars: (A and B) 2.2 μ m; (C and D) 500 nm; (E) 20 μ m; (F) 800 nm.

variant of the β 1 integrin subunit called β 1D integrin, which is found at the MTJs and costameres (Belkin et al., 1996; van der Flier et al., 1997). Western blotting and immunostaining revealed strong β 1D integrin expression at MTJs and lower levels at the sarcolemma both in control and HSACre-ILK muscle (Fig. 6, A and B). Although similar amounts were detected by immunoblotting, immunostaining for α 7A β 1 and α 7B β 1 integrins revealed irregular staining patterns with reduced signals in some areas of the muscle tissue (Fig. 6 B). Furthermore, unlike in control muscle, the α 5 staining was not restricted to the tendon but partly extended into the muscle fibers (Fig. 6 B).

The BM around myofibers is assembled by integrins and the DGC (Mayer et al., 1997; Miosge et al., 1999; Nawrotzki et al., 2003; Guo et al., 2006; Rooney et al., 2006). Immunostaining

Figure 6. Expression and distribution of ILK-associated proteins. (A) ILK, Pinch, and parvin are decreased in HSACre-ILK muscle, whereas $\beta 1$, $\beta 1D$, $\alpha 5$, $\alpha 7A$, and $\alpha 7B$ integrin and phosphopaxillin (p-paxillin), β -dystroglycan (β -DG), and caveolin-3 are not changed. GAPDH was used as the loading control. (B) Immunofluorescence staining of $\alpha 7A$, $\alpha 7B$, $\alpha 5$, and $\beta 1D$ integrins and β -dystroglycan. Note the prominent $\alpha 7A$ integrin signals (red) at MTJ of control muscles and the reduction at MTJs of HSACre-ILK muscles. Although $\alpha 7B$ integrin (red) is expressed on the sarcolemma of all myofibers in the control, it shows an irregular staining pattern in HSACre-ILK muscle. In contrast to the control muscle, $\alpha 5$ integrin signals are not restricted to the tendon of HSACre-ILK muscles. $\beta 1D$ Integrin and β -dystroglycan signals are comparable between control and HSACre-ILK muscles. Bars: ($\alpha 7A$ integrin, $\alpha 5$ integrin, and β -dystroglycan) 40 μ m; ($\alpha 7B$ integrin) 35 μ m; ($\beta 1D$ integrin) 60 μ m.



revealed normal expression of β -dystroglycan, laminin $\alpha 2$, and dystrophin (Fig. 6 B and Fig. S4, available at <http://www.jcb.org/cgi/content/full/jcb.200707175/DC1>). Collectively, we conclude that ILK deficiency in muscle does not affect F-actin anchorage and BM assembly but affects the distribution of integrins.

Normal myoblast fusion in vitro

Because of the long half-life of the *ILK* mRNA and/or protein, HSACre-ILK embryos still contained significant levels of ILK in skeletal muscle tissue around the time of myoblast migration and fusion (Fig. 1 D). Therefore, we isolated primary myoblasts from the hindlimbs of 2-d-old control and HSACre-ILK mice and compared their ability to form myotubes in vitro. Western blotting of freshly isolated myoblasts cultured in growth medium (GM) or differentiation medium (DM) revealed faint levels of ILK (Fig. 7 A), which were most likely derived from fibroblast contaminations (desmin-negative cells; not depicted). The switch from GM to DM induced the expression of the myogenic marker myogenin and repressed the expression of MyoD to a similar extent in both control and HSACre-ILK cells. PINCH1 levels decreased concomitantly with ILK, whereas the levels of integrin $\beta 1D$, phosphorylated PKB/Akt, and phosphorylated

Erk1/2 were similar between control and HSACre-ILK myoblasts (Fig. 7 A). When the primary myoblasts were induced to form myotubes, we observed that HSACre-ILK myoblasts were able to efficiently form multinucleated myotubes (Fig. 7, B–D). Neither the number of myotubes nor the kinetic of their formation differed between the cultures of control and HSACre-ILK myoblasts. Furthermore, quantitative analysis revealed similar numbers of nuclei per myotube in control and HSACre-ILK cultures (Fig. 7, C and D). These data indicate that ILK plays no obvious role in myoblast proliferation, differentiation, and fusion.

Abnormal mechanical stress response

To test how mechanical stress affects the integrity of HSACre-ILK muscles, we subjected 5-mo-old control and HSACre-ILK mice, respectively, to daily treadmill exercise with an upward inclination of 10° at 18 m/min for 60 min, 5 d/wk. In the first 3 wk, both control and HSACre-ILK mice maintained the required speed of 18 m/min at the 10° inclination during the whole training sessions. Because HSACre-ILK mice were unable to run at this speed without breaks after the 3-wk training period, we terminated the treadmill exercise and analyzed the muscle tissue.

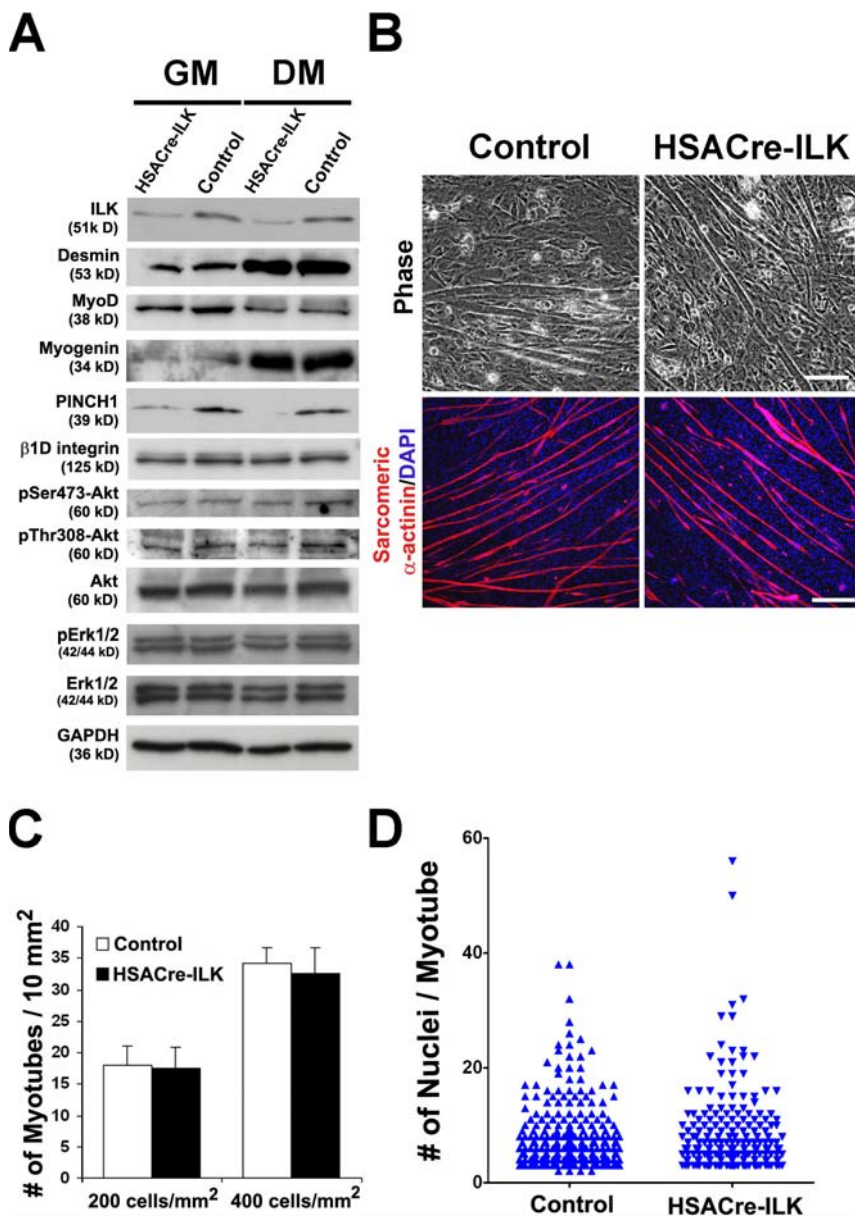


Figure 7. **Normal fusion of HSACre-ILK myoblasts.** (A) Protein levels of ILK and PINCH1 are dramatically decreased in primary HSACre-ILK myoblasts both in GM and DM. Signals of desmin and myogenin increase and MyoD decreases in response to differentiation in both cell types. The levels of β1D integrin, pSer473-Akt, pThr308-Akt, Akt, pErk1/2, and Erk1/2 are comparable. GAPDH was used as the loading control. (B) Myoblast cells were isolated from postnatal day 2 control and HSACre-ILK hindlimbs, incubated in DM, and evaluated microscopically. Differentiated myoblasts and myotubes were stained with sarcomeric α-actinin antibody (red) and DAPI (blue). (C) Quantification of myotube numbers from control and HSACre-ILK myoblasts plated at different cell densities. Data are expressed as mean ± SD ($n = 3$; 200 and 400 cells/mm²). (D) Determination of the number of nuclei per fused myotube. No difference between control and HSACre-ILK mice was observed ($P = 0.253$). Bars: (phase) 50 μm; (sarcomeric α-actinin) 80 μm.

Hematoxylin/eosin and trichrome staining of trained HSACre-ILK muscles revealed an increase in fibrosis which was not detected in control muscles (Fig. 8 A). The myofibers of untrained HSACre-ILK mice showed mild dystrophic changes and were positive for methylene blue staining (Fig. 8 B). In contrast, fibers of trained HSACre-ILK muscle were frequently negative for methylene blue, indicating muscle damage (Fig. 8 B). To evaluate the mechanical stress-induced damage more quantitatively, we investigated the levels of stretch/injury-responsive muscle ankyrin-repeat proteins Ankrd2 and CARP (Miller et al., 2003b; Hentzen et al., 2006). Both Ankrd2 and CARP mRNA were found to be significantly up-regulated in trained HSACre-ILK muscles, further confirming the exercise-induced muscle damage in HSACre-ILK mice (Fig. S5, A and B, available at <http://www.jcb.org/cgi/content/full/jcb.200707175/DC1>).

Furthermore, we observed profound abnormalities in MTJs of HSACre-ILK muscles at the ultrastructural level. Although control mice had normal MTJs after the exercise program (Fig. S5, C and D), the MTJs from HSACre-ILK mice almost completely lost their digit-like interdigitations and instead formed irregular membrane protrusions and invaginations (Fig. S5, E and F). Concomitantly with these defects, the BM detachment from the sarcolemma was further aggravated (Fig. S5, F and G) when compared with untrained muscle (Fig. 5 F). In addition, in some areas the BM was replaced by an electron-dense material (Fig. S5 F).

Training experiments with 9-mo-old HSACre-ILK mice showed that they were unable to exercise at a speed of 18 m/min. This age-dependent decline in running capacity made it impossible to perform a training intervention comparable to the 5-mo-old mice.

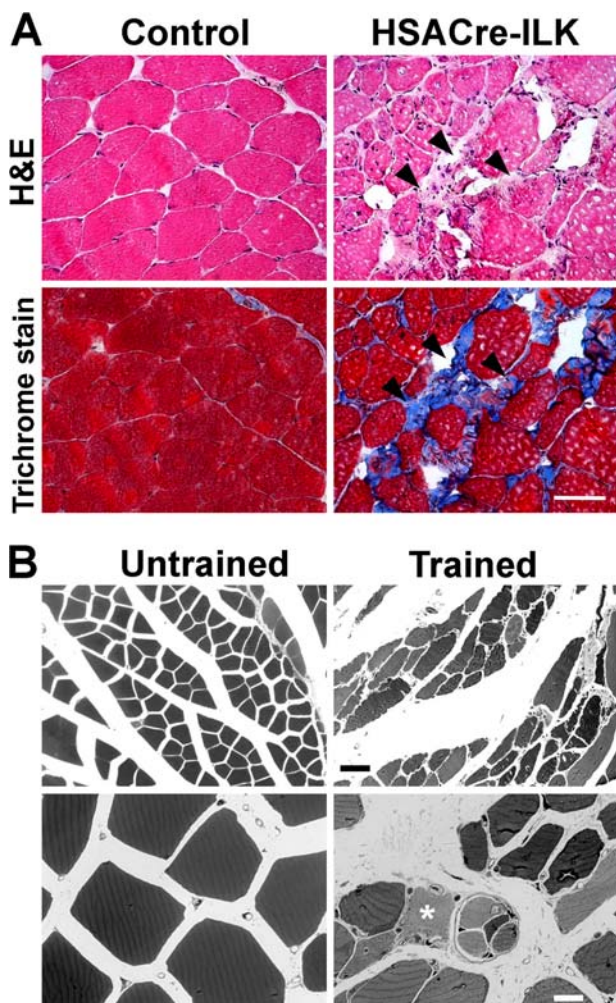


Figure 8. Exercise-induced alterations in myofibers of HSACre-ILK mice. (A) Hematoxylin/eosin (H&E)- and trichrome-stained cryosections of the GC muscle of trained control and HSACre-ILK mice. Arrowheads indicate fibrotic regions. Bar, 50 μ m. (B) Methylene blue-stained skeletal muscle fibers of untrained and trained HSACre-ILK mice. Trained HSACre-ILK muscles contain necrotic fibers (asterisk). Bars: (top) 35 μ m; (bottom) 900 nm.

Collectively, these data demonstrate that ILK-deficient skeletal muscle is highly susceptible to mechanical stress.

ILK modulates IGF signaling

Growth of skeletal muscle critically depends on the activation of mTOR kinase by PKB/Akt (Glass, 2003; Hoffman and Nader, 2004). ILK phosphorylates Ser473 of PKB/Akt and is thought to be required for full PKB/Akt activation. To test PKB/Akt activity, we isolated muscle tissue and performed Western blotting using phosphospecific antibodies. Untrained HSACre-ILK muscle displayed levels of Ser473 and Thr308 phosphorylation comparable with those of control muscle (Fig. 9 A). Upon training, however, we observed a significant increase in the phosphorylation of Ser473 as well as of Thr308 residues of PKB/Akt in control muscle, whereas the HSACre-ILK muscle showed a strongly attenuated response (Fig. 9 A).

In muscle, PKB/Akt can be activated by an intracellular signaling cascade that is triggered through the activation of IGF-1R (Mourkioti and Rosenthal, 2005). Therefore, we tested whether IGF-1R levels and/or activation were altered in exercised HSACre-ILK muscle. Western blotting and real-time PCR revealed that the total protein and RNA levels of IGF-1R were similar before and after exercise in control and HSACre-ILK mice (Fig. 9, B and C). Upon exercise, the phosphorylation of cytoplasmic tyrosines in the activation loop of IGF-1R (Tyr1131/1135/1136), which are known to induce PKB/Akt-activation (Vasilcanu et al., 2004), significantly increased by $57.9 \pm 0.19\%$ in exercised control muscle (Fig. 9, B and D). In contrast, there was no increase in phosphorylation of IGF-1R in HSACre-ILK muscle upon exercise (Fig. 9, B and D). Importantly, the failure of increased IGF-1R phosphorylation upon training was not caused by diminished IGF-1 secretion because IGF-1 levels were even higher in trained HSACre-ILK muscle than in that of trained controls (Fig. 9 E). These findings suggest that ILK acts in concert with growth factors to protect muscle from mechanical damage by regulating the IGF-1R–PKB–Akt signaling pathway.

The β 1 integrin subunit can associate with the IGF-1R in several cell types (Goel et al., 2006). To test whether a similar association occurs before and/or during the formation of myofibers, we cultured C2C12 cells for different days in fusion medium in the presence or absence of IGF-1, cross-linked and immunoprecipitated β 1 integrin subunits, and finally probed the precipitate with antibodies against IGF-1R, EGFR, β -dystroglycan, and β 1 integrin. As shown in Fig. 9 F, the β 1 integrin associated with the IGF-1R, with or without IGF-1 treatment and before and after myoblast fusion. Interestingly, the amount of IGF-1R– β 1 integrin complexes increased in response to IGF-1 treatment. The association was specific because β 1 subunits neither coimmunoprecipitated with EGFR (Fig. 9 F) nor with β -dystroglycan (not depicted).

Discussion

In this paper, we report the skeletal muscle-specific ablation of the ILK gene, which leads to a mild muscular dystrophy and increased susceptibility to stress-induced damage. The exercise-induced defects are associated with reduced PKB/Akt activation, which is likely caused by an impaired cross talk between β 1 integrin–ILK and the IGF-1R–insulin receptor substrate 1–PI-3K signaling pathway.

ILK maintains MTJs of untrained muscle

Loss of ILK resulted in a very mild phenotype characterized by a persistent shamble without affecting weight or life span and damaged muscle fibers with increased presence of centralized nuclei and large variation of myofiber size. Other alterations were restricted to the MTJs and included increased fibrosis, infiltration of a few inflammatory cells, and detachment of BMs at the base of the interdigitations. Because we observed normal Erk1/2 activation and normal levels of activated PKB/Akt in ILK-deficient muscle, we conclude that muscle regeneration works efficiently in the absence of ILK, and that muscle damage likely results from a mechanical rather than a signaling failure. Furthermore, it seems that

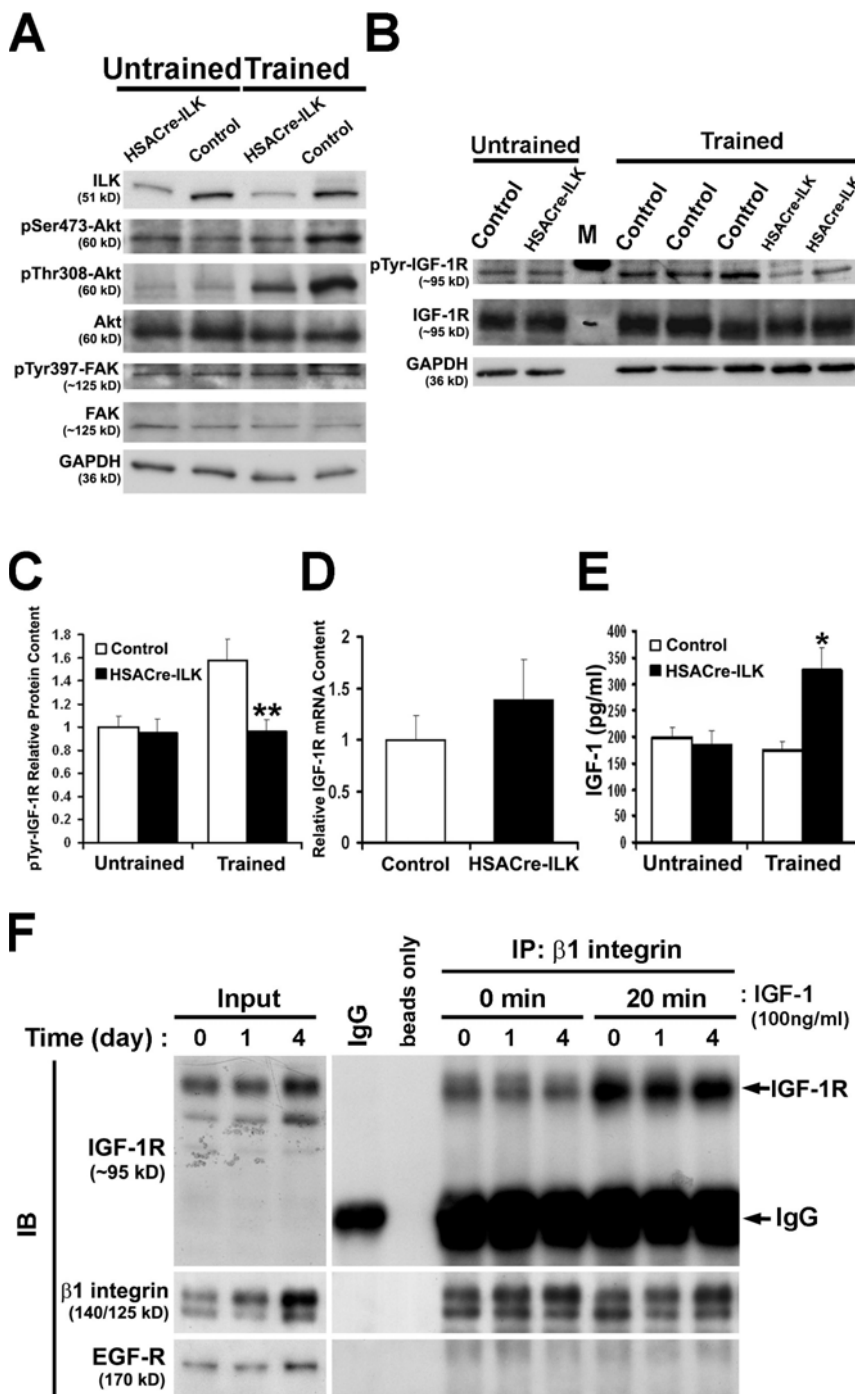


Figure 9. Altered IGF signaling after endurance exercise training. (A and B) Western blot analysis of untrained and endurance exercise-trained control and HSACre-ILK GC muscle for ILK, pSer473-Akt, pThr308-Akt, total Akt, pTyr397-FAK, and total FAK (A) and pTyr1131/1135/1136-IGF-1R and total IGF-1R (B). GAPDH was determined to show equal loading. (C) Densitometric quantification of pTyr-IGF-1R levels from resting and endurance exercised-trained control and HSACre-ILK muscles. The increase of pTyr-IGF-1R was significantly reduced in muscle from HSACre-ILK mice ($n = 4$; **, $P < 0.01$). (D) Real-time PCR analysis of IGF-1R mRNA expression of control and HSACre-ILK muscles. The levels were not significantly different between control and HSACre-ILK mice ($n = 4$; $P = 0.199$). (E) Measurement of autocrine IGF-1 levels of control and HSACre-ILK muscles by ELISA. The level of IGF-1 in trained HSACre-ILK was 75% higher than in trained control muscles. Data are expressed as mean \pm SD ($n = 4$; *, $P < 0.05$). (F) C2C12 mouse myoblasts were lysed before (0) and after 1 and 4 d of differentiation with or without IGF-1 treatment, immunoprecipitated with rabbit anti- $\beta 1$ integrin antiserum or rabbit IgG (as control), and immunoblotted with rabbit anti-IGF-1R, rabbit anti- $\beta 1$ integrin, or rabbit anti-EGF-R antiserum. 8 μ g of lysates were used as inputs.

ILK is important for the stabilization of adhesion sites exposed to high mechanical forces, such as MTJs, whereas at costameres, where less force is transmitted, ILK seems to be dispensable.

The destabilization of MTJs is caused by a detachment of the BM rather than a detachment of F-actin from the sarcolemma, indicating that loss of ILK primarily affects ligand binding of integrins. This observation differs from the loss-of-function studies of ILK in flies (Zervas et al., 2001), where ILK is primarily required to attach the actin cytoskeleton at the plasma membrane

and, to a lesser extent, for integrin binding to the ECM. It is possible that the requirements of ILK are slightly different between invertebrate and vertebrate muscle. Alternatively, it could also be that our mice have subtle actin defects that escaped detection.

ILK is not required for myoblast fusion and sarcomere assembly

Although the $\beta 1$ integrins were shown to regulate myoblast fusion and sarcomere assembly (Menko and Boettiger, 1987; Hirsch

et al., 1998; Schwander et al., 2003), it is still unclear how $\beta 1$ integrins execute these functions. Two studies reported that ILK is acting downstream of $\beta 1$ integrin to control fusion and sarcomere formation. The studies overexpressed wild-type and mutant ILK cDNAs in either mouse or rat myoblast cell lines and came to opposite conclusions. Although one study showed that ILK antagonizes myoblast fusion by sustained Erk1/2 activation, preventing cell cycle withdrawal and myogenic determination, another study reported that ILK stimulates fusion and myogenic determination (Huang et al., 2000; Miller et al., 2003a).

Unfortunately, the long half-life time of the ILK mRNA and/or protein did not permit us to study myoblast fusion and sarcomere assembly in vivo. Therefore, we isolated primary myoblasts from newborn control and HSACre-ILK mice and tested whether they fuse and assemble sarcomeres in vitro. We found that primary ILK-deficient myoblasts exhibit normal fusion and sarcomere assembly, indicating that ILK does not play an obvious and very prominent role during myogenic differentiation. These findings are in line with recent zebrafish data showing that loss of ILK function results in severe heart failure but normal development of skeletal muscle.

ILK protects myofibers from force-induced damage

Contrary to the mild defects of ILK-deficient skeletal muscle, disruption of ILK function in zebrafish or the myocardium of mice leads to lethality with progressive contraction defects, heart dilation, and fibrosis (Bendig et al., 2006; White et al., 2006). The strong phenotype suggests that mechanical loading triggers the severe defects. We tested this assumption by exposing control and mutant mice to forced treadmill and found that mutant mice could not complete the 4-wk training protocol with a treadmill speed of 18 m/min, demonstrating that the function of HSACre-ILK muscle was profoundly compromised. After training for 3 wk, the MTJs of HSACre-ILK muscle displayed an almost complete loss of interdigitations, extensive BM detachments, and myofiber necrosis.

Although treadmill profoundly augmented the defects at the MTJs, we still observed normal insertions of actin filaments at the sarcolemma at MTJs. This could have several reasons. It is possible that the training protocol was not vigorous enough to trigger actin filament detachment as observed in flies and nematodes. It is also conceivable that ILK plays no or only a minor role as a mechanical linkage for the terminal sarcomeres at MTJs. Finally, loss of ILK may be compensated by other actin-linked adhesion molecules such as the DGC. Consistent with the latter assumption, it was demonstrated that *mdx/ $\alpha 7$ integrin^{-/-}* double mutant mice develop a more severe muscle dystrophy than dystrophin or $\alpha 7$ integrin single mutant mice (Guo et al., 2006; Rooney et al., 2006).

ILK is required for the mechanical stress-induced activation of PKB/Akt

ILK is believed to phosphorylate and, thereby, modulate the activity of several target proteins, including PKB/Akt, which, in turn, plays a central role during the repair of skeletal muscle by activating the mTOR complex and downstream targets such

as S6K and 4E-BP (Bodine et al., 2001; Rommel et al., 2001). Several reports have recently challenged this view and showed that the phosphorylation of Ser473 is mediated by the mTOR kinase rather than ILK, that the phosphorylation of Thr308 is sufficient for activation of PKB/Akt, and that the phosphorylation of Ser473 determines the specificity of PKB/Akt toward FOXO1 and FOXO3 and, to a lesser extent, the absolute activity of PKB/Akt (Frias et al., 2006; Guertin et al., 2006; Jacinto et al., 2006; Shiota et al., 2006). Despite these novel findings, ablation of the ILK gene in cardiomyocytes of mice led to a dramatically reduced Ser473 phosphorylation of PKB/Akt. Because the phosphorylation levels of Thr308 were not determined in ILK-deficient cardiomyocytes, it is unclear whether loss of ILK affected the specificity of PKB/Akt only or also the overall activity of PKB/Akt.

We observed similar phosphorylation levels of Ser473 and Thr308 in control and HSACre-ILK muscle of untrained mice, suggesting that the mild muscular dystrophy upon ILK loss is not a result of diminished ILK-dependent PKB/Akt activation. In sharp contrast, forced treadmill triggered an increase of Ser473 phosphorylation in the skeletal muscle of control mice, whereas phospho-Ser473 levels failed to rise in HSACre-ILK muscle. Moreover, the reduced PKB/Akt phosphorylation was not restricted to the potential ILK target Ser473 but was also observed on Thr308, indicating that mechanical load-induced activation of both the PDK-1 and Ser473 kinase activities requires ILK.

These findings suggest that loss of ILK likely affects an activator, which is upstream of both the PDK-1–Thr308–PKB–Akt and the Ser473–PKB/Akt pathways in mechanically challenged muscle. A potential candidate for such an upstream activator is IGF-1R, which plays a central role during muscle repair (Musaro et al., 2001), acts through PI-3K/PKB/Akt/mTOR signaling (Bodine et al., 2001; Rommel et al., 2001), cross talks with the $\beta 1$ integrin signaling pathway (Goel et al., 2004, 2006), and was shown to activate ILK (Attwell et al., 2000). We performed Western blot assays with antibodies against the phosphorylated form of IGF-1R and could indeed demonstrate that IGF-1R activation is severely impaired in trained HSACre-ILK muscle. It is well known that physical training triggers IGF-1R phosphorylation and the downstream activation of PKB/Akt and the mTOR complexes, which in turn give rise to the formation of new myofibrils. Consistent with the reduced PKB/Akt phosphorylation, the training-induced phosphorylation of IGF-1R at tyrosine residues (Tyr1131/1135/1136) in the activation loop of the kinase domain was almost completely abrogated in HSACre-ILK muscle. Phosphorylation of Tyr1136 was shown to be required for the IGF-1-induced phosphorylation of insulin receptor substrate 1, the interaction of the regulatory p85 subunit of PI-3K with IGF-1R, and the downstream-activation of PKB/Akt (Vasilcanu et al., 2004). Moreover, we observed that the $\beta 1$ integrin subunit can form a complex with IGF-1R in C2C12 cells before and after fusion into myotubes. Interestingly, IGF-1 treatment increases the amount of $\beta 1$ integrin–IGF-1R complex, corroborating that the complex formation has a functional role in IGF signaling. Collectively, our data suggest that the $\beta 1$ integrin–IGF-1R complex is using ILK to activate the IGF-1R signaling machinery, leading to PKB/Akt activation and regeneration of exercise-induced muscle damage.

Materials and methods

Mouse strains

To obtain mice with a skeletal muscle-restricted deletion of the *ILK* gene, floxed *ILK* mice (Grashoff et al., 2003) were crossed with transgenic mice expressing the Cre gene under the control of the *HSA* promoter (Schwander et al., 2003). All animals were fed ad libitum and housed according to the guidelines of the Society of Laboratory Animal Science.

Antibodies

Antibodies used in this study were mouse anti-GAPDH (Millipore), mouse anti-sarcomeric α -actinin (Sigma-Aldrich), rabbit anti-caveolin3 (Abcam), rabbit anti-Erk1/2 (Cell Signaling Technology), rabbit anti-phospho-Erk1/2 (Thr202/Tyr204; Cell Signaling Technology), mouse anti-desmin (BD Biosciences), mouse anti-paxillin (Transduction Laboratories), rabbit anti-phosphopaxillin (Tyr118; Cell Signaling Technology), mouse anti-myogenin (BD Biosciences), rabbit anti-MyoD (Santa Cruz Biotechnology, Inc.), rabbit anti-FAK (Millipore), rabbit anti-phospho-FAK (Tyr397; Invitrogen), mouse anti-dystrophin (Abcam), goat anti- β -dystroglycan (Santa Cruz Biotechnology, Inc.), rabbit anti-EGFR (Cell Signaling Technology), rabbit anti-phospho-IGF-1R (Tyr1131/1135/1136; Acris Antibodies), rabbit anti-IGF-1R (Cell Signaling Technology), and mouse anti-IGF-1R (Millipore). Fluorescent dye-conjugated secondary antibodies were obtained from Invitrogen. All other antibodies used have been described previously (Nawrotzki et al., 2003; Sakai et al., 2003; Stanchi et al., 2005; Chu et al., 2006; Guo et al., 2006).

Western blotting

Muscle tissue was homogenized in modified RIPA buffer (50 mM Tris-HCl, pH 7.4, 150 mM NaCl, 5 mM EDTA, 0.1% SDS, 1% Triton X-100, 1% sodium deoxycholate, protease inhibitors [Roche], and phosphatase inhibitors [Sigma-Aldrich]). Extracted proteins were gel separated and immunoprobed as previously described (Grashoff et al., 2003).

Histology, immunofluorescence, and electron microscopy

Muscle tissues from embryos or newborn or adult mice was excised and either frozen in liquid nitrogen-cooled isopentane or dehydrated and embedded in paraffin. 8 μ m of transverse sections were cut and collected onto SuperFrost Plus (Menzel-Gläser) slides. The area of myofibers was determined on hematoxylin/eosin-stained paraffin sections using the Axiovision software (Version 4.6.3.0; Carl Zeiss, Inc.).

Immunofluorescence was done on cryosections as described in Mayer et al. (1997). Images were collected by confocal microscopy (DMIRE2; Leica) using Leica Confocal Software (version 2.5, build 1227) with 40 or 63 \times oil objectives, by fluorescence microscopy (DMRA2; Leica) using SimplePCI software (version 5.1.0.0110; GTI Microsystems) with 20, 40, or 63 \times oil objectives, or by bright field microscopy (Axiovert; Carl Zeiss, Inc.) using IM50 software (Leica) with 10 or 40 \times objectives. All images were collected at RT. Digital images were manipulated and arranged using Photoshop CS2 (Adobe). Transmission electron microscopy was performed using an electron microscope (902A; Carl Zeiss, Inc.) as described in Hirsch et al. (1998).

In brief, muscle biopsies were fixed in 4% buffered PFA, rinsed three times in cacodylate buffer, and then treated with 1% uranyl acetate in 70% ethanol for 8 h. The biopsies were subsequently dehydrated in a graded series of ethanol and then embedded in Araldite (SERVA). Semithin sections (500 μ m) were cut with a glass knife on an ultramicrotome (Reichert) and stained with Methylene blue. Ultrathin sections (30–60 nm) for electron microscopic observation were processed on the same microtome with a diamond knife and placed on copper grids.

Isolation and differentiation of primary myoblasts

Primary myoblasts were isolated as described by Rando and Blau (1994). In brief, hindlimbs were dissected from 1–2-d-old mice, placed in PBS, minced with a razor blade, and enzymatically dissociated with a mixture of collagenase II (0.1%; Worthington Biochemical) and dispase (2.4 U/ml; grade II; Roche). The slurry, maintained at 37°C for 30–45 min, was triturated every 15 min with a 5-ml plastic pipette. After centrifugation at 350 g for 10 min, the pellet was resuspended in DME containing 20% FCS, 2 mM glutamin, and 1% Pen/Strep (Invitrogen) and preplated into noncoated tissue culture dishes for 20 min for attaching fibroblasts to the dish surface. The nonadherent cells were then transferred into 0.2% gelatin-coated 6-well plates (approximately two limbs for one well). Differentiation was induced with 5% horse serum (Invitrogen) in DME for 2–4 d. A myotube was defined as having three or more nuclei.

Endurance exercise training

Experiments were performed with 5-mo-old control (seven mice; weight: 27.0 \pm 0.7 g) and HSACre-ILK (six mice; weight: 25.1 \pm 0.9 g) mice. The treadmill (Exer3/6; Columbus Instruments) endurance training consisted of a 60-min treadmill exercise 5 d a week at a velocity of 18 m/min at an angle of 10°. Mice were elicited to run by touching their back with a pencil. Mice were accommodated to the situation for 1 wk before starting the experiments. The velocity of 18 m/min was chosen because in these preexperiments, control and HSACre-ILK mice were able to constantly run for 1 h at this velocity. An angle of 10° was chosen to increase the muscle load during the training. The training was performed for 4 wk. At the end of this period, animals were killed and the vastus lateralis and GC muscles were isolated, fixed in 4% buffered PFA for 6 h, and prepared for ultrastructural analysis.

An additional test was initiated with 9-mo-old control ($n = 6$) and HSACre-ILK ($n = 6$) mice under the conditions described in the previous paragraph. Because HSACre-ILK mice were unable to abide the exercise, the experiment was terminated. The local Animal Care Committee approved all experimental procedures.

Real-time PCR

Muscle RNA was isolated with the RNeasy Mini kit (QIAGEN). 1 μ l cDNA generated from 200 ng RNA with the iScript cDNA Synthesis kit (Bio-Rad Laboratories) was subjected to real-time PCR using the iQ SYBR Green Supermix (Bio-Rad Laboratories) and the iCycler (Bio-Rad Laboratories). The following primers (Mouse Genome Informatics number 1204415) were used for detecting IGF-1R: forward, 5'-TGGCACCTACAGGTTCCAG-3'; and reverse, 5'-TGATGGACACCTGCATG-3'. The following primers were used for CARP: forward, 5'-GAGAAGTTAATGGAGGCTGG-3'; and reverse, 5'-GTTCCAGCAACAGTTCCAGGAC-3'. The following primers were used for Ankr2: forward, 5'-CCACAGAGCTCATCGAGCAG-3'; and reverse, 5'-CTAGCACTAGCATGTCCATGG-3'. Gene expression was quantified using the Gene Expression Analysis Program for the iCycler iQ Real-Time PCR Detection system (Bio-Rad Laboratories) and normalized to GAPDH levels.

Cross-linking and immunoprecipitation

C2C12 mouse myoblasts were maintained in GM and differentiation was induced with DM. Treatment with 100 ng/ml IGF-1 (R&D Systems) in DME was performed 14 h after starvation.

Cross-linking reaction was performed in 1 mM DSP (Thermo Fisher Scientific) in PBS for 20 min on ice. Cells were lysed in IP buffer containing 1% Triton X-100, 0.05% sodium deoxycholate, 150 mM NaCl, and 50 mM Tris-HCl, pH 8, with protease inhibitors and phosphatase inhibitors (cocktails 1 and 2). For coimmunoprecipitation of β 1 integrin, 700 μ g of lysates were incubated with anti- β 1 integrin antiserum for 30 min at 4°C and then with 35 μ l of protein A-Agarose for another 1 h. Protein complexes were washed three times in wash buffer (0.1% Triton X-100, 0.005% sodium deoxycholate, 150 mM NaCl, and 50 mM Tris-HCl, pH 8) and subsequently extracted with 5 \times SDS loading buffer for 5 min at 95°C.

Myosin ATPase, pH 4.6, staining

Unfixed cryosections were preincubated for 10 min at RT in incubation buffer (0.1 M NaOAc and 1 mM EDTA adjusted to pH 4.6). Slides were dipped in incubation buffer, pH 9.6, and then immediately incubated in ATP solution (10 mg ATP in 10 ml incubation buffer, pH 9.6) for 10 min at 37°C. After washing with double-distilled H₂O (ddH₂O), slides were immersed in 2% CoCl₂ for 5 min. After another wash with ddH₂O, slides were immersed in 0.1% ammonium sulfide solution for 30 s. Finally, the slides were washed under running water for 5 min, dehydrated, and mounted in glycerine jelly.

NADH staining

Unfixed cryosections were incubated for 30 min in 0.2M Tris-HCl, pH 7.4, 1.5 mM NADH, and 1.5 mM Nitroblue tetrazolium (Sigma-Aldrich) at 37°C. After incubation, slides were rinsed three times with ddH₂O and mounted in Evanol.

Masson's trichrome staining

Slides were mordant in preheated Bouin's solution (saturated picric acid/formaldehyde/glacial acetic acid = 15:5:1) for 15 min at 56°C. After cooling to RT, slides were washed under running water to remove the yellow color and stained in Weigert's iron hematoxylin solution for 5 min. Slides were then washed for 5 min under running water, rinsed in ddH₂O, and stained in Biebrich scarlet-acid Fuchsin for 5 min. After rinsing in ddH₂O, slides were transferred to Aniline blue Solution for 5 min and, subsequently, to 1% acetic acid for 2 min. Finally, the slides were rinsed, dehydrated through alcohol, cleared in xylene, and mounted. All chemicals were from Sigma-Aldrich.

IGF-1 measurement

Muscle tissue was homogenized in PBS, pH 7.4. After two freeze-thaw cycles, the homogenates were centrifuged for 5 min at 5,000 g. The supernatant was then removed and stored at -80°C . IGF-1 measurement was performed as described in the manual of the Quantikine Mouse IGF-1 kit (R&D Systems).

Statistical analysis

Statistical evaluation was performed with GraphPad Prism software (GraphPad, Inc.). Statistical significance between data groups was determined by the Mann-Whitney test and subdivided into three groups (*, $P < 0.05$; **, $P < 0.01$; ***, $P < 0.001$).

Online supplemental material

Fig. S1 shows the centralized nuclei in soleus, extensor digitorum longus, and tibialis anterior muscle of HSACre-ILK mice. Fig. S2 shows the measurements of myofiber density and size in HSACre-ILK and control mice. Fig. S3 shows that the sarcolemmal F-actin is unaffected in HSACre-ILK muscle. Fig. S4 shows the normal distribution and expression of $\beta 1$ integrin, vinculin, laminin $\alpha 2$, and dystrophin in HSACre-ILK muscle. Fig. S5 shows the analysis of Ankrd2 and CARP levels as markers of muscle damage in trained mice as well as ultrastructural analysis showing detachment of the BM in trained HSACre-ILK muscle. Online supplemental material is available at <http://www.jcb.org/cgi/content/full/jcb.200707175/DC1>.

We thank the members of the Fässler laboratory for lively discussions and careful reading of the manuscript.

S.A. Wickström is supported by the Sigrid Juselius Foundation and the Finnish Cultural Foundation. This work was funded by the Wellcome Trust (grant 060549 to U. Mayer), the Austrian Science Fund (grant SFB021), and the Max Planck Society (to R. Fässler).

Submitted: 25 July 2007

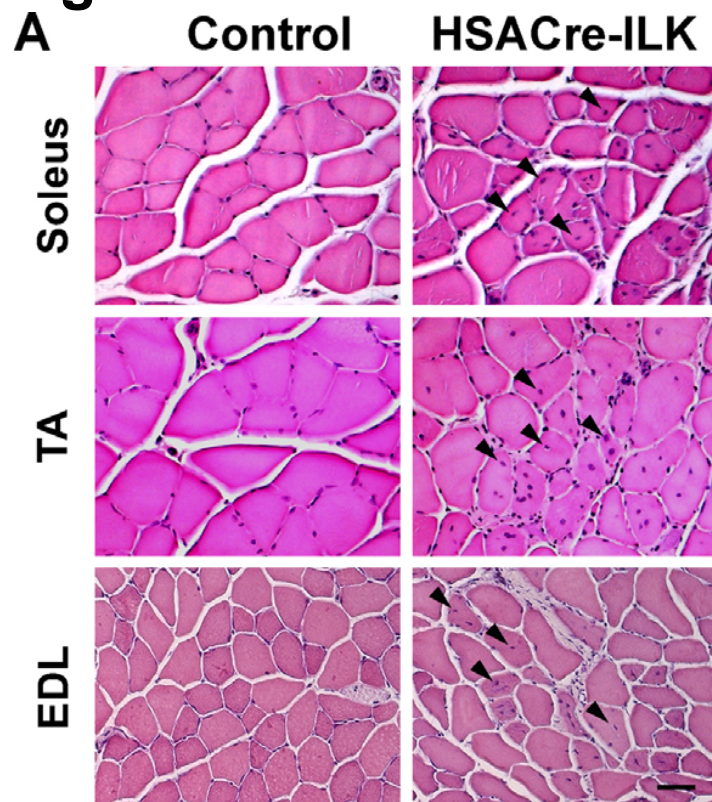
Accepted: 7 February 2008

References

- Attwell, S., C. Roskelley, and S. Dedhar. 2000. The integrin-linked kinase (ILK) suppresses anoikis. *Oncogene*. 19:3811–3815.
- Baron, W., S.J. Shattil, and C. French-Constant. 2002. The oligodendrocyte precursor mitogen PDGF stimulates proliferation by activation of $\alpha v \beta 3$ integrins. *EMBO J.* 21:1957–1966.
- Belkin, A.M., N.I. Zhidkova, F. Balzac, F. Altruda, D. Tomatis, A. Maier, G. Tarone, V.E. Kotliansky, and K. Burridge. 1996. $\beta 1$ D integrin displaces the $\beta 1$ A isoform in striated muscles: localization at junctional structures and signaling potential in nonmuscle cells. *J. Cell Biol.* 132:211–226.
- Bendig, G., M. Grimmer, I.G. Huttner, G. Wessels, T. Dahme, S. Just, N. Trano, H.A. Katus, M.C. Fishman, and W. Rottbauer. 2006. Integrin-linked kinase, a novel component of the cardiac mechanical stretch sensor, controls contractility in the zebrafish heart. *Genes Dev.* 20:2361–2372.
- Bodine, S.C., T.N. Stitt, M. Gonzalez, W.O. Kline, G.L. Stover, R. Bauerlein, E. Zlotchenko, A. Scrimgeour, J.C. Lawrence, D.J. Glass, and G.D. Yancopoulos. 2001. Akt/mTOR pathway is a crucial regulator of skeletal muscle hypertrophy and can prevent muscle atrophy in vivo. *Nat. Cell Biol.* 3:1014–1019.
- Bouvard, D., C. Brakebusch, E. Gustafsson, A. Aszodi, T. Bengtsson, A. Berna, and R. Fässler. 2001. Functional consequences of integrin gene mutations in mice. *Circ. Res.* 89:211–223.
- Brakebusch, C., and R. Fässler. 2003. The integrin-actin connection, an eternal love affair. *EMBO J.* 22:2324–2333.
- Chu, H., I. Thievensen, M. Sixt, T. Lammernann, A. Waisman, A. Braun, A.A. Noegel, and R. Fässler. 2006. γ -Parvin is dispensable for hematopoiesis, leukocyte trafficking, and T-cell-dependent antibody response. *Mol. Cell Biol.* 26:1817–1825.
- Condorelli, G., A. Drusco, G. Stassi, A. Bellacosa, R. Roncarati, G. Iaccarino, M.A. Russo, Y. Gu, N. Dalton, C. Chung, et al. 2002. Akt induces enhanced myocardial contractility and cell size in vivo in transgenic mice. *Proc. Natl. Acad. Sci. USA.* 99:12333–12338.
- DeBosch, B., I. Treskov, T.S. Lupu, C. Weinheimer, A. Kovacs, M. Courtois, and A.J. Muslin. 2006. Akt1 is required for physiological cardiac growth. *Circulation*. 113:2097–2104.
- Delcomenne, M., C. Tan, V. Gray, L. Rue, J. Woodgett, and S. Dedhar. 1998. Phosphoinositide-3-OH kinase-dependent regulation of glycogen synthase kinase 3 and protein kinase B/AKT by the integrin-linked kinase. *Proc. Natl. Acad. Sci. USA.* 95:11211–11216.
- Frias, M.A., C.C. Thoreen, J.D. Jaffe, W. Schroder, T. Sculley, S.A. Carr, and D.M. Sabatini. 2006. mSin1 is necessary for Akt/PKB phosphorylation, and its isoforms define three distinct mTORC2s. *Curr. Biol.* 16:1865–1870.
- Glass, D.J. 2003. Signalling pathways that mediate skeletal muscle hypertrophy and atrophy. *Nat. Cell Biol.* 5:87–90.
- Goel, H.L., M. Fornaro, L. Moro, N. Teider, J.S. Rhim, M. King, and L.R. Languino. 2004. Selective modulation of type 1 insulin-like growth factor receptor signaling and functions by $\beta 1$ integrins. *J. Cell Biol.* 166:407–418.
- Goel, H.L., L. Moro, M. King, N. Teider, M. Centrella, T.L. McCarthy, M. Holgado-Madruga, A.J. Wong, E. Marra, and L.R. Languino. 2006. Beta1 integrins modulate cell adhesion by regulating insulin-like growth factor-II levels in the microenvironment. *Cancer Res.* 66:331–342.
- Grashoff, C., A. Aszodi, T. Sakai, E.B. Hunziker, and R. Fässler. 2003. Integrin-linked kinase regulates chondrocyte shape and proliferation. *EMBO Rep.* 4:432–438.
- Grashoff, C., I. Thievensen, K. Lorenz, S. Ussar, and R. Fässler. 2004. Integrin-linked kinase: integrin's mysterious partner. *Curr. Opin. Cell Biol.* 16:565–571.
- Guertin, D.A., D.M. Stevens, C.C. Thoreen, A.A. Burds, N.Y. Kalaany, J. Moffat, M. Brown, K.J. Fitzgerald, and D.M. Sabatini. 2006. Ablation in mice of the mTORC components raptor, rictor, or mLST8 reveals that mTORC2 is required for signaling to Akt-FOXO and PKC α , but not S6K1. *Dev. Cell.* 11:859–871.
- Guo, C., M. Willem, A. Werner, G. Raivich, M. Emerson, L. Neyses, and U. Mayer. 2006. Absence of $\alpha 7$ integrin in dystrophin-deficient mice causes a myopathy similar to Duchenne muscular dystrophy. *Hum. Mol. Genet.* 15:989–998.
- Hoffman, E.P., and G.A. Nader. 2004. Balancing muscle hypertrophy and atrophy. *Nat. Med.* 10:584–585.
- Hentzen, E.R., M. Lahey, D. Peters, L. Mathew, I.A. Barash, J. Fridén, and R.L. Lieber. 2006. Stress-dependent and -independent expression of the myogenic regulatory factors and the MRP genes after eccentric contractions in rats. *J. Physiol.* 570:157–167.
- Hirsch, E., L. Lohikangas, D. Gullberg, S. Johansson, and R. Fässler. 1998. Mouse myoblasts can fuse and form a normal sarcomere in the absence of $\beta 1$ integrin expression. *J. Cell Sci.* 111:2397–2409.
- Huang, Y., J. Li, Y. Zhang, and C. Wu. 2000. The roles of integrin-linked kinase in the regulation of myogenic differentiation. *J. Cell Biol.* 150:861–872.
- Hynes, R.O. 2002. Integrins: bidirectional, allosteric signaling machines. *Cell.* 110:673–687.
- Jacinto, E., V. Facchinetti, D. Liu, N. Soto, S. Wei, S.Y. Jung, Q. Huang, J. Qin, and B. Su. 2006. SIN1/MIP1 maintains rictor-mTOR complex integrity and regulates Akt phosphorylation and substrate specificity. *Cell.* 127:125–137.
- Legate, K.R., E. Montanez, O. Kudlacek, and R. Fässler. 2006. ILK, PINCH and parvin: the tIPP of integrin signalling. *Nat. Rev. Mol. Cell Biol.* 7:20–31.
- Mackinnon, A.C., H. Qadota, K.R. Norman, D.G. Moerman, and B.D. Williams. 2002. *C. elegans* PAT-4/ILK functions as an adaptor protein within integrin adhesion complexes. *Curr. Biol.* 12:787–797.
- Mayer, U. 2003. Integrins: redundant or important players in skeletal muscle? *J. Biol. Chem.* 278:14587–14590.
- Mayer, U., G. Saher, R. Fässler, A. Bornemann, F. Echtermeyer, H. von der Mark, N. Miosge, E. Poschl, and K. von der Mark. 1997. Absence of integrin $\alpha 7$ causes a novel form of muscular dystrophy. *Nat. Genet.* 17:318–323.
- Menko, A.S., and D. Boettiger. 1987. Occupation of the extracellular matrix receptor, integrin, is a control point for myogenic differentiation. *Cell.* 51:51–57.
- Michele, D.E., and K.P. Campbell. 2003. Dystrophin-glycoprotein complex: post-translational processing and dystroglycan function. *J. Biol. Chem.* 278:15457–15460.
- Miller, M.G., I. Naruszewicz, A.S. Kumar, T. Ramlal, and G.E. Hannigan. 2003a. Integrin-linked kinase is a positive mediator of L6 myoblast differentiation. *Biochem. Biophys. Res. Commun.* 310:796–803.
- Miller, M.K., M.L. Bang, C.C. Witt, D. Labeit, C. Trombitas, K. Watanabe, H. Granzier, A.S. McElhinny, C.C. Gregorio, and S. Labeit. 2003b. The muscle ankyrin repeat proteins: CARP, ankrd2/Arpp and DARP as a family of titin filament-based stress response molecules. *J. Mol. Biol.* 333:951–964.
- Miosge, N., C. Klenczar, R. Herken, M. Willem, and U. Mayer. 1999. Organization of the myotendinous junction is dependent on the presence of $\alpha 7 \beta 1$ integrin. *Lab. Invest.* 79:1591–1599.
- Moro, L., M. Venturino, C. Bozzo, L. Silengo, F. Altruda, L. Beguinot, G. Tarone, and P. Defilippi. 1998. Integrins induce activation of the EGF receptor: role in MAP kinase induction and adhesion-dependent cell survival. *EMBO J.* 17:6622–6632.
- Moro, L., L. Dolce, S. Cabodi, E. Bergatto, E. Boeri Erba, M. Smeriglio, E. Turco, S.F. Retta, M.G. Giuffrida, M. Venturino, et al. 2002. Integrin induced

- epidermal growth factor (EGF) receptor activation requires c-src and p130Cas and leads to phosphorylation of specific EGF receptor tyrosines. *J. Biol. Chem.* 277:9405–9414.
- Mourkioti, F., and N. Rosenthal. 2005. IGF-1, inflammation and stem cells. Interactions during muscle regeneration. *Trends Immunol.* 26:535–542.
- Musaro, A., K. McCullagh, A. Paul, L. Houghton, G. Dobrowolny, M. Molinaro, E.R. Barton, H.L. Sweeney, and N. Rosenthal. 2001. Localized Igf-1 transgene expression sustains hypertrophy and regeneration in senescent skeletal muscle. *Nat. Genet.* 27:195–200.
- Nawrotzki, R., M. Willem, N. Miosge, H. Brinkmeier, and U. Mayer. 2003. Defective integrin switch and matrix composition at $\alpha 7$ -deficient myotendinous junctions precede the onset of muscular dystrophy in mice. *Hum. Mol. Genet.* 12:483–495.
- Novak, A., S.C. Hsu, C. Leung-Hagesteijn, G. Radeva, J. Papkoff, R. Montesano, C. Roskelley, R. Grosschedl, and S. Dedhar. 1998. Cell adhesion and the integrin-linked kinase regulate the LEF-1 and beta-catenin signaling pathways. *Proc. Natl. Acad. Sci. USA.* 95:4374–4379.
- Persad, S., S. Attwell, V. Gray, M. Delcommenne, A. Troussard, J. Sanghera, and S. Dedhar. 2000. Inhibition of integrin-linked kinase (ILK) suppresses activation of protein kinase B/Akt and induces cell cycle arrest and apoptosis of PTEN-mutant prostate cancer cells. *Proc. Natl. Acad. Sci. USA.* 97:3207–3212.
- Rando, T.A., and H.M. Blau. 1994. Primary mouse myoblast purification, characterization, and transplantation for cell-mediated gene therapy. *J. Cell Biol.* 125:1275–1287.
- Rommel, C., S.C. Bodine, B.A. Clarke, R. Rossman, L. Nunez, T.N. Stitt, G.D. Yancopoulos, and D.J. Glass. 2001. Mediation of IGF-1-induced skeletal myotube hypertrophy by PI(3)K/Akt/mTOR and PI(3)K/Akt/GSK3 pathways. *Nat. Cell Biol.* 3:1009–1013.
- Rooney, J.E., J.V. Welsch, M.A. Dechert, N.L. Flintoff-Dye, S.J. Kaufman, and D.J. Burkin. 2006. Severe muscular dystrophy in mice that lack dystrophin and $\alpha 7$ integrin. *J. Cell Sci.* 119:2185–2195.
- Sakai, T., S. Li, D. Docheva, C. Grashoff, K. Sakai, G. Kostka, A. Braun, A. Pfeifer, P.D. Yurchenco, and R. Fässler. 2003. Integrin-linked kinase (ILK) is required for polarizing the epiblast, cell adhesion, and controlling actin accumulation. *Genes Dev.* 17:926–940.
- Sastry, S.K., M. Lakonishok, D.A. Thomas, J. Muschler, and A.F. Horwitz. 1996. Integrin α subunit ratios, cytoplasmic domains, and growth factor synergy regulate muscle proliferation and differentiation. *J. Cell Biol.* 133:169–184.
- Schneller, M., K. Vuori, and E. Ruoslahti. 1997. $\alpha v \beta 3$ integrin associates with activated insulin and PDGF β receptors and potentiates the biological activity of PDGF. *EMBO J.* 16:5600–5607.
- Schwander, M., M. Leu, M. Stumm, O.M. Dorchies, U.T. Rugg, J. Schittny, and U. Müller. 2003. $\beta 1$ integrins regulate myoblast fusion and sarcomere assembly. *Dev. Cell.* 4:673–685.
- Shiota, C., J.T. Woo, J. Lindner, K.D. Shelton, and M.A. Magnuson. 2006. Multiallelic disruption of the rictor gene in mice reveals that mTOR complex 2 is essential for fetal growth and viability. *Dev. Cell.* 11:583–589.
- Soldi, R., S. Mitola, M. Strasly, P. Defilippi, G. Tarone, and F. Bussolino. 1999. Role of $\alpha v \beta 3$ integrin in the activation of vascular endothelial growth factor receptor-2. *EMBO J.* 18:882–892.
- Stanchi, F., R. Bordoy, O. Kudlacek, A. Braun, A. Pfeifer, M. Moser, and R. Fässler. 2005. Consequences of loss of PINCH2 expression in mice. *J. Cell Sci.* 118:5899–5910.
- Taverna, D., M.H. Disatnik, H. Rayburn, R.T. Bronson, J. Yang, T.A. Rando, and R.O. Hynes. 1998. Dystrophic muscle in mice chimeric for expression of $\alpha 5$ integrin. *J. Cell Biol.* 143:849–859.
- van der Flier, A., A.C. Gaspar, S. Thorsteinsdottir, C. Baudoin, E. Groeneveld, C.L. Mummery, and A. Sonnenberg. 1997. Spatial and temporal expression of the $\beta 1 D$ integrin during mouse development. *Dev. Dyn.* 210:472–486.
- Vasilcanu, D., A. Girmata, L. Girmata, R. Vasilcanu, M. Axelson, and O. Larsson. 2004. The cyclolignan PPP induces activation loop-specific inhibition of tyrosine phosphorylation of the insulin-like growth factor-1 receptor. Link to the phosphatidylinositol-3 kinase/Akt apoptotic pathway. *Oncogene.* 23:7854–7862.
- Volk, T., L.I. Fessler, and J.H. Fessler. 1990. A role for integrin in the formation of sarcomeric cytoarchitecture. *Cell.* 63:525–536.
- White, D.E., P. Couto, Y.F. Shi, J.C. Tardif, S. Nattel, R. St Arnaud, S. Dedhar, and W.J. Muller. 2006. Targeted ablation of ILK from the murine heart results in dilated cardiomyopathy and spontaneous heart failure. *Genes Dev.* 20:2355–2360.
- Zervas, C.G., S.L. Gregory, and N.H. Brown. 2001. *Drosophila* integrin-linked kinase is required at sites of integrin adhesion to link the cytoskeleton to the plasma membrane. *J. Cell Biol.* 152:1007–1018.

Figure S1



B

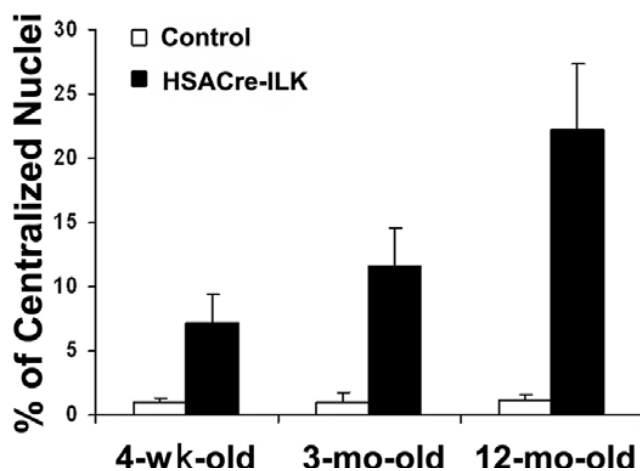


Figure S1 HSACre-ILK muscle displays centralized nuclei in different type of muscles. (A) Hematoxylin and eosin–stained paraffin sections of soleus, tibialis anterior (TA), and extensor digitorum longus (EDL) of 5-mo-old control and HSACre-ILK mice. Note the irregular diameter and centrally located nuclei (arrowheads) in myofibers of HSACre-ILK mice. Bar, 30 μ m. (B) The number of myofibers with central nuclei increased from $7.2 \pm 2.1\%$ in 4-wk-old HSACre-ILK mice, to $11.6 \pm 2.9\%$ in 3-mo-old HSACre-ILK mice, to $22.2 \pm 5.1\%$ in 12-mo-old HSACre-ILK mice, whereas the numbers in control mice were $1.0 \pm 0.3\%$, 1.1 ± 0.7 , and 1.2 ± 0.6 , respectively, at the ages analyzed. Data are expressed as mean \pm SD ($P < 0.01$).

Figure S2

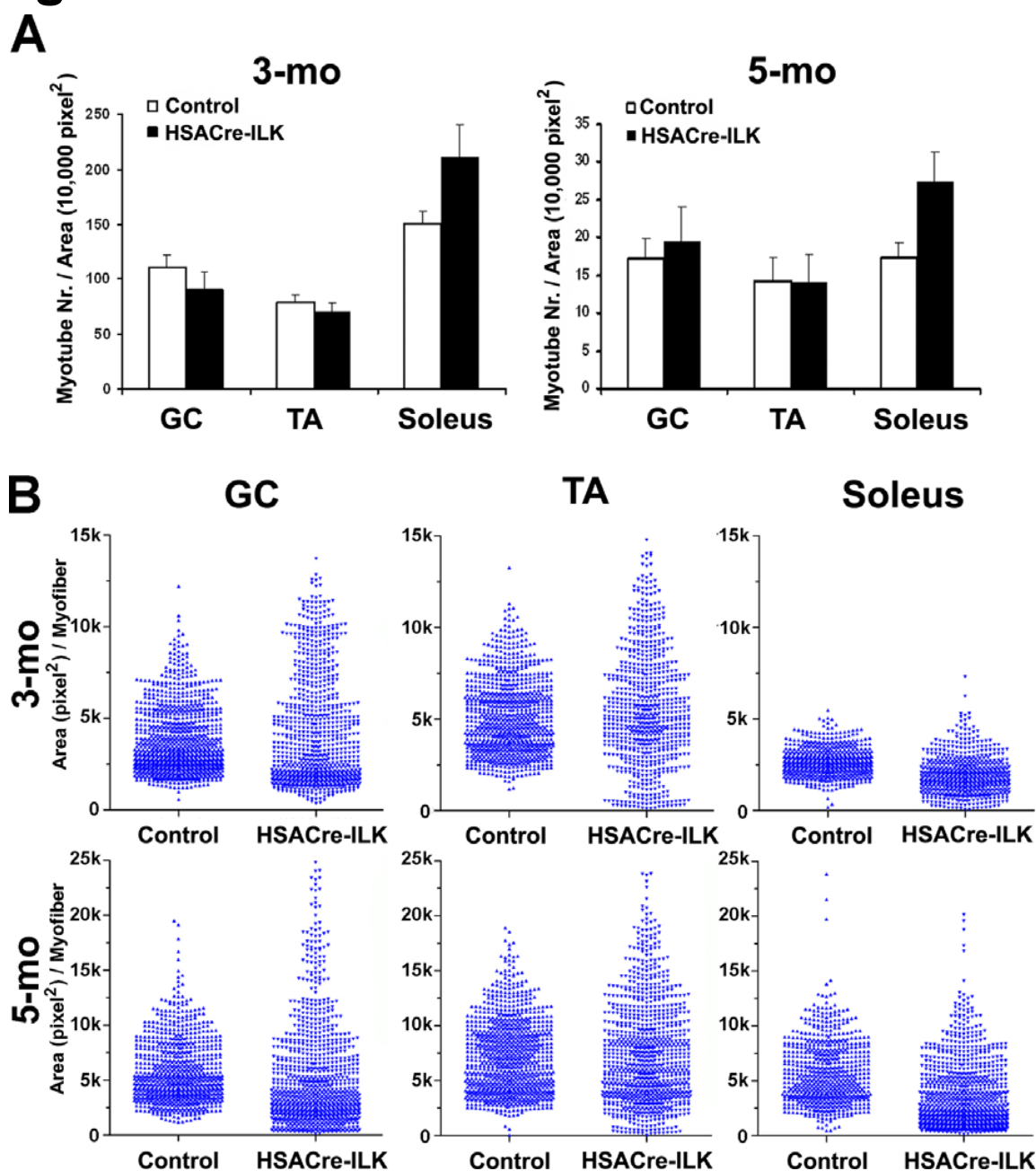


Figure S2. **Measurement of myofiber density and size.** (A) The density of myofibers was defined by the number of myofibers per area (10,000 pixel²). GC, tibialis anterior (TA), and soleus muscles from 3- and 5-mo-old control and HSACre-ILK mice were measured. The soleus myofiber density was 150.4 ± 11.6 and 210.6 ± 29.8 in 3-mo-old control and HSACre-ILK ($P < 0.001$) mice, respectively, and 17.5 ± 1.8 and 27.5 ± 3.9 in 5-mo-old control and HSACre-ILK ($P < 0.001$) mice, respectively. Data are expressed as mean \pm SD. (B) Myofiber size of GC, soleus, and TA muscles of 3- and 5-mo-old control and HSACre-ILK mice was measured by pixel² per myofiber and shown by dot-plots. The HSACre-ILK muscles show an altered distribution of fiber size with a prevalence of fibers with a smaller diameter.

Figure S3

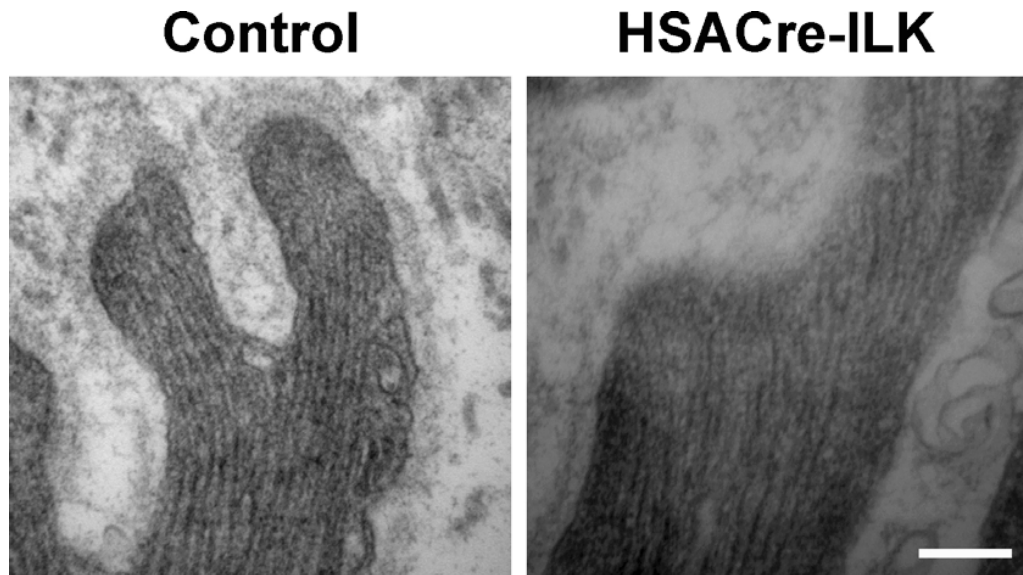


Figure S3. **Normal F-actin of control and HSACre-ILK sarcolemma.** Ultrastructural analysis of control and HSACre-ILK muscles. Bar, 150 nm.

Figure S4

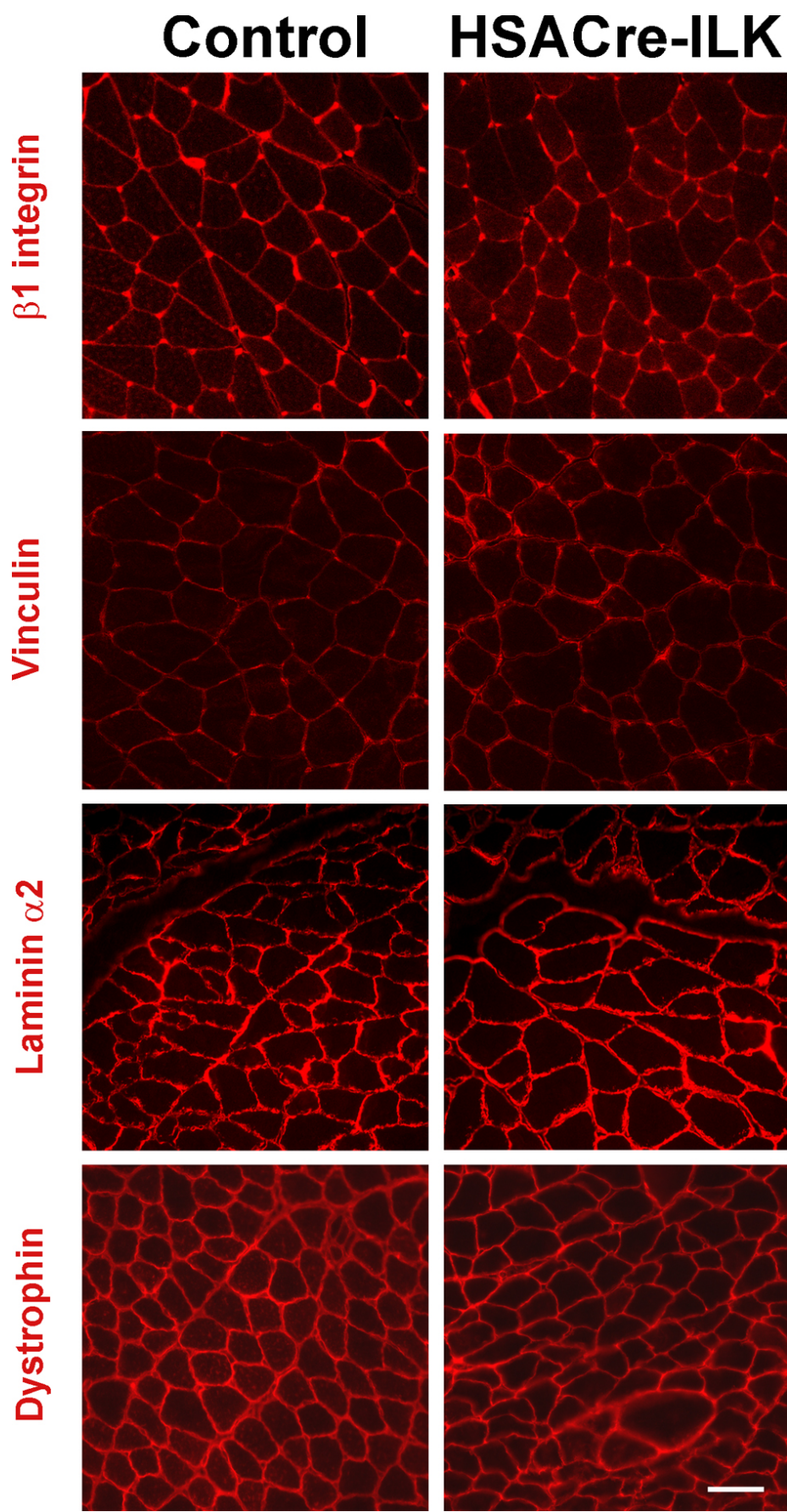


Figure S4. **Normal distribution and expression of $\beta 1$ integrin, vinculin, laminin $\alpha 2$, and dystrophin.** Immunofluorescence analysis of the control and HSACre-ILK muscle sections using $\beta 1$ integrin, vinculin, laminin $\alpha 2$, and dystrophin antibodies. Bar, 30 μm .

Figure S5

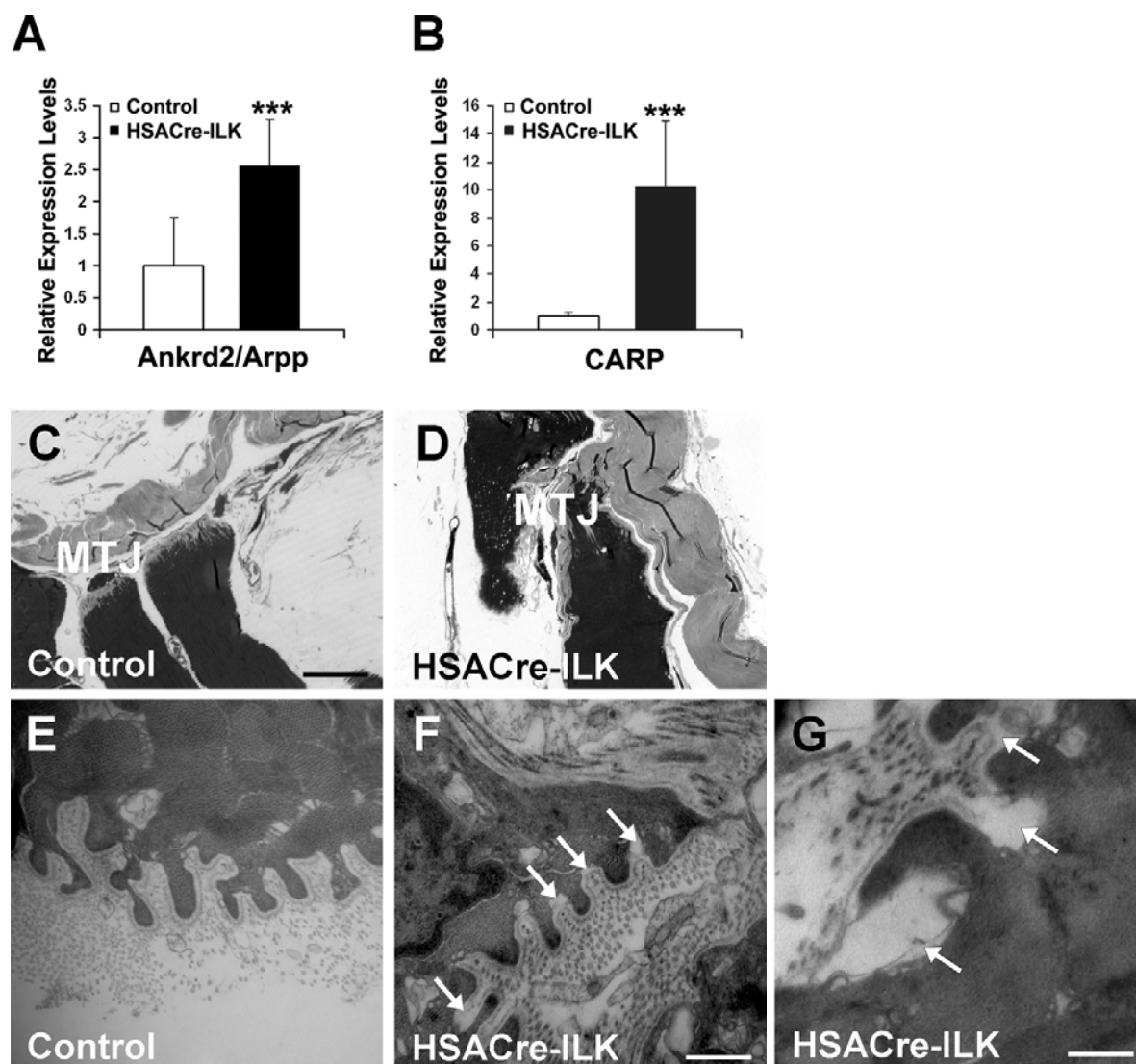
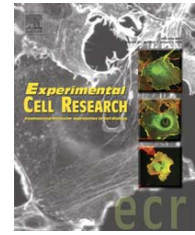


Figure S5. **Muscle damage and detachment of BM in trained HSACre-ILK muscle.** (A and B) Relative mRNA levels of Ankrd2/Arpp and CARP are shown, measured by quantitative PCR in GC muscle from trained control and HSACre-ILK mice. The levels of both Ankrd2/Arpp and CARP are significantly elevated in HSACre-ILK muscle. Data are expressed as mean \pm SD ($n = 3$; ***, $P < 0.001$). (C–G) Light (C and D) and electron (E–G) micrographs of skeletal muscle fibers of control (C and E) and HSACre-ILK (D, F, and G) mice. (C) Normal MTJ with regular short interdigitations. (D) HSACre-ILK MTJ lost the typical shape and shows cytoplasmic processes and invaginations with variable size and shape. (E–G) The fingerlike folds of MTJ are covered by a closely attached BM in trained control (E) muscle. The BM (arrows) is frequently detached at less affected fingerlike folds (F) and almost completely between irregularly shaped cytoplasmic processes of severely affected MTJ in HSACre-ILK (G) mice. Bars: (C and D) 35 μ m; (E and F) 900nm; (G) 1.4 μ m.

Paper II

available at www.sciencedirect.comwww.elsevier.com/locate/yexcr

Research Article

The Kindlins: Subcellular localization and expression during murine development

Siegfried Ussar^a, Hao-Ven Wang^a, Stefan Linder^b, Reinhard Fässler^a, Markus Moser^{a,*}

^aMax-Planck-Institute of Biochemistry, Department of Molecular Medicine, D-82152 Martinsried, Germany

^bInstitut für Prophylaxe und Epidemiologie der Kreislaufkrankheiten, Ludwig-Maximilians-Universität, 80336 Munich, Germany

ARTICLE INFORMATION

Article Chronology:

Received 28 March 2006

Revised version received

6 June 2006

Accepted 13 June 2006

Available online 29 June 2006

Keywords:

Kindler Syndrome

Integrins

Cell-cell adhesion

Cell-matrix adhesion

ABSTRACT

The three Kindlins are a novel family of focal adhesion proteins. The Kindlin-1 (URP1) gene is mutated in Kindler syndrome, the first skin blistering disease affecting actin attachment in basal keratinocytes. Kindlin-2 (Mig-2), the best studied member of this family, binds ILK and Migfilin, which links Kindlin-2 to the actin cytoskeleton. Kindlin-3 is expressed in hematopoietic cells. Here we describe the genomic organization, gene expression and subcellular localization of murine Kindlins-1 to -3. In situ hybridizations showed that Kindlin-1 is preferentially expressed in epithelia, and Kindlin-2 in striated and smooth muscle cells. Kindlins-1 and -2 are both expressed in the epidermis. While both localize to integrin-mediated adhesion sites in cultured keratinocytes Kindlin-2, but not Kindlin-1, colocalizes with E-cadherin to cell-cell contacts in differentiated keratinocytes. Using a Kindlin-3-specific antiserum and an EGFP-tagged Kindlin-3 construct, we could show that Kindlin-3 is present in the F-actin surrounding ring structure of podosomes, which are specialized adhesion structures of hematopoietic cells.

© 2006 Elsevier Inc. All rights reserved.

Introduction

The Kindlin gene family is named after the gene mutated in Kindler syndrome, an autosomal recessive genodermatosis in humans [1]. Kindlin-1 is a member of a new family of focal adhesion (FA) proteins. The family consists of three members in mice and men. The Kindlin proteins are composed of a centrally located FERM (Band 4.1/Ezrin/Radixin/Moesin) domain interrupted by a pleckstrin homology (PH) domain. The first member of this family was identified in a differential cDNA library screen as mitogen inducible gene-2 (Mig2 now termed Kindlin-2) [2]. The two other genes were initially named Unc-112 Related Protein 1 (URP1 now termed Kindlin-1) and URP2 (now termed Kindlin-3), due to their homology to the *Caenorhabditis elegans* gene *unc-112* [3]. Siegel et al. [5]

proposed to name the three different genes Kindlin-1 (URP1), Kindlin-2 (Mig2) and Kindlin-3 (URP2/Mig2B [4]), which we will also do throughout this article.

Kindlin-1 and Kindlin-2 have been shown to play an essential role in integrin-mediated adhesion and spreading. Both proteins localize to FAs and loss of either leads to delayed cell spreading in different cell lines [6,7]. These studies also showed that Kindlin-1 can interact with the cytoplasmic tails of $\beta 1$ and $\beta 3$ integrins and Kindlin-2 with the integrin-linked kinase (ILK). Binding partners for Kindlin-3 are not known. The ability of Kindlin-2 to bind Migfilin, a LIM domain containing protein capable of binding Filamin, revealed a novel linkage between integrins and the actin cytoskeleton [7]. Whether Kindlin-1 also binds Migfilin has not been investigated yet, although the high homology

* Corresponding author.

E-mail address: moser@biochem.mpg.de (M. Moser).

between Kindlin-1 and Kindlin-2 makes such a binding activity very likely [8].

Genetic studies have so far been performed in humans and *C. elegans*. Null mutations of the Kindlin orthologue Unc-112 in nematodes are embryonic lethal due to a paralyzed arrested elongation at twofold (PAT) phenotype. Unc-112 localizes together with PAT3/ β -integrin and PAT4/ILK to dense bodies and M-lines at muscle attachment sites, which link the muscle to the body wall. Loss of Unc-112 impairs cell–matrix adhesion and integrin function resulting in muscle detachment from the body wall and severe paralysis [9].

Loss of Kindlin-1 in humans gives rise to Kindler syndrome. Kindler syndrome patients show different skin pathologies that undergo changes during the patients' lifetime. The syndrome is characterized by skin atrophy and trauma-induced skin blisters at early life. During infancy, the blistering becomes less and instead photosensitivity and progressive poikiloderma develops. In addition, there are indications that Kindler Syndrome patients may be prone to squamous cell carcinoma development [10]. Kindler Syndrome is the first skin blistering disease resulting from defects in actin cytoskeleton anchorage to cell matrix adhesion sites [5,11,12,13]. However, the molecular mechanism leading to the multiple defects of Kindler Syndrome is only poorly understood and simple actin anchorage insufficiencies cannot completely explain the phenotype.

Several reports describe a transcriptional misregulation of Kindlins in various types of cancer. Kindlin-1 is overexpressed in lung and colon carcinomas, whereas Kindlins-2 and -3 were unchanged or even reduced [3]. Kindlin-2 expression has been shown to be elevated in leiomyomas and greatly decreased in leiomyosarcomas [14]. Interestingly, an almost exclusive nuclear staining of Kindlin-2 was observed in both tumors, suggesting additional functions of Kindlin-2. This observation is of note since Migfilin has been shown function in the nucleus as transcriptional coactivator during cardiomyocyte differentiation in mice [15]. Finally, increased expression of Kindlin-3 has been reported in different kinds of B cell lymphomas [4]. However, the molecular role of Kindlin proteins during tumor formation is so far completely unclear.

In the present paper, we report the expression of the three Kindlins during murine development and in adult tissues and characterize their subcellular localization in different cell types.

Materials and methods

Northern blotting

Total RNA was extracted with Trizol (Invitrogen) following the manufacturer's protocol. Total RNA (8 μ g) was separated on a denaturing agarose gel and transferred to Hybond N+ membranes (Amersham). The following primers were used to amplify the Kindlin probes:

Kindlin-1 forward: TCTGAGGTTGACGAGGTTAG (Exon 6);
Kindlin-1 reverse: ACTTCATTCATACCATCAGC (Exon 9);
Kindlin-2 forward: CTAGATGACCAGTCTGAAGACG (Exon 4);
Kindlin-2 reverse: TGAATCGGAGCAGCAAGGCC (Exon 6);

Kindlin-3 forward: GAGAAGGAGCCTGAAGAGGAG (Exon 4);
Kindlin-3 reverse: TAAATCGCAGCCAAAGCACATC (Exon 6).

The amplified probes were radiolabeled using the Redi-Prime II random prime labeling kit (Amersham). Membranes were hybridized overnight at 65°C in Church buffer, washed and exposed for 1–8 days at –80°C with Kodak Biomax MS screens (Kodak).

RT-PCR

Total RNA (1 μ g) was used for first strand cDNA synthesis according to the protocol of the manufacturer using Super-Script III polymerase (Invitrogen) and random hexamer primers. Specific cDNA fragments were amplified using the following primers:

Kindlin-1 forward: CTACACCTTCTTTGACTTG;
Kindlin-1 reverse: AGGGATGTCAGTTATGTC.
Kindlin-2 forward: GTACCGAAGTAGACTGCAAGG;
Kindlin-2 reverse: CATACGGCATATCAAGTAGGC.
Kindlin-3 forward: AGCTGTCTCTGCTGCGTGCTC;
Kindlin-3 reverse: ATACCTTGCTGCATGAGGCAC.

Radioactive in situ hybridization

³³P-UTP-labeled sense and antisense riboprobes were generated by in vitro transcription from linearized vectors containing Kindlins-1/-2/-3-specific cDNA fragments (see Northern Blotting). Paraffin sections from mouse embryos at different embryonic stages were dewaxed, rehydrated and hybridized as previously described [16].

Antibody production and affinity purification

A Kindlin-3-specific peptide (EPEEEVHDLTKVFLA; aa 156–170) was coupled to Imject Maleimide Activated mCKLH (Pierce) and used to immunize rabbits. The antiserum was subsequently affinity purified using a commercial kit (SulfoLink Kit, Pierce Biotechnology Inc., Rockford, IL, USA). High affinity antibodies were eluted from the column using 100 mM Glycine buffer, pH 2.7 and then dialyzed against phosphate-buffered saline (PBS).

Western blotting

Both cells and tissues from adult C57BL/6 mice were homogenized in lysis buffer (1% Triton X-100, 50 mM Tris–Cl pH 7.4, 300 mM NaCl, 5 mM EDTA and protease inhibitors (Roche)). Equal amounts of total protein (about 20 μ g) per lane were separated on a 10% polyacrylamide gel and transferred to PVDF membranes (Millipore). Kindlin-3 (1:1000), tubulin (1:5000), GAPDH antibodies (1:5000; Chemicon) were used together with the appropriate secondary antibody (1:50000 in 5% bovine serum albumin (BSA); Biorad).

Constructs

All Kindlin cDNAs were cloned into the pEGFP-C1 vector (Clontech). A partial Kindlin-1 cDNA was obtained from Image

clone 3157716. The missing N-terminal part was amplified from epidermal cDNA by PCR using CAGGTCGAC-CATCTGCCTGGGCCACAATG as forward primer and CAAGT-CAAAGAAGGTGTAG as reverse primer. Kindlin-2 full-length cDNA was obtained from Image clone 3596509. Kindlin-3 was cloned by amplifying a 558 bp fragment from the N-terminus (CAGGTCGACATGGCGGTATGAAGACAG; AGAA-GTGTGCTGGCATGC) containing the start codon combined with the residual nucleotides from the Image clone 4187161. Final expression constructs were confirmed by sequencing.

Immunostaining

Paraffin sections were dewaxed, rehydrated and endogenous peroxidase was blocked by incubating the slides for 20 min in 2.5 ml H₂O₂/75 ml methanol. Blocking was performed for 1 h in PBS supplemented with 10% goat serum and 1% BSA. Subsequently, the Kindlin-3 antibody (1:500) was incubated at 4°C over night. Sections were incubated with a 1:200 dilution of biotinylated anti-rabbit secondary antibody for one hour and transferred to ABC solution (Vector Laboratories) for an additional 30 min. Secondary antibody was detected with diaminobenzidine (DAB). Counterstaining of the sections was performed with methylene green and sections were mounted with Entellan.

Immunohistochemistry

Cells were grown on fibronectin (5 µg/ml, Calbiochem) coated glass cover slips, fixed with PBS supplemented with 4% paraformaldehyde (PFA) and 3% sucrose, permeabilized with 0.25% Triton X-100 in PBS for 10 min, blocked in PBS containing 3% BSA and 5% goat serum for 1 h. Cells were immunostained for paxillin (monoclonal antibodies, BD Transduction), α -actinin (monoclonal antibodies, Sigma), vinculin (monoclonal antibodies, Sigma) and TRITC-labeled phalloidin (1:500; Sigma) to visualize F-actin. Alexa647 and Cy3-conjugated secondary antibodies were purchased from Molecular Probes. Stained cells were mounted in Elvanol and pictures were taken with a Leica DMRA2 microscope and a Hamamatsu camera.

Transfections

Immortalized wild-type mouse embryonic fibroblasts, mouse keratinocytes, primary cardiomyocytes and dendritic cells were transfected with the EGFP-Kindlin-1, EGFP-Kindlin-2 and EGFP-Kindlin-3 cDNA constructs using Lipofectamine 2000 (Invitrogen) following the manufacturer's instructions.

Cell culture

Primary wild-type macrophages and dendritic cells were derived from bone marrow of 5-day-old mice and cultured on bacterial petri dishes for 7 days in DMEM, supplemented with glutamine, 10% FCS, Pen/Strep (all Invitrogen), M-CSF (to derive macrophages) or GM-CSF (to generate dendritic cells). Both cytokines were derived from a hybridoma supernatant. The supernatant was used in a 1:10 dilution.

Immortalized newborn mouse keratinocytes were maintained in MEM supplemented with 5 µg/ml insulin (Sigma),

10 ng/ml EGF (Roche), 10 µg/ml transferrin (Sigma), 10 µM phosphoethanolamine (Sigma), 10 µM ethanolamine, 0.36 µg/ml hydrocortisone (Calbiochem), glutamine (Invitrogen), Pen/Strep (Invitrogen), 45 µM CaCl₂ and 8% chelated FCS. For differentiation keratinocytes were cultured in growth medium containing 1 mM CaCl₂ over night. Immortalized mouse embryonic kidney fibroblasts were maintained in DMEM supplemented with 10% FCS.

Isolation and culture of neonatal mouse cardiomyocytes

Cardiomyocytes were isolated from hearts of P1 newborn mice by treatment with 0.4 mg/ml collagenase II (Worthington, Freehold, NJ) and 1 mg/ml pancreatin (Sigma) in ADS buffer (116 mM NaCl, 0.8 mM NaH₂PO₄, 1 g/l glucose, 5.4 mM KCl, 0.8 mM MgSO₄ and 20 mM 2,3-butanedione monoxime in 20 mM HEPES, pH 7.35) for 10 min at 37°C. Fresh enzyme solution (0.3 ml/heart) was added and tissue was incubated for 8 min. The supernatant containing dispersed cardiac cells was transferred to a new tube containing 1 ml FCS (per heart) and centrifuged at low speed (80×g, 6 min), resuspended in 2 ml FCS and kept at 37°C. The remaining tissue fragments were incubated with fresh enzyme solution (0.3 ml/heart) as above for additional 5 times. Cell suspensions were pooled and centrifuged at low speed (80×g, 6 min) and resuspended in 4 ml ADS buffer.

Cells were grown on glass coverslips coated with fibronectin (10 µg/ml) at a cell density of 3.0×10⁵ cells/35-mm culture dish in plating medium (67% DMEM, 17% M199 medium, 10% horse serum, 5% FCS, 1% Pen/Strep and 4 mM glutamine). Cells were incubated at 37°C in a 5% CO₂ humidified incubator. The next day the plating medium was replaced with maintenance medium (75% DMEM, 23.5% M199 medium, 0.5% horse serum, 1% Pen/Strep, 4 mM glutamine and 0.1 mM phenylephrine).

MAC sorting of primary T and B cells

A whole spleen from an adult C57BL/6 mouse was strained to obtain a single cell suspension. 3×10⁷ cells were incubated in 300 µl PBS with 3 µl FITC conjugated B220 (PharMingen) and CD3 (eBioscience) antibodies for 10 min at 4°C. Cells were washed with PBS and incubated with 30 µl anti-FITC MACS-beads (Miltenyi Biotec) for 10 min, washed with PBS, isolated in a magnetic field and eluted from beads, following the manufacturer's recommendations.

Results and discussion

Genomic organization of the murine Kindlin gene family

All three murine Kindlin genes were identified in a genomic search of the Ensembl database using the human Kindlin cDNAs. The chromosomal localization of the three human and murine Kindlin genes is shown in Table 1. The human as well as the murine Kindlin genes are composed of 15 exons with the translation start site in exon 2. The murine Kindlin-1 gene spans 38.5 kb resulting in a transcript of approximately 4.6 kb. The murine Kindlin-2 gene has a length of 70 kb and gives rise

Table 1 – Genomic localization of the human and murine Kindlin genes

	Mouse	Human
Kindlin-1	2F2	20p12.3
Kindlin-2	14B	14q22.1
Kindlin-3	19A	11q13.1

to a 3.2 kb transcript. Kindlin-3 represents the smallest gene with 19.8 kb encoding a 2.5 kb mRNA.

Kindlin protein structure

Translation of the murine cDNAs results in proteins of 637 aa (Kindlin-1), 680 aa (Kindlin-2) and 655 aa (Kindlin-3), respectively. A sequence alignment between the three murine Kindlin proteins revealed that Kindlins-1 and -2 are most closely related, sharing 60% identity and 74% similarity, while Kindlin-3 is more distantly related sharing 53% identity and 69% similarity to Kindlin-1 and 49% identity and 67% similarity to Kindlin-2.

Kindlin proteins have a unique domain architecture. They are composed of a centrally located FERM domain interrupted

by a PH domain [6]. FERM domains are found in a number of proteins linking the membrane to the cytoskeleton [17]. Among these proteins, the FERM domain of talin is most homologous to the Kindlin FERM domains. In vitro assays have shown an interaction between Kindlin-1 and the cytoplasmic tails of $\beta 1$ and $\beta 3$ integrins [6]. Therefore, it has been proposed that Kindlins bind to $\beta 1$ and $\beta 3$ integrins with a similar mechanism as it has been described for talin [18,19].

The second common domain within Kindlins is the PH domain. Although PH domains are known to mediate binding to phosphatidylinositol phosphates [20], the function and specificity of this domain have not been further characterized in Kindlin proteins.

A nuclear localization signal (NLS), amino acids 55–72, is exclusively present in Kindlin-2 only. In accordance with this finding, nuclear localization of Kindlin-2 has been reported in leiomyosarcomas and leiomyomas. Furthermore, the Kindlin-2 interacting protein Migfilin can localize to the nucleus. There it functions as a coactivator for the CSX/NKX2-5 transcription factor to promote cardiomyocyte differentiation [14].

Taken together, Kindlin proteins are typical adaptor proteins with two domains known to mediate membrane association. However, both the molecular regulation of

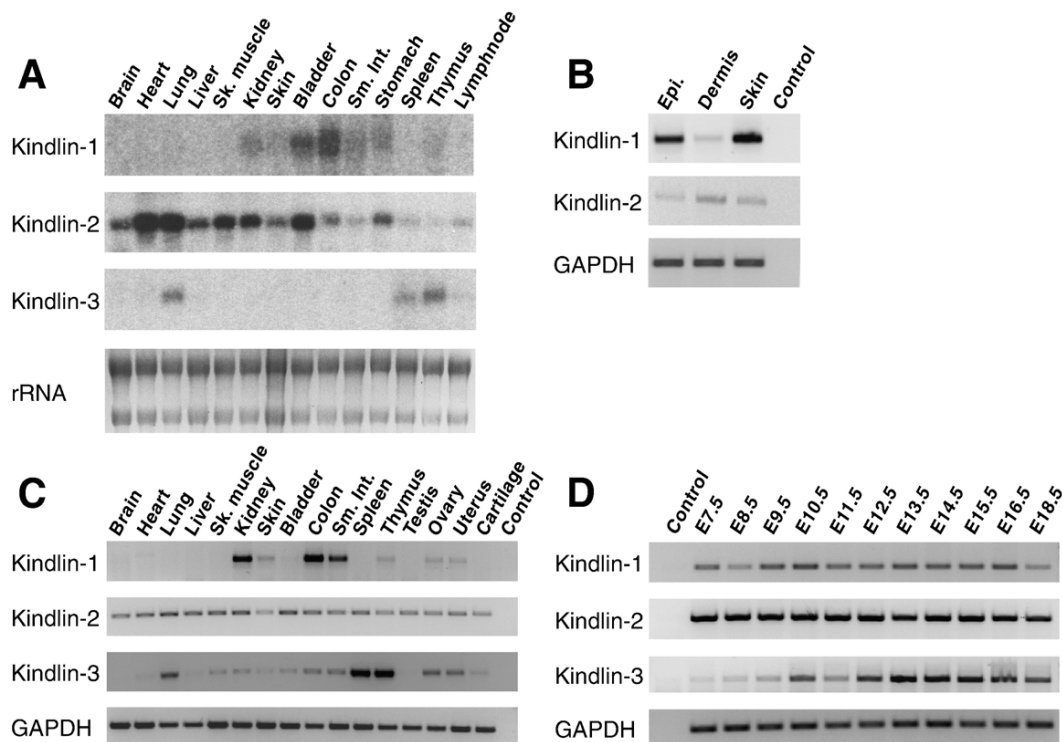


Fig. 1 – Expression pattern of Kindlins-1/-2/-3. (A) Northern blot from different tissues. Total RNA was extracted from organs of 2-week-old C57BL/6 mice. Staining of ribosomal RNA with ethidium bromide was used to control loading. **(B)** Skin from adult C57BL/6 mice was separated into epidermis and dermis by trypsin digestion and total RNA was reverse transcribed to detect differential expression of Kindlin-1 and Kindlin-2 in epidermis, dermis and whole skin. **(C)** Total RNA from 2-week-old C57BL/6 mice was reverse transcribed into cDNA and expression of the three Kindlins was checked by RT-PCR. GAPDH was used as loading control. **(D)** Total RNA was extracted from total embryos at different embryonic stages. RT-PCR was performed for all three Kindlins with cDNA derived from the total RNA. GAPDH was used to show equal loading. Sk. muscle: skeletal muscle; Sm. Int.: small intestine; Epi: epidermis.

Kindlin proteins and the specific binding of certain interactors to individual Kindlin proteins are only poorly understood.

Expression patterns of murine Kindlin-1 to -3 in adult tissues and during embryonic development

The tissue distribution of the murine Kindlin genes was analyzed by multiple tissue Northern blots and RT-PCR of total RNA from 2-week-old mice using specific cDNA fragments and primer pairs (Fig. 1A). The specificity of the cDNA probes was confirmed in a Southern blot containing all three murine Kindlin cDNAs (data not shown).

Kindlin-1 transcripts were detected in bladder and colon and at lower expression levels in kidney, skin, small intestine, stomach and thymus with Northern blot assays. RT-PCR revealed additional weak Kindlin-1 expression in ovary and uterus. Recently, a larger splice variant of Kindlin-1 was detected in human intestine [5]. This isoform is generated by including intron 7 into the coding sequence and was recently found in a thymus cDNA (AK_030947). This alternative splicing event gives rise to a 5.2 kb transcript, a premature translation stop, and a short protein isoform of 352 amino acids. Using primer pairs located in exon 6 and intron 7 we could detect the long transcript in kidney, colon and small intestine (data not shown). The existence of this isoform became also apparent in our Northern blots, which revealed a second, approximately 5.2 kb large transcript in colon and small intestine (Fig. 2A). Since no antibody against the N-terminus of Kindlin-1 is currently available, it remains to be seen whether this transcript is translated and if so, which function this short Kindlin-1 protein might fulfil.

Since there is a strong interest in a detailed expression analysis of Kindlin-1 in skin, we separated epidermis from dermis. RT-PCR analysis indicated strong expression of

Kindlin-1 in the epidermis, and much weaker expression in the dermis (Fig. 1B). Whether the dermal expression is indeed derived from dermal cells or alternatively from hair follicle keratinocytes is unclear. Interestingly, Kindlin-2 is inversely expressed, with higher expression levels in the dermis than in the epidermis (Fig. 1B). This finding is particularly interesting, since Kindlin-2 seems not to compensate for the loss of Kindlin-1 in Kindler Syndrome. Whether this is due to the distinct expression in different cell layers of the skin or because of differences in the subcellular localization of both proteins within the keratinocytes needs to be addressed in the future.

Northern blot and RT-PCR analyses confirmed Kindlin-2 expression in all tissues analyzed. The levels differed between tissues and were high in heart, lung, skeletal muscle, kidney, bladder and stomach. In contrast to the broad expression pattern of Kindlin-2, Kindlin-3 showed a restricted expression pattern with signals in lung, spleen, thymus and very low in lymph nodes (Fig. 1A). RT-PCR confirmed a strong Kindlin-3 expression in hematopoietic tissues and much lower in other tissues, which may be due to contamination of these tissues by blood cells (Fig. 1C).

Expression of Kindlin genes during embryonic development was tested by RT-PCR from RNA samples derived from E7.5 to 18.5 embryos. All Kindlin genes are expressed throughout the analyzed time points, although Kindlin-3 expression was low at E7.5 and increases until E13.5 (Fig. 1D).

To determine the distribution of the Kindlin mRNAs during mouse development, we performed radioactive in situ hybridizations on mouse embryo sections from different developmental stages.

The same probes that were used for Northern blot experiments were subcloned into pBluescript to derive sense and antisense transcripts. As expected from the RT-PCR and

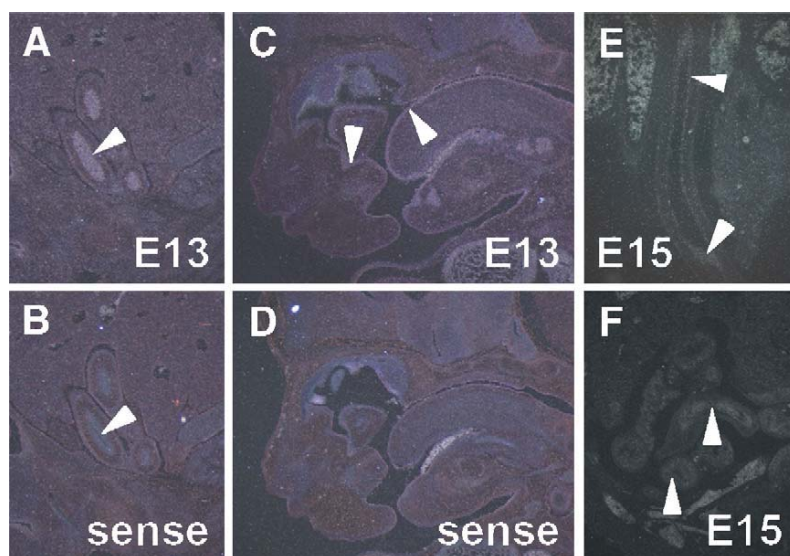


Fig. 2 – Radioactive in situ hybridizations on E13 and E15 mouse embryo sections reveal Kindlin-1 expression in the developing gut epithelium (arrowhead in panel A) and epithelium of the oral cavity and tongue at E13 (arrowheads in panel C). Consecutive sections hybridized with the sense probe indicate signal specificity (B, D). At E15, Kindlin-1 expression is found in the oesophageal epithelium (E) and gut epithelium (F).

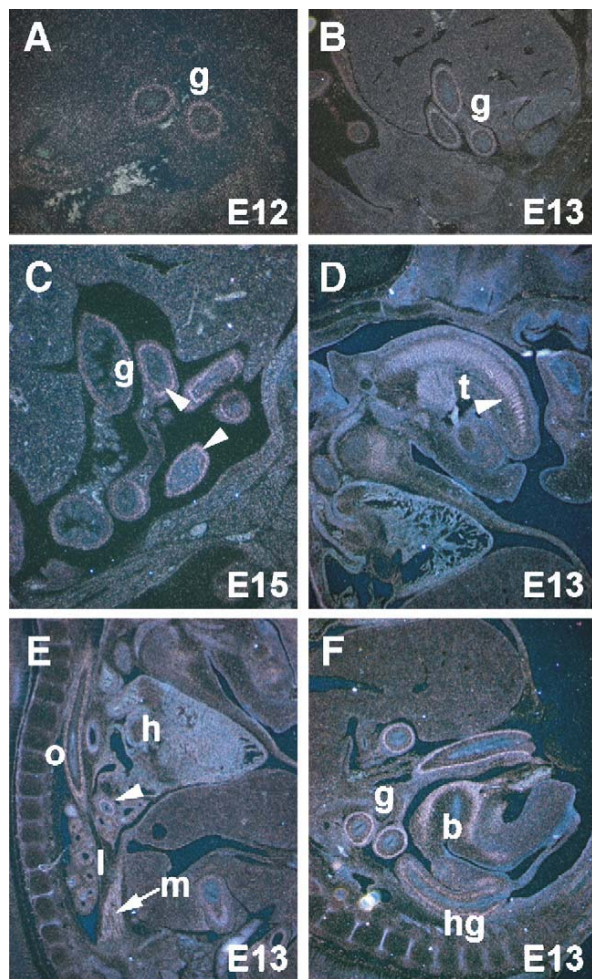


Fig. 3 – In situ hybridizations reveal Kindlin-2 expression in all three muscle types. Kindlin-2 is expressed in the smooth muscle layer of the developing gut at E12 (A), E13 (B) and E15 (C). In addition, Kindlin-2 expression is found in the smooth muscle layers surrounding the oesophagus (E), large vessels (arrowhead in panel E), around the bronchial epithelium of the lung (E), in the bladder and hindgut (both F). Expression in skeletal muscle is seen in the tongue and the diaphragm (D,E). A weaker signal is detected in cardiac muscle (E). b, bladder; g, gut; h, heart; hg, hindgut; l, lung; m, skeletal muscle; o, oesophagus; t, tongue.

Northern blot analyses, Kindlin-1 expression was hardly detected in the embryo. Weak signals could be detected in the epithelium of the gut from E12.5 onwards, as well as in the oral epithelium and oesophagus. Control hybridizations with the sense probe revealed no signal in these organs (Fig. 2). All attempts to detect Kindlin-1 in other embryonic or adult tissues were unsuccessful.

In contrast, Kindlin-2 expression was seen in many organs with strongest expression in the not sooth but smooth muscle cell layer of a number of organs including the developing gut, bladder, oesophagus and blood vessels (Fig. 3). Strong expression was also found in striated muscle such as tongue and

heart. In agreement with Northern blot and RT-PCR data, Kindlin-3 expression was restricted to hematopoietic organs such as the fetal liver and thymus. Interestingly, between E12.5 and E16.5 Kindlin-3 signals were detectable throughout the whole liver with strong signals in large multinucleated cells that most likely represent megakaryocytes (Figs. 4A–F). Weak staining was detected in the thymus (Figs. 4G, H). Based on the restricted expression of Kindlin-3 in adult hematopoietic tissues, the uniform signal in the embryonic liver was likely derived from lymphoid progenitor cells rather than from hepatocytes. In line with this notion, neither Northern blot nor RT-PCR revealed Kindlin-3 expression in adult liver (Figs. 1A and C).

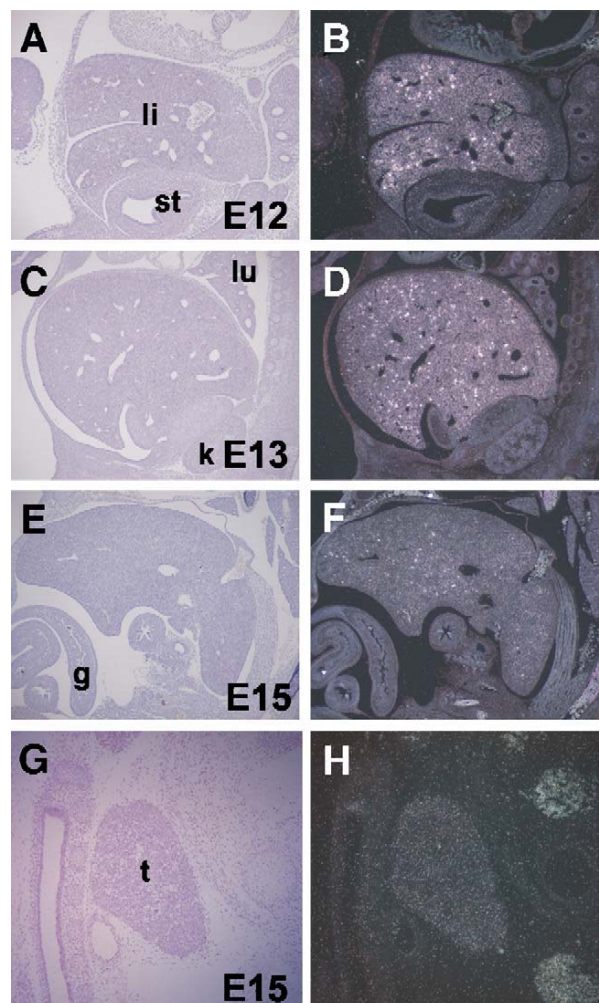


Fig. 4 – In situ hybridizations on sagittal sections of murine embryos at E12 (A, B), E13 (C, D), and E15 (E–H). Panels A, C, E, and G show brightfield views of panels B, D, F, and H, respectively. Kindlin-3 expression is mainly restricted to the developing liver with particularly strong signals in large multinucleated cells, most likely representing megakaryocytes (A–F). (G,H) Kindlin-3 is also expressed in thymus at E15. g, gut; k, kidney; li, liver; lu, lung; st, stomach; t, thymus.

Altogether these data indicate that Kindlin-1 expression is confined to epithelial cells of the skin and gut, Kindlin-2 expression is broad with high expression in striated and smooth muscle cells and Kindlin-3 expression is restricted to hematopoietic tissues.

Kindlin-3 is expressed in different hematopoietic cell types and is localized to podosomes

To date, the Kindlin-3 protein has not been investigated in any study. Therefore we generated a rabbit polyclonal antiserum against Kindlin-3 (see Materials and methods). The affinity purified antibody reacted with an approximately 100 kDa protein from mouse embryonic fibroblasts transfected with EGFP-tagged murine Kindlin-3 cDNA. As a control, cell lysates from fibroblasts transfected with EGFP-Kindlin-1 or -2 constructs showed no crossreactivity with the Kindlin-3 antibody (Fig. 5A). The anti-Kindlin-3 antibody was then used to immunoblot lysates derived from multiple organs of adult C57BL/6 mice. In accordance with the RNA data Kindlin-3 protein could be detected in spleen, thymus, lymph node and lung (Fig. 5B).

Due to this very broad expression pattern of Kindlin-3 within hematopoietic tissues, we addressed the expression in different hematopoietic cell types. Western Blots from MACS sorted T and B cells and in vitro differentiated macrophages, immature and mature dendritic cells were performed. Interestingly, Kindlin-3 was expressed in all these hematopoietic cell types at similar levels and seems not to be restricted to a specific hematopoietic lineage (Fig. 5C). Since Northern blot and RT-PCR analyses revealed weak expression of Kindlins-1 and -2 in spleen and thymus, we investigated expression of both genes in different hematopoietic cell types by RT-PCR. Interestingly, both Kindlins-1 and -2 are expressed in T cells and very weak in B cells (Fig. 5D).

Furthermore, the anti-Kindlin-3 antibody was used for immunohistochemical stainings of mouse embryo sections. The Kindlin-3 protein was observed in the developing liver with particularly high signals in megakaryocytes (Fig. 5E), confirming our in situ hybridization data (Figs. 4A-F).

To investigate the subcellular localization of Kindlin-3, we first overexpressed EGFP-tagged Kindlin-3 in murine fibroblasts. Unexpectedly, we could not observe any specific localization to FA but rather a diffuse cytoplasmatic staining

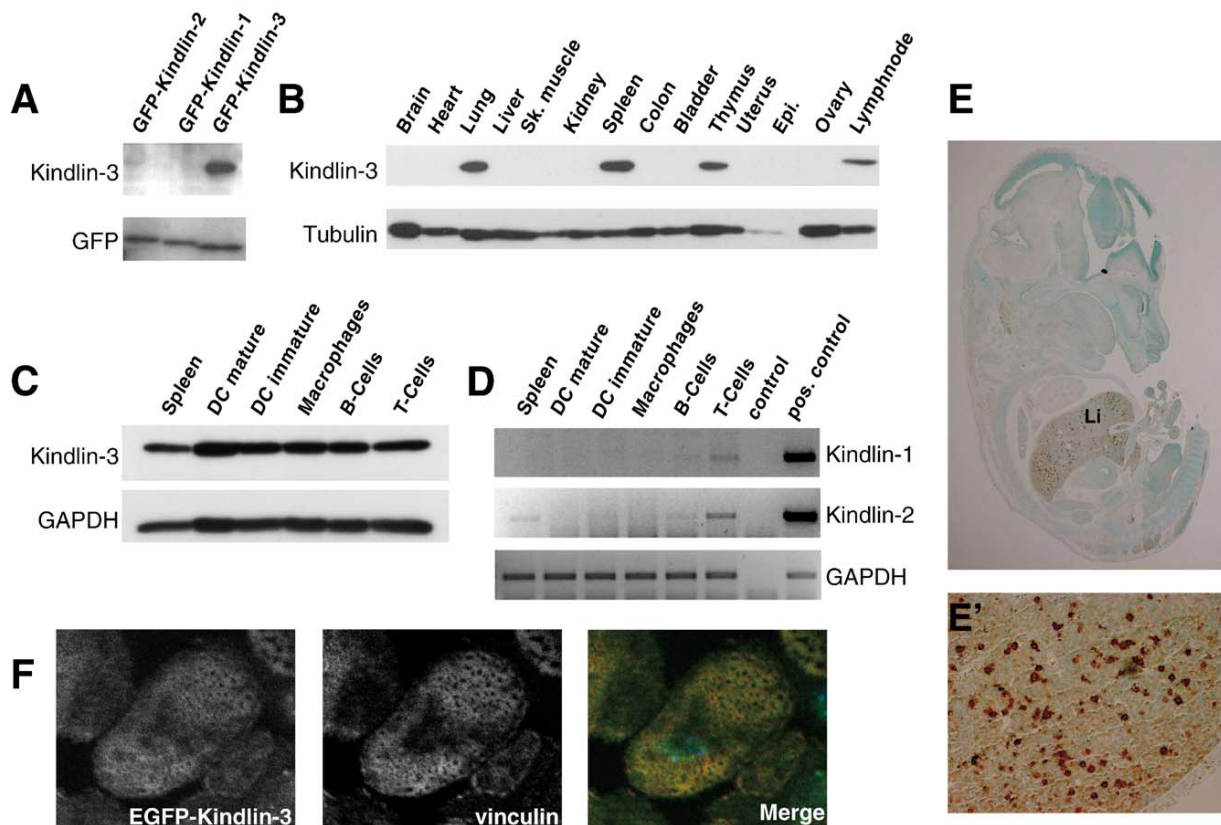


Fig. 5 – Hematopoietic expression pattern and typical subcellular localization of Kindlin-3. (A) Western blot of NIH3T3 cells transfected with EGFP-Kindlins-1/-2/-3 with the Kindlin-3 antibody. A GFP antibody was used to control loading. (B) Western blot of different mouse tissues from adult C57BL/6 probed with the Kindlin-3 antibody. Tubulin was used to control loading. (C) Western blot for Kindlin-3 from different hematopoietic cell types (DC: dendritic cells). GAPDH was used to control loading. (D) RT-PCR for Kindlin-1 and Kindlin-2 from different hematopoietic cell types. GAPDH was used to control loading. (E) Immunostaining of E14.5 embryo sections with Kindlin-3 antibody (Li: liver). (E') Higher magnification of the liver. (F) EGFP-Kindlin-3 colocalizes with vinculin in podosomes of cultured dendritic cells.

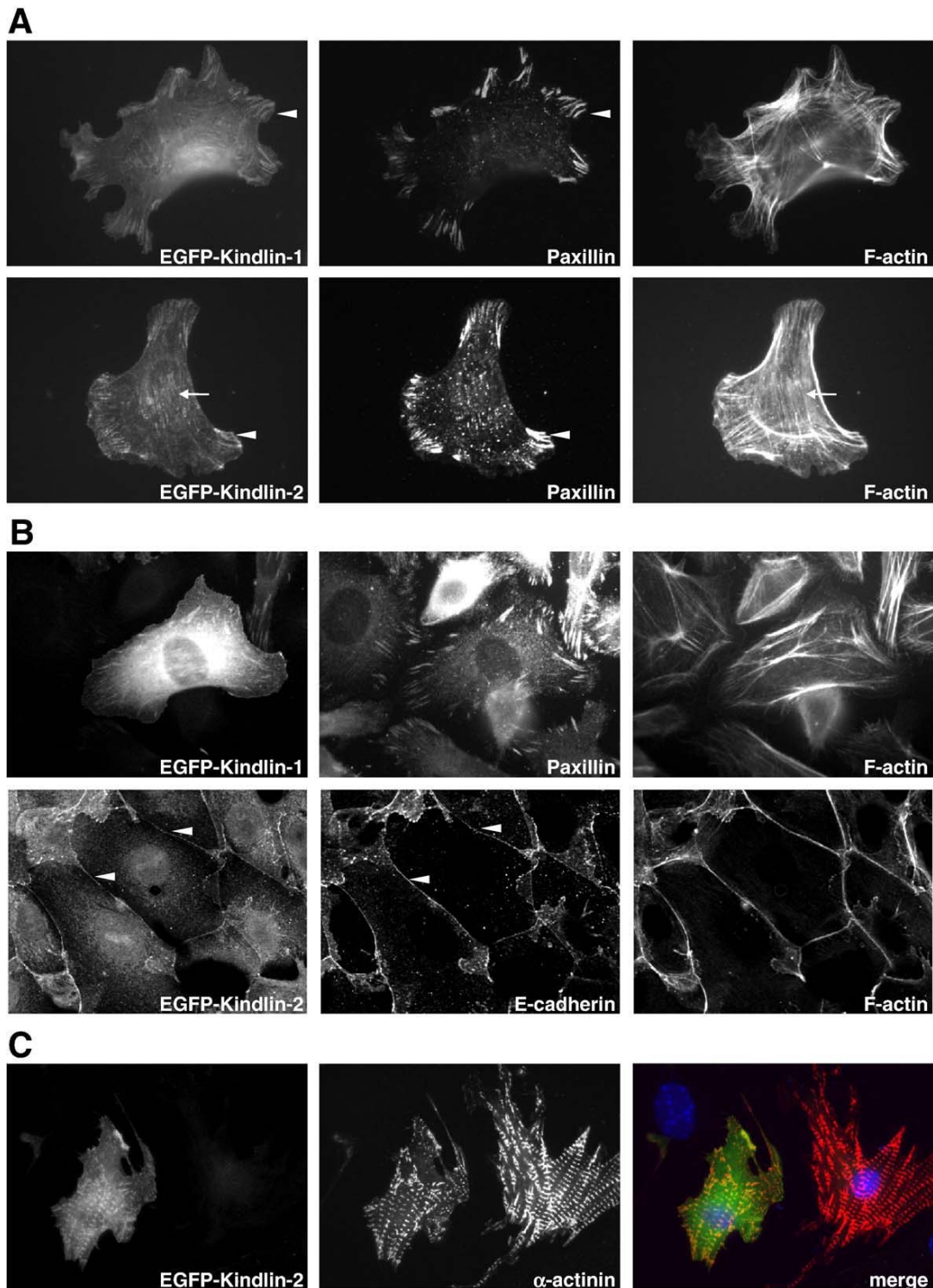


Fig. 6 – Subcellular localization of Kindlin-1 and Kindlin-2. (A) Mouse embryonic fibroblasts (MEFs) were seeded onto fibronectin and transiently transfected with EGFP-Kindlin-1 and EGFP-Kindlin-2, respectively. 24 h after transfection cells were costained for paxillin and F-actin. Arrowheads indicate focal adhesion sites. Arrows indicate colocalization with F-actin. (B) Spontaneously immortalized mouse keratinocytes were transiently transfected with EGFP-Kindlin-1. Cells were costained for paxillin and F-actin. EGFP-Kindlin-2 transfected cells were differentiated with 1 mM CaCl_2 overnight, and costained for E-cadherin and F-actin. Arrowheads show colocalization of EGFP-Kindlin-2 and E-cadherin at cell-cell contacts. (C) Primary mouse cardiomyocytes were transfected with EGFP-Kindlin-2 and after fixation costained with α -actinin.

(data not shown). This indicates that either Kindlin-3 differs in its localization from the other two family members or cannot compete with the endogenous Kindlin-2 for FA recruitment in these cells. Kindlin-1 and Kindlin-3 expression could not be detected in these cells by RT-PCR (data not shown). Therefore, we used immunofluorescence stainings of in vitro differentiated macrophages and dendritic cells. In contrast to fibroblasts or epithelial cells, hematopoietic cells do not form classical FA. Instead, they form podosomes, adhesion structures characterized by a core of F-actin and actin-associated proteins surrounded by a ring consisting of plaque proteins such as talin or vinculin (reviewed in [21] and [22]). Coimmunofluorescence stainings with phalloidin revealed that Kindlin-3 colocalizes to podosomes (data not shown). Therefore, a more detailed analysis of Kindlin-3 localization within podosomes was performed. Transfection of immature dendritic cells with EGFP-Kindlin-3 and subsequent staining for vinculin (Fig. 5F) and talin (data not shown) revealed Kindlin-3 localization to the actin surrounding ring of podosomes. Altogether these data show that Kindlin-3 is present in hematopoietic adhesion complexes and expressed in multiple hematopoietic cell lineages.

Kindlins-1 and -2 localize to different cell adhesion sites

Previous studies have localized human Kindlin-1 and Kindlin-2 to FAs. Using EGFP-tagged cDNA constructs transiently transfected into mouse embryonic fibroblasts, we tested the localization of murine Kindlins. Transfection of neither Kindlin constructs nor the EGFP control affected cell morphology during cell spreading when compared to untransfected cells (data not shown).

Kindlin-1 colocalized with paxillin to focal complexes and FAs (Fig. 6A). A similar staining pattern was also observed for Kindlin-2 suggesting that Kindlins-1 and -2 are recruited to newly formed focal contacts, and hence may play an important role during the assembly of the cell–matrix adhesion complex. In addition to the integrin-containing adhesion structures, Kindlin-2 also localized to actin stress fibers. Altogether these data indicate that all three Kindlin proteins localize to specific cell–matrix adhesion sites in vitro.

Our in situ hybridizations suggested a preferential expression of Kindlin-1 in epithelial cells and Kindlin-2 in striated and smooth muscle cells in vivo. Therefore we investigated the localization of Kindlins-1 and -2 in immortalized mouse keratinocytes and of Kindlin-2 in addition in primary cardiomyocytes.

Keratinocytes transfected with EGFP-Kindlin-1 revealed fluorescent labeling of paxillin-positive FAs and phalloidin-positive actin stress fibers (Fig. 6B). A similar staining pattern could be observed for Kindlin-2 (data not shown). However, cells transfected with EGFP-Kindlin-1 often revealed a strong perinuclear and a weak filamentous signal that failed to colocalize with F-actin. Whether these signals are a consequence of Kindlin-1 overexpression or indeed represent an additional subcellular localization of Kindlin-1 outside of FAs remains to be addressed. Furthermore, we investigated the localization of Kindlins-1 and -2 in calcium differentiated keratinocytes. Surprisingly, we could not observe localization of EGFP-Kindlin-1 to cell–cell contacts, as previously assumed [8] (data not shown). In contrast, EGFP-Kindlin-2 colocalized

with E-cadherin to cell–cell contacts (Fig. 6B). This result is the first indication that Kindlins-1 and -2 can localize to different subcellular compartments. It could explain why Kindlin-2 cannot compensate for Kindlin-1 loss in Kindler Syndrome. Unfortunately, no Kindlin-1 or -2-specific antibodies are available, which would be required to investigate the subcellular localization in vivo.

To test the localization of Kindlin-2 in muscle cells, we isolated primary cardiomyocytes from newborn mice and transfected them with EGFP-tagged Kindlin-2. Kindlin-2 colocalized with α -actinin to Z-discs of cardiomyocytes (Fig. 6C). This observation implies that Kindlin-2 like UNC-112 plays an important role in the organization of cell–matrix adhesion sites in muscle cells.

In summary, our analyses revealed that all three Kindlins are expressed during early development, but expression of each isoform is restricted to certain tissues and cell types. This is most evident for Kindlin-3, which is exclusively expressed in cells of hematopoietic origin. The expression pattern of Kindlins-1 and -2 show a partial overlap, although with a preference for Kindlin-1 expression in epithelial cells of the skin and the gastrointestinal tract and Kindlin-2 in striated and smooth muscle cells. Kindlins-1 and -2-specific antibodies will be important tools to investigate their subcellular localization in more detail in vivo. This is medically relevant, since our analyses demonstrate that Kindlin-2 is expressed in the epidermis but can apparently not compensate for the loss of Kindlin-1 expression in Kindler syndrome patients. This observation is in line with our in vitro data indicating that in contrast to Kindlin-1, Kindlin-2 localizes to cell–cell contacts of differentiated keratinocytes and might therefore be less involved in the cell–matrix adhesion of keratinocytes. Identification of novel Kindlin binding partners will be one important aim to understand the cellular functions of Kindlin proteins. Additionally, Kindlin-deficient mice could give important insights into the function of this gene family during development and disease.

Acknowledgments

We thank Melanie Ried for excellent technical assistance, Michael Sixt, Kyle Legate, Julia Schlehe and Tim Lämmermann for helpful suggestions and critical reading of the manuscript. Peter C. Weber and Jürgen Heesemann for the continuous support and Barbara Böhlig for expert technical assistance.

The work was supported by the DFG, the Max-Planck-Society and the Fonds der Chemischen Industrie to R.F.

REFERENCES

- [1] F. Jobard, B. Bouadjar, F. Caux, S. Hadj-Rabia, C. Has, F. Matsuda, J. Weissenbach, M. Lathrop, J.F. Prud'homme, J. Fischer, Identification of mutations in a new gene encoding a FERM family protein with a pleckstrin homology domain in Kindler syndrome, *Hum. Mol. Genet.* 12 (2003) 925–935.
- [2] M. Wick, C. Burger, S. Brusselbach, F.C. Lucibello, R. Muller, Identification of serum-inducible genes: different patterns of

- gene regulation during G0→S and G1→S progression, *J. Cell Sci.* 107 (1994) 227–239.
- [3] E.J. Weinstein, M. Bourner, R. Head, H. Zakeri, C. Bauer, R. Mazzarella, URP1: a member of a novel family of PH and FERM domain-containing membrane-associated proteins is significantly over-expressed in lung and colon carcinomas, *Biochim. Biophys. Acta* 1637 (2003) 207–216.
- [4] R.S. Boyd, P.J. Adam, S. Patel, J.A. Loader, J. Berry, N.T. Redpath, H.R. Poyser, G.C. Fletcher, N.A. Burgess, A.C. Stamps, L. Hudson, P. Smith, M. Griffiths, T.G. Willis, E.L. Karran, D.G. Oscier, D. Catovsky, J.A. Terrett, M.J. Dyer, Proteomic analysis of the cell-surface membrane in chronic lymphocytic leukemia: identification of two novel proteins, BCNP1 and MIG2B, *Leukemia* 17 (2003) 1605–1612.
- [5] D.H. Siegel, G.H. Ashton, H.G. Penagos, J.V. Lee, H.S. Feiler, K.C. Wilhelmson, A.P. South, F.J. Smith, A.R. Prescott, V. Wessagowit, N. Oyama, M. Akiyama, D. Al Aboud, K. Al Aboud, A. Al Githami, K. Al Hawsawi, A. Al Ismaili, R. Al-Suwaid, D.J. Atherton, R. Caputo, J.D. Fine, I.J. Frieden, E. Fuchs, R.M. Haber, T. Harada, Y. Kitajima, S.B. Mallory, H. Ogawa, S. Sahin, H. Shimizu, Y. Suga, G. Tadini, K. Tsuchiya, C.B. Wiebe, F. Wojnarowska, A.B. Zaghoul, T. Hamada, R. Mallipeddi, R.A. Eady, W.H. McLean, J.A. McGrath, E.H. Epstein, Loss of kindlin-1, a human homolog of the *Caenorhabditis elegans* actin-extracellular-matrix linker protein UNC-112, causes Kindler syndrome, *Am. J. Hum. Genet.* 73 (2003) 174–187.
- [6] S. Kloeker, M.B. Major, D.A. Calderwood, M.H. Ginsberg, D.A. Jones, M.C. Beckerle, The Kindler syndrome protein is regulated by transforming growth factor-beta and involved in integrin-mediated adhesion, *J. Biol. Chem.* 279 (2004) 6824–6833.
- [7] Y. Tu, S. Wu, X. Shi, K. Chen, C. Wu, Migfilin and Mig-2 link focal adhesions to filamin and the actin cytoskeleton and function in cell shape modulation, *Cell* 113 (2003) 37–47.
- [8] V. Gkretsi, Y. Zhang, Y. Tu, K. Chen, D.B. Stolz, Y. Yang, S.C. Watkins, C. Wu, Physical and functional association of migfilin with cell–cell adhesions, *J. Cell Sci.* 118 (2005) 697–710.
- [9] T.M. Rogalski, G.P. Mullen, M.M. Gilbert, B.D. Williams, DG. Moerman, The UNC-112 gene in *Caenorhabditis elegans* encodes a novel component of cell–matrix adhesion structures required for integrin localization in the muscle cell membrane, *J. Cell Biol.* 150 (2000) 253–264.
- [10] M. Lotem, M. Raben, R. Zeltser, M. Landau, M. Sela, M. Wygoda, Z.A. Tochner, Kindler syndrome complicated by squamous cell carcinoma of the hard palate: successful treatment with high-dose radiation therapy and granulocyte-macrophage colony-stimulating factor, *Br. J. Dermatol.* 144 (2001) 1284–1286.
- [11] T. Kindler, Congenital poikiloderma with traumatic bulla formation and progressive cutaneous atrophy, *Br. J. Dermatol.* 66 (1954) 104–111.
- [12] G.H. Ashton, W.H. McLean, A.P. South, N. Oyama, F.J. Smith, R. Al-Suwaid, A. Al-Ismaïly, D.J. Atherton, C.A. Harwood, I.M. Leigh, C. Moss, B. Didona, G. Zambruno, A. Patrizi, R.A. Eady, J.A. McGrath, Recurrent mutations in kindlin-1, a novel keratinocyte focal contact protein, in the autosomal recessive skin fragility and photosensitivity disorder, Kindler syndrome, *J. Invest. Dermatol.* 122 (2004) 78–83.
- [13] S.J. White, W.H. McLean, Kindler surprise: mutations in a novel actin-associated protein cause Kindler syndrome, *J. Dermatol. Sci.* 38 (2005) 169–175.
- [14] K. Kato, T. Shiozawa, J. Mitsushita, A. Toda, A. Horiuchi, T. Nikaido, S. Fujii, I. Konishi, Expression of the mitogen-inducible gene-2 (mig-2) is elevated in human uterine leiomyomas but not in leiomyosarcomas, *Hum. Pathol.* 35 (2004) 55–60.
- [15] H. Akazawa, S. Kudoh, N. Mochizuki, N. Takekoshi, H. Takano, T. Nagai, I. Komuro, A novel LIM protein Cal promotes cardiac differentiation by association with CSX/NKX2-5, *J. Cell Biol.* 164 (2004) 395–405.
- [16] M. Moser, A. Imhof, A. Pscherer, R. Bauer, W. Amselgruber, F. Sinowatz, F. Hofstadter, R. Schule, R. Buettner, Cloning and characterization of a second AP-2 transcription factor: AP-2 beta, *Development* 121 (1995) 2779–2788.
- [17] A.H. Chishtî, A.C. Kim, S.M. Marfatia, M. Lutchman, M. Hanspal, H. Jindal, S.C. Liu, P.S. Low, G.A. Rouleau, N. Mohandas, J.A. Chasis, J.G. Conboy, P. Gascard, Y. Takakuwa, S.C. Huang, E.J. Benz Jr., A. Bretscher, R.G. Fehon, J.F. Gusella, V. Ramesh, F. Solomon, V.T. Marchesi, S. Tsukita, S. Tsukita, M. Arpin, D. Louvard, N.K. Tonks, J.M. Anderson, A.S. Fanning, P.J. Bryant, D.F. Woods, K.B. Hoover, The FERM domain: a unique module involved in the linkage of cytoplasmic proteins to the membrane, *Trends Biochem. Sci.* 23 (1998) 281–282.
- [18] D.A. Calderwood, B. Yan, J.M. de Pereda, B.G. Alvarez, Y. Fujioka, R.C. Liddington, M.H. Ginsberg, The phosphotyrosine binding-like domain of talin activates integrins, *J. Biol. Chem.* 277 (2002) 21749–21758.
- [19] B. Garcia-Alvarez, J.M. de Pereda, D.A. Calderwood, T.S. Ulmer, D. Critchley, I.D. Campbell, M.H. Ginsberg, R.C. Liddington, Structural determinants of integrin recognition by talin, *Mol. Cell.* 11 (2003) 49–58.
- [20] M.A. Lemmon, K.M. Ferguson, Signal-dependent membrane targeting by pleckstrin homology (PH) domains, *Biochem. J.* 350 (2000) 1–18.
- [21] S. Linder, P. Kopp, Podosomes at a glance, *J. Cell Sci.* 118 (2005) 2079–2082.
- [22] S. Linder, M. Aepfelbacher, Podosomes: adhesion hot-spots of invasive cells, *Trends Cell Biol.* 13 (2003) 376–385.

Paper III

Identification and Embryonic Expression of a New AP-2 Transcription Factor, AP-2 ϵ

Hao-Ven Wang,¹ Kristina Vaupel,¹ Reinhard Buettner,² Anja-Katrin Bosserhoff,³ and Markus Moser^{1*}

AP-2 proteins comprise a family of highly related transcription factors, which are expressed during mouse embryogenesis in a variety of ectodermal, neuroectodermal, and mesenchymal tissues. AP-2 transcription factors were shown to be involved in morphogenesis of craniofacial, urogenital, neural crest-derived, and placental tissues. By means of a partial cDNA fragment identified during an expressed sequence tag search for AP-2 genes, we identified a fifth, previously unknown AP-2-related gene, AP-2 ϵ . AP-2 ϵ encodes an open reading frame of 434 amino acids, which reveals the typical modular structure of AP-2 transcription factors with highly conserved C-terminal DNA binding and dimerization domains. Although the N-terminally localized activation domain is less homologous, position and identity of amino acids essential for transcriptional transactivation are conserved. Reverse transcriptase-polymerase chain reaction analyses of murine embryos revealed AP-2 ϵ expression from gestational stage embryonic day 7.5 throughout all later embryonic stages until birth. Whole-mount in situ hybridization using a specific AP-2 ϵ cDNA fragment demonstrated that during embryogenesis, expression of AP-2 ϵ is mainly restricted to neural tissue, especially the midbrain, hindbrain, and olfactory bulb. This expression pattern was confirmed by immunohistochemistry with an AP-2 ϵ -specific antiserum. By using this antiserum, we could further localize AP-2 ϵ expression in a hypothalamic nucleus and the neuroepithelium of the vomeronasal organ, suggesting an important function of AP-2 ϵ for the development of the olfactory system. *Developmental Dynamics* 231:128–135, 2004.

© 2004 Wiley-Liss, Inc.

Key words: AP-2; transcription factor; mouse embryogenesis; gene expression

Received 29 September 2003; Revised 3 March 2004; Accepted 31 March 2004

INTRODUCTION

AP-2 α was identified due to its ability to bind to the SV40 and the human metallothionein IIa gene promoters and initially was considered to represent a unique transcription factor without any homology to other transcriptional regulators (Mitchell et al., 1987). In 1995, a second homologous gene, AP-2 β , was cloned (Moser et al., 1995) and, subsequently, two further AP-2 genes, AP-2 γ (also known as AP-2.2) and

AP-2 δ , enlarged the family of AP-2 transcription factors (Bosher et al., 1996; Chazaud et al., 1996; Oulad-Abdelghani et al., 1996; Zhao et al., 2001). All currently known AP-2 proteins share a modular structure consisting of an N-terminal proline- and glutamine-rich transactivation domain, followed by a positively charged α -helical DNA binding region and a helix-span-helix motif, which mediates homo- and heterodimerization of AP-2 proteins (Wil-

liams and Tjian, 1991a,b; Bosher et al., 1996). The C-terminal domains of AP-2 proteins share the highest degree of similarity and were also highly conserved during evolution, as cloning of the *Drosophila* AP-2 protein revealed 68% identity with AP-2 α in this region (Bauer et al., 1998; Monge and Mitchell, 1998). In contrast, the N-terminal transactivation domain appears to be structurally more flexible and, therefore, less conserved between the individual

¹Max-Planck-Institute of Biochemistry, Martinsried, Germany

²Institute of Pathology, University Hospital Bonn, Bonn, Germany

³Institute of Pathology, University Hospital Regensburg, Regensburg, Germany

Grant sponsor: Deutsche Forschungsgemeinschaft.

*Correspondence to: Markus Moser, Max-Planck-Institute for Biochemistry, Am Klopferspitz 18A, D-82152 Martinsried, Germany.

E-mail: moser@biochem.mpg.de

DOI 10.1002/dvdy.20119

Published online 29 June 2004 in Wiley InterScience (www.interscience.wiley.com).

TABLE 1. Overview of Exons and Exon-Intron Junction of AP-2 ϵ

Exon number	Exon size (bp)	Sequence at exon-intron junction	
		3'splice acceptor	5'splice donor
1	>144		TCC GCC ATG <u>gtg agt</u>
2	573	ctt ctg <u>cag GAG</u> CGC CCC	GAA TTG <u>CAG gta agc</u>
3	52	tat ttg <u>cag GCG</u> ATA GAT	TCA AGA <u>AAG gta agg</u>
4	223	gtt cca <u>cag TCC</u> CCA TTC	CCT CCG AAG <u>gta gga</u>
5	119	tac gtt <u>aag GGC</u> CAA GTC	TGG TGG <u>AAG gta agc</u>
6	142	ttt ccc <u>cag GAG</u> AAG CTG	GGC TGC <u>CAA gta agt</u>
7	>283	ccc cac <u>cag GCA</u> \acute{G} AT CTG	CAT CGG AAG <u>taa ctg</u>

TABLE 2. Chromosomal Locations of Human and Murine AP-2 Genes

AP-2	Chromosome location	
	Human	Mouse
α	6p24	13 A5-B1
β	6p12	1 A2-A4
γ	20q13.2	2 H3-H4
δ	6p12.1	1 A3
ϵ	1p34.3	4 D2.2

AP-2 proteins, although, with the exception of AP-2 δ , certain critical residues and motifs involved in transcriptional activation are conserved. A limited number of only 36 critical amino acid residues was mapped previously and is believed to interact with coactivators of the transcription machinery (Wankhade et al., 2000).

Expression analyses in mammals, birds, and amphibians showed that AP-2 genes are involved in the formation of craniofacial, neuroectodermal, ectodermal structures, limb buds, and urogenital tissues (Mitchell et al., 1991; Snape et al., 1991; Moser et al., 1995, 1997a; Shen et al., 1997; Epperlein et al., 2000). The functional relevance of AP-2 proteins for mammalian development was demonstrated by the lethal phenotypes of AP-2 α , AP-2 β , and AP-2 γ mouse mutants. Of interest, the phenotypes of these mutants differ significantly, despite that the expression patterns of AP-2 α , AP-2 β , and AP-2 γ genes overlap in many tissues during mouse development. AP-2 α knockout mice exhibit severe craniofacial defects and defective closure of the anterior neural tube and body wall (Schorle et al., 1996; Zhang et al., 1996; Nottoli et al., 1998; Brewer et al., 2002). AP-2 β -deficient mice complete embryogenesis, but die shortly after birth due to impaired kidney function (Moser et al., 1997b, 2003). Finally, AP-2 γ mutant embryos die very early after gastrulation as a result of defective placental development (Auman et al., 2002; Werling and Schorle, 2002).

Recently, germ line missense mutations in the human AP-2 β gene have been linked to Char syndrome, characterized by patent ductus arteriosus, facial malformations, and

hand anomalies. AP-2 β mutations in patients with Char syndrome result in a transdominant negative AP-2 β protein with defective DNA binding properties (Satoda et al., 1999, 2000). These results clearly indicate that AP-2 genes execute also essential nonredundant functions during human development.

In this study, we describe a new fifth member of the AP-2 transcription factor family, AP-2 ϵ , which is mainly expressed in the central nervous system during murine embryogenesis. We additionally describe here the generation and characterization of an AP-2 ϵ -specific antiserum that can be used for Western blots, gel mobility shift assays, and immunohistochemistry.

RESULTS AND DISCUSSION

Identification of the Mouse AP-2 ϵ cDNA

By a BLAST search for AP-2 genes, we identified a partial cDNA clone, which encoded a predicted peptide with significant homology to the central region of AP-2 proteins (AA414551; IMAGE 778986). By using this partial cDNA sequence, an extended expressed sequence tag (EST) BLAST search identified several overlapping EST clones (described in the Experimental Procedures section). Because all of these independent ESTs encoded the same predicted peptide with significant homology to the DNA binding and dimerization domains of the four previously known AP-2 proteins, we assumed that they were derived from a distinct, fifth AP-2 protein, which we designated AP-2 ϵ . Unfortunately, all these clones lacked the 5' region

of the new AP-2 ϵ gene. Specific primer pairs were chosen to amplify a 551-bp cDNA fragment by reverse transcriptase-polymerase chain reaction (RT-PCR) that was subsequently used as a probe to screen an embryonic day (E) 14 mouse embryo cDNA library. The cDNA library screen identified one positive lambda phage clone and the identity of the AP-2 ϵ cDNA was verified by sequencing. Again, this cDNA clone only covered the 3' region of the murine AP-2 ϵ cDNA. Finally, a BLAST search to human EST clones identified a full-length AP-2 ϵ cDNA clone (IMAGE 5786430). In addition to the coding sequence, this clone contained 232-bp 5'- and 664-bp 3'-untranslated regions (UTRs) and the insert was used to generate a cytomegalovirus (CMV) promoter-driven AP-2 ϵ expression plasmid.

By using the NIX software package, the murine genomic sequence from Celera and the NCBI database, we determined the genomic organization of the murine AP-2 ϵ gene. The overall structure of the mAP-2 ϵ gene is highly conserved and, as known from AP-2 α , β , and γ genes, consists of seven exons spanning approximately 20,000 bp. The genomic organization suggests that these genes were most likely derived by gene duplication of a single ancestor. The exon-intron boundaries follow the conserved splice donor and acceptor sites (Table 1). The NCBI database maps the AP-2 ϵ gene to human chromosome 1 and mouse chromosome 4. Table 2 summarizes the chromosomal loci of all five human and murine AP-2 genes.

The AP-2 ϵ gene encodes a predicted peptide of 434 amino acids harboring all modular domains

shared by the classic AP-2 genes, AP-2 α , β , and γ . Highly conserved DNA binding and dimerization motifs homologous to the other murine AP-2 proteins are present in the C-terminal half starting from amino acid 208 (Fig. 1). The transcriptional activation domain located in the N-terminal half is much less conserved between the different AP-2 proteins. However, functionally important residues, including the PY motif at positions 47 to 51 in AP-2 ϵ , the aspartic acid residue corresponding to position 52 in AP-2 α and the two leucine residues at positions 107 and 108 of AP-2 α (Wankhade et al., 2000), are present in AP-2 ϵ and in all other AP-2 isoforms, except for AP-2 δ (Fig. 1). Of interest, AP-2 ϵ lacks a short N-terminal peptide, a feature that has been also observed in *Xenopus* AP-2 (Winning et al., 1991).

Tissue-Specific Expression of AP-2 ϵ During Murine Embryogenesis and in Adult Tissues

To determine the expression profile of AP-2 ϵ during murine embryogenesis, RT-PCR was performed with AP-2 ϵ -specific primers chosen from the 3' end and the 3' UTR of the AP-2 ϵ cDNA (see Experimental Procedures section). Gel electrophoresis revealed bands on ethidium bromide-stained agarose gels for all analyzed embryonic stages from E7.5 to E17.5. The expression signal strikingly increases from E8.5 to E14.5 and declines thereafter. Of interest, expression levels at E7.5 were higher compared with later stages, probably due to the fact that these RNA samples were prepared from whole conceptuses, suggesting that AP-2 ϵ , as well as AP-2 α and AP-2 γ (Moser et al., 1997a; Auman et al., 2002), is also expressed in extraembryonic structures (Fig. 2A).

Next, we transcribed sense and antisense digoxigenin-labeled riboprobes from an AP-2 ϵ -specific cDNA fragment obtained from the 3' UTR to determine embryonic expression patterns by whole-mount in situ hybridization. Specificity was verified by hybridizing the probe to a Southern blot with full-length cDNAs of AP-2 α , β , γ , and δ and the partial murine

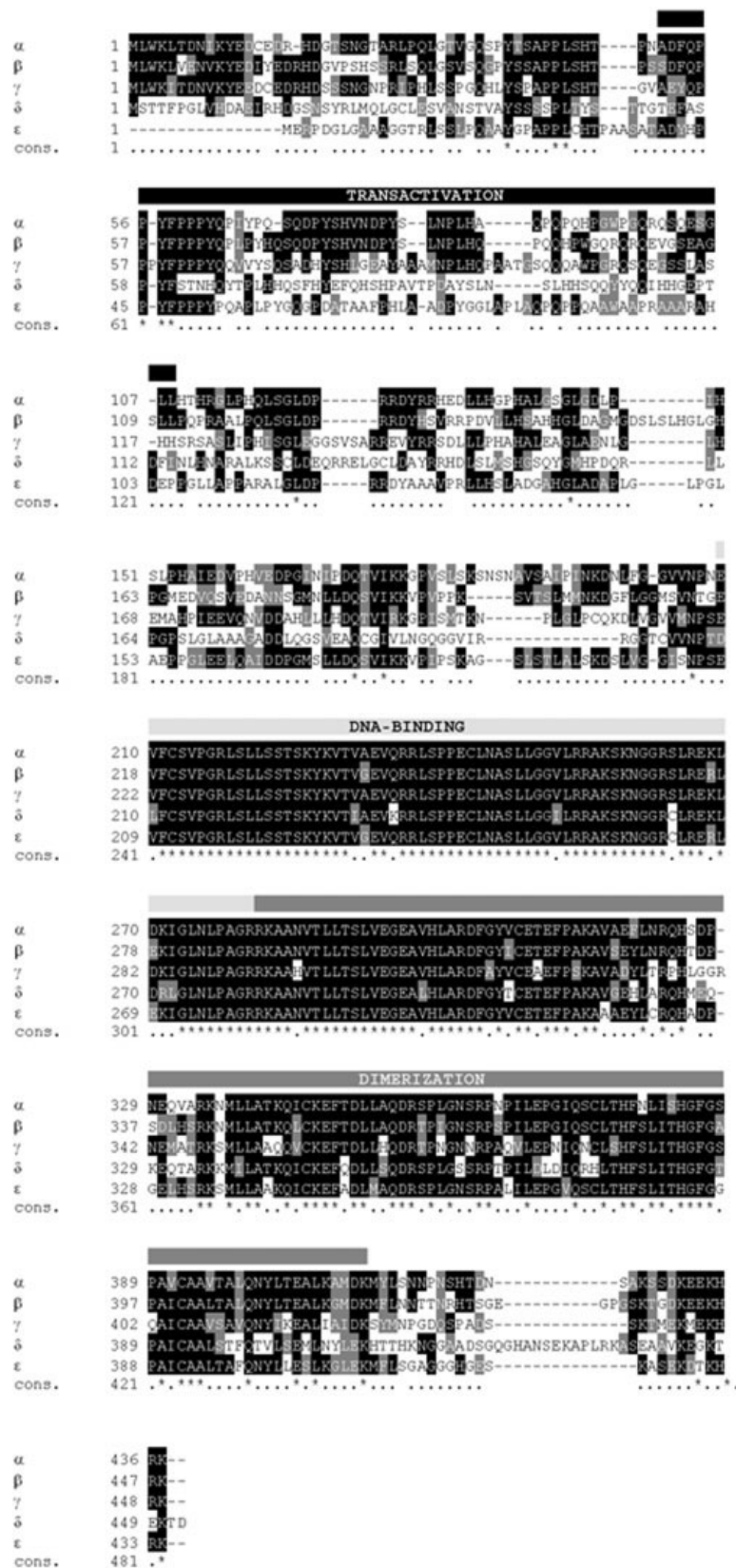


Fig. 1. Clustal W alignment of murine AP-2 ϵ and the previously known AP-2 α , β , γ , and δ proteins. Identical amino acid residues are boxed in black with white lettering, whereas similar residues are shown in gray boxes. Gaps between amino acids are filled with a dash. Functional AP-2 domains are indicated above by horizontal bars.

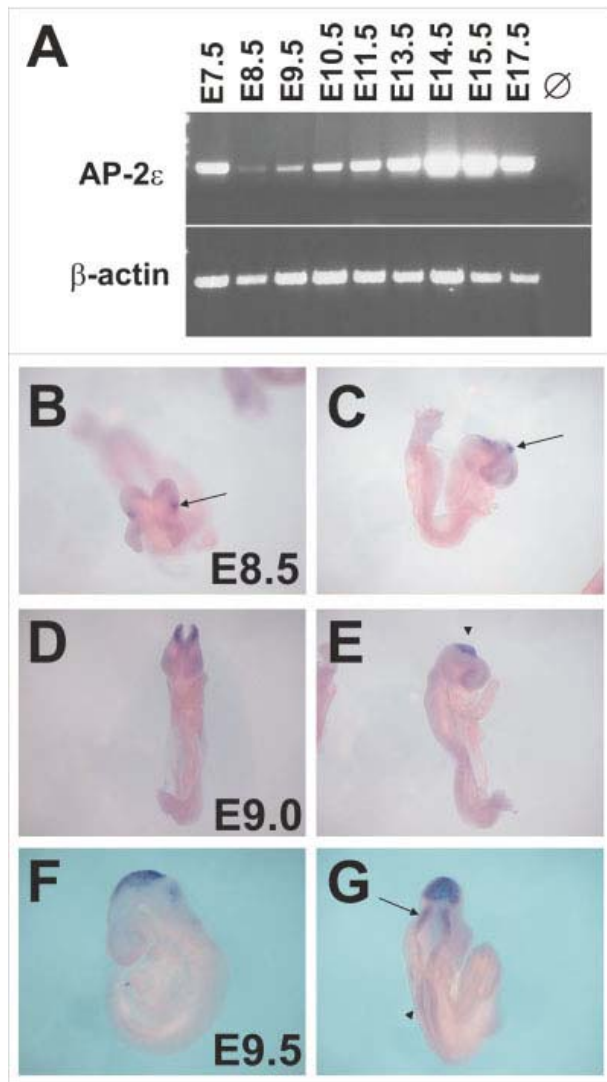


Fig. 2. AP-2 ϵ expression during murine embryogenesis. **A:** Reverse transcriptase-polymerase chain reaction with an AP-2 ϵ -specific primer set reveals AP-2 ϵ expression during embryogenesis from embryonic day (E) 7.5 until E17.5. As a control, the quality and amount of cDNA preparations were tested by amplification of a β -actin fragment. **B–G:** Whole-mount in situ hybridization of E8.5 (B,C), E9.0 (D,E), and E9.5 (F,G) mouse embryos. AP-2 ϵ -specific signals are present in a restricted region of the neural folds of the future midbrain at E8.5 (marked by an arrow in B and C). At E9.0 and E9.5, AP-2 ϵ is expressed in the midbrain region (arrowheads) the hindbrain (arrow in G) and spinal cord (arrowhead in G).

AP-2 ϵ cDNA clone (data not shown). Whole-mount in situ hybridization of E8.5 embryos revealed AP-2 ϵ expression in a distinct patch of cells in the neural folds of the prospective midbrain region (Fig. 2B,C). This region increased in size, when neural folds started to fuse at E9.0 (Fig. 2D,E). From E9.5 on, AP-2 ϵ signals were abundant in the hindbrain primor-

dial anterior of the fourth ventricle and in the spinal cord. In addition, strong signals were detected in the midbrain and midbrain–hindbrain junction (Fig. 2F,G). Of interest, a pair of distinct patches of cells in the anterior midbrain became evident at E10.5 (Fig. 3A,B). Thus, AP-2 ϵ expression partially overlaps with expression of other AP-2 genes in these re-

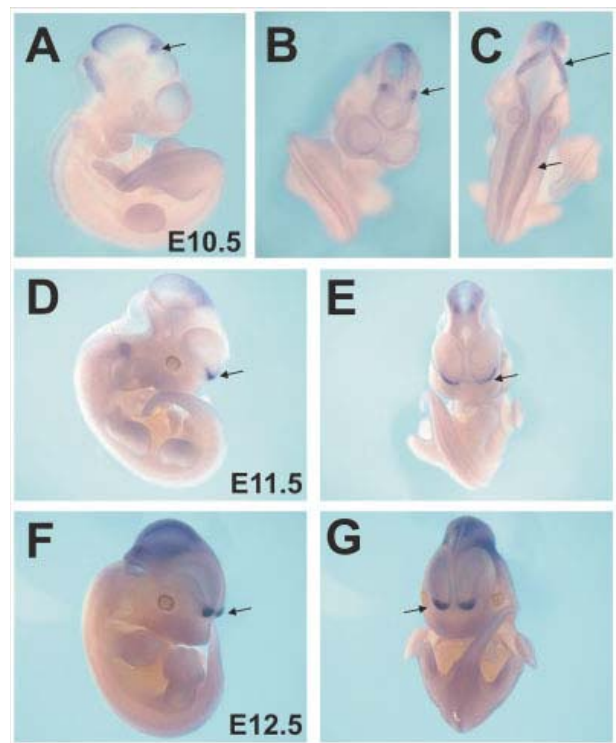


Fig. 3. Whole-mount in situ hybridization of embryonic day (E) 10.5 (A–C), E11.5 (D,E), and E12.5 (F,G) mouse embryos hybridized with an AP-2 ϵ -specific probe. **A,C:** AP-2 ϵ is expressed in the midbrain and hindbrain. **B:** Note the two lateral regions of AP-2 ϵ expression in the anterior midbrain. **C:** Backside view indicates staining anterior of the fourth ventricle (long arrow) and the spinal cord (arrow). **D–G:** Arrows indicate AP-2 ϵ expression in the primordium of the olfactory bulbs of E11.5 and E12.5 embryos. Control hybridizations performed with a sense probe did not reveal any signals (data not shown).

gions. In particular, AP-2 α and AP-2 β were previously detected in the midbrain, the midbrain–hindbrain junction, the primordia of the cerebellum and the spinal cord (Moser et al., 1995, 1997a). Additionally, AP-2 δ expression has also been localized to the midbrain region at this time point (Zhao et al., 2003). Of interest, AP-2 ϵ expression was also observed in the developing olfactory bulb, in which no other AP-2 genes are expressed at this early stage of development (Fig. 3D–G). Sectioning of these embryos confirmed the restricted AP-2 ϵ expression in the neuroepithelium and did not reveal any signals in neural crest cells (data not shown).

To analyze AP-2 ϵ expression in the brain at later stages, we dissected brains from E12.5 to E15.5 embryos and performed whole-mount in situ hybridizations. Figure 4 shows differ-

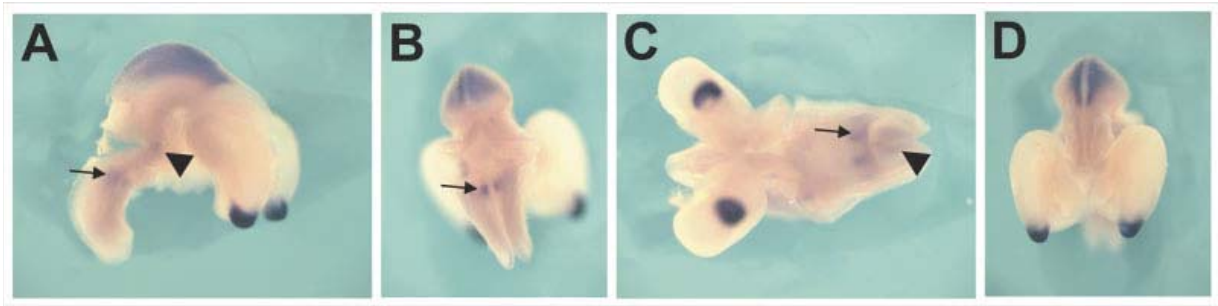


Fig. 4. Whole-mount in situ hybridizations of brain from embryonic day 14.5 embryos hybridized with an AP-2 ϵ -specific cDNA probe. A–D: Lateral (A), backside (B), ventral (C), and frontal (D) view of the same brain showing AP-2 ϵ expression in the olfactory bulb and the mesencephalon. Additional sites of AP-2 ϵ expression are distinct regions in the pons (arrowhead in A), medulla oblongata (arrows in A, B, and C), and spinal cord (arrowhead in C).

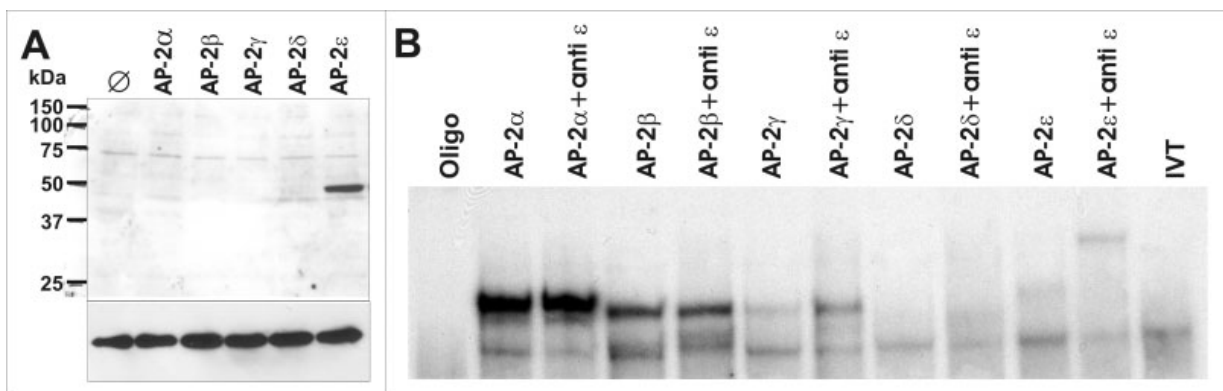


Fig. 5. Characterization of an AP-2 ϵ -specific antiserum. A: Western-blot analysis from RIPA extracts of HepG2 cells transfected with expression plasmids of all five AP-2 isoforms probed with the anti-AP-2 ϵ antiserum. Equal loading was confirmed by anti-tubulin staining. B: Gel mobility shift assays of in vitro translated (IVT) AP-2 proteins incubated with radioactively labeled optimized hM11a and the AP-2 ϵ -specific antiserum shows the formation of a supershifted AP-2 ϵ -DNA antibody complex.

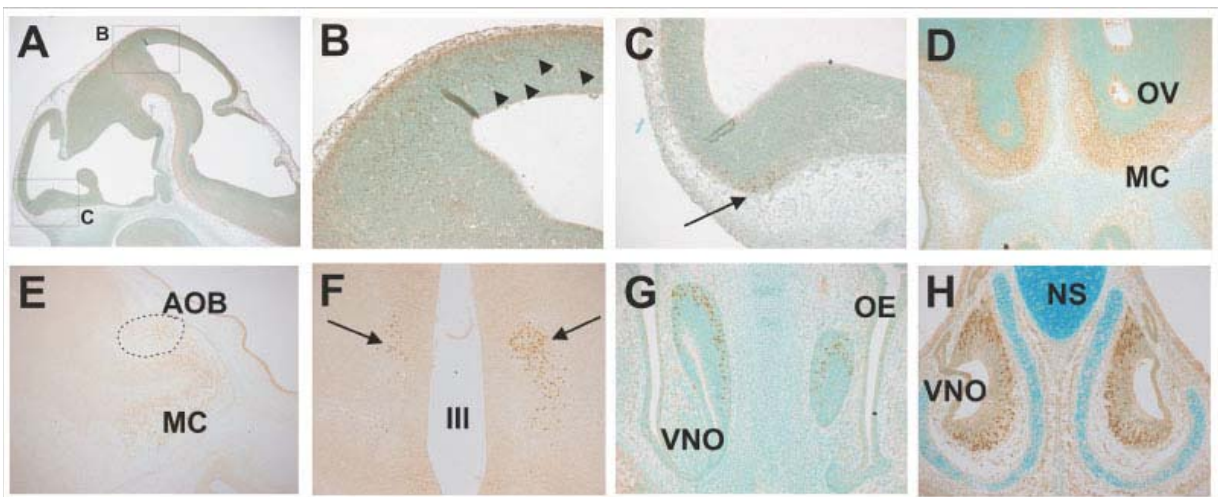


Fig. 6. A–C: Immunohistochemical staining with the AP-2 ϵ -specific antiserum of sagittal sections of the head region of embryonic day (E) 12.5 embryos. B and C show magnifications of the boxed area in A. Single AP-2 ϵ -positive cells in the midbrain (arrowheads in B) and the most cranial telencephalon (arrow in C). D,E: Coronal and sagittal sections of the olfactory bulb from E15.5 embryos, respectively. AP-2 ϵ is expressed in mitral cells of the olfactory bulb and the rostral accessory olfactory bulb (encircled by a dashed line in E). F: AP-2 ϵ is further expressed in the ventrolateral nucleus of the hypothalamus (indicated by arrows). G,H: Transverse (G) and coronal (H) sections of E15.5 and newborn mice of the vomeronasal organ, respectively. AP-2 ϵ -positive cells are found in the sensory neuroepithelium of the vomeronasal organ. AOB, accessory olfactory bulb; III, third ventricle; MC, mitral cells; NS, nasal septum; OE, olfactory epithelium; OV, olfactory ventricle; VNO, vomeronasal organ.

ent perspectives of an E14.5 brain hybridized with the AP-2 ϵ probe. This stage reveals very strong expression of AP-2 ϵ in the olfactory bulb and a much weaker signal in the midbrain. In addition, signals could also be detected in distinct nuclei of the pons and medulla oblongata and the spinal cord (Fig. 4A–D). In parallel, we performed radioactive in situ hybridizations on sections of E12 to E16.5 embryos. Of interest, we were not able to detect AP-2 ϵ in the midbrain any longer at E16.5, suggesting a down-regulation of AP-2 ϵ in this structure, whereas expression in the olfactory bulb was still detectable (data not shown). Finally, we were unable to detect any AP-2 ϵ expression in the brain of 1.5- and 3-month-old mice by in situ hybridization (data not shown). The decrease in AP-2 ϵ expression was also confirmed by RT-PCR analyses from adult tissue preparations showing only very weak signals in the brain and ovary (data not shown).

Generation of AP-2 ϵ -Specific Antiserum and Immunohistochemical Analysis of AP-2 ϵ Expression

To analyze AP-2 ϵ protein expression in more detail, we aimed to generate an AP-2 ϵ -specific polyclonal antiserum (see Experimental Procedures section). AP-2 ϵ -transfected NIH3T3 cells showed strong nuclear staining when incubated with the antiserum raised against an N-terminal peptide of the AP-2 ϵ protein (data not shown). Specificity was tested by Western blot analysis of lysates from HepG2 cells that were transfected with cDNAs of all five AP-2 isoforms (Fig. 5A). In addition, we performed gel mobility shift assays of in vitro translated AP-2 isoforms together with the optimized hMtila binding sequence (Mohibullah et al., 1999). Here, a supershift was only formed with the AP-2 ϵ -DNA complex (Fig. 5B). Both assays confirmed that the antiserum specifically recognizes the AP-2 ϵ protein without any cross-reactivity.

Finally, we used this antiserum for immunohistochemistry of paraformaldehyde-fixed sections of E12.5 and E15.5 embryos. Again, the specificity

of this antiserum was proven by the nuclear staining and the staining pattern itself, which clearly confirmed the data obtained from in situ hybridizations. At E12.5, we detected labeled cells in the midbrain and the most cranial region of the telencephalon (Fig. 6A–C). Of interest, AP-2 ϵ -positive cells are not limited to the roof of the midbrain, where three other members of the AP-2 family, AP-2 α , AP-2 β , and AP-2 δ , are expressed at that time point in more differentiated neuronal cells (Moser et al. 1995; Zhao et al. 2003; own unpublished data). In contrast, AP-2 ϵ -positive cells are distributed throughout the neuroepithelium in neuroblasts that have left the proliferative ventricular zone (Fig. 6B). These data indicate that (1) AP-2 ϵ is expressed already earlier during the maturation process of neuronal cells and (2) its expression does not overlap at the cellular level with the other members of the AP-2 family in the midbrain. Although, we were able to show an interaction between AP-2 ϵ with other members of the AP-2 gene family in vitro, by performing pull down analysis and gel shift assays, our data here do not support any in vivo relevance of this interaction. Therefore, this point needs further examinations (data not shown).

From E12.5 onward, strongest AP-2 ϵ expression is seen in the olfactory system. At E15.5, no AP-2 ϵ -positive cells were stained in the midbrain. In contrast AP-2 ϵ protein expression could be detected in the mitral cell layer of the olfactory bulb and the rostral portion of the accessory olfactory bulb (Fig. 6D,E).

Chemosensation in most mammals is achieved by at least two distinct nasal tissues: the main olfactory epithelium and the vomeronasal organ. The axonal processes of both structures project to mitral cells of the olfactory bulb and the accessory olfactory bulb, respectively. In both structures, AP-2 ϵ is expressed. Of interest, AP-2 ϵ is also expressed in the vomeronasal organ, which represents the sensory organ of social chemical stimuli, like pheromones, whereas no expression is found in the olfactory epithelium. In the vomeronasal organ, AP-2 ϵ is only

present in the crescent-shaped sensory epithelium and not in the laterally located nonsensory epithelium at E15.5 and in newborn animals (Fig. 6G,H). The vomeronasal neuroepithelium is divided into an apical and basal zone of sensory epithelium. Axons of apical vomeronasal neurons terminate on mitral neurons in the rostral zone of the accessory olfactory bulb, where AP-2 ϵ is also expressed (Zufall et al., 2002; reviewed in Halpern and Martinez-Marcos, 2003). At the moment, we cannot claim, that AP-2 ϵ -positive cells only belong to the apical zone of the vomeronasal neuroepithelium, it rather seems that it is expressed in neuroepithelial cells of both layers. Finally, pheromonal stimuli induce endocrinological changes in the animal, which are mainly regulated by certain hypothalamic nuclei controlling the secretion of hormones by the hypophysis. Of interest, AP-2 ϵ expression could be also detected in a ventrolateral nucleus of the hypothalamus (Fig. 6F). Whether these cells control hypophyseal function needs further investigation.

Taken together, our expression data reveal a restriction of AP-2 ϵ expression to neuronal cells of the midbrain, hindbrain, olfactory bulb, and vomeronasal neuroepithelium, which clearly differs with respect to time and spatial pattern from all other members of the AP-2 family. We therefore speculate that AP-2 ϵ fulfills essential and nonredundant functions for embryonic development in these organs.

EXPERIMENTAL PROCEDURES

Identification of AP-2 ϵ and Cloning of a Partial Murine AP-2 ϵ cDNA Clone

Computer searches using the BLAST algorithm identified a murine cDNA clone with high homology to the AP-2 gene family (AA414551; IMAGE 778986). An extended database search using the NCBI-BLAST software revealed several EST clones containing partial cDNA clones of the murine AP-2 ϵ gene (BF464155, B1134735, BF461668, BE987978, A150520).

The predicted cDNA sequences were used to design primer sets to amplify an AP-2 ϵ probe (mAP-2 ϵ sense1: GTC TTC CAG GAT TGG CGG AG; mAP-2 ϵ anti2: GGC TGG AAA CTC AGT CTC AC). As a template, we used total cellular RNA extracted from a mouse embryo at gestational stage E14. The resulting cDNA fragment of 551 bp was then used to screen a murine embryonic E14 cDNA library (AMS Biotechnology Europe LTD, Lugano, Switzerland). Handling of lambda phages and plaque lifting was performed as described previously (Moser et al., 1995). After screening 4.5×10^5 lambda phages, one positive clone was identified, which contained the 3' part of the AP-2 ϵ cDNA (see Fig. 1).

Both the lambda clone and, in parallel, the IMAGE cDNA clone (IMAGE 778986) were sequenced on both strands using an ABI377 DNA sequencer. Finally, a full-length human EST clone (IMAGE 5786430) containing 5' and 3' UTRs was also obtained, sequenced, and used for further experiments. The genomic organization of the mouse AP-2 ϵ gene was mapped by using the NIX software package and the NCBI database, together with a comparison of the cDNA sequences.

RT-PCR and Whole-Mount In Situ Hybridization

Total cellular RNA from mouse embryos of different stages and tissues from adult C57BL/6 mice were isolated by using Trizol (Invitrogen, Karlsruhe, Germany) following the manufacturer's instructions. cDNA synthesis was performed with 2 μ g of total RNA using the Superscript II cDNA synthesis kit (Invitrogen). For RT-PCR studies, the following primer set were taken: mAP-2 ϵ spec sense: CAA GCA TCG GAA GTA ACT GGC; mAP-2 ϵ spec anti: CAC CTC TGA TGT GTT ATC AGC.

Whole-mount in situ hybridization was performed essentially as described (Wilkinson, 1993). As a probe, a 526-bp fragment obtained from the 3' UTR region of the murine AP-2 ϵ cDNA was excised with *StuI/SalI* from the murine IMAGE clone (IMAGE 778986) and subcloned into pBlue-

script. Digoxigenin-labeled cRNA sense and antisense probes were in vitro transcribed from the linearized plasmid as described previously (Moser et al., 1995). The same fragment was gel-purified and labeled with (32 P)dCTP by using a random primed labeling kit (Amersham, Braunschweig, Germany). Southern blot hybridization to linearized plasmids of the AP-2 α , AP-2 β , AP-2 γ , AP-2 δ , and AP-2 ϵ cDNAs indicated that the probe hybridized specifically to AP-2 ϵ but not to any other AP-2 gene.

Generation of AP-2 ϵ -Specific Antiserum and Western Blotting

Polyclonal AP-2 ϵ -specific antiserum was raised in rabbits by using peptide immunogens fused to KLH. The AP-2 ϵ -specific peptide was MERPDGLGGAAAGGTR, which represents the N-terminus of the protein. For Western-blot analysis, 20 μ g of RIPA cell lysates of HepG2 cells transfected with each of the five AP-2 expression plasmids were loaded per well, separated on 10% sodium dodecyl sulfate-polyacrylamide gel and transferred to nitrocellulose. A 1:5,000 dilution of the AP-2 ϵ antiserum was used before specific antibody binding was detected with the ECL system (Amersham).

Immunohistochemical Analysis

Paraffin sections of E12.5, E15.5, and newborn mice were rehydrated in alcohol solutions, endogenous peroxidase activity was blocked with 3% H₂O₂/methanol for 15 min, followed by antigen retrieval by heat treatment in 10 mM sodium citrate buffer (pH 6.0). After incubation with 10% goat serum/3% bovine serum albumin, sections were incubated with AP-2 ϵ -specific antiserum (at a dilution of 1:2,500) at 4°C overnight. Positive signals were developed with peroxidase-conjugated secondary antibody using diaminobenzidine followed by counterstaining with methyl green.

ACKNOWLEDGMENTS

M.M., A.K.B., and R.B. were funded by grants from the Deutsche Forschungsgemeinschaft.

REFERENCES

- Auman HJ, Nottoli T, Lakiza O, Winger Q, Donaldson S, Williams T. 2002. Transcription factor AP-2 γ is essential in the extra-embryonic lineages for early postimplantation development. *Development* 129:2733-2747.
- Bauer R, McGuffin ME, Mattox W, Tainsky MA. 1998. Cloning and characterization of the Drosophila homologue of the AP-2 transcription factor. *Oncogene* 17:1911-1922.
- Bosher JM, Totty NF, Hsuan JJ, Williams T, Hurst HC. 1996. A family of AP-2 proteins regulates c-erbB-2 expression in mammary carcinoma. *Oncogene* 13:1701-1707.
- Brewer S, Jiang X, Donaldson S, Williams T, Sucov HM. 2002. Requirement for AP-2 α in cardiac outflow tract morphogenesis. *Mech Dev* 110:139-149.
- Chazaud C, Oulad-Abdelghani M, Bouillet P, Decimo D, Chambon P, Dolle P. 1996. AP-2.2, a novel gene related to AP-2, is expressed in the forebrain, limbs and face during mouse embryogenesis. *Mech Dev* 54:83-94.
- Epperlein H, Meulemans D, Bronner-Fraser M, Steinbeisser H, Selleck MA. 2000. Analysis of cranial neural crest migratory pathways in axolotl using cell markers and transplantation. *Development* 127:2751-2761.
- Halpern M, Martinez-Marcos A. 2003. Structure and function of the vomeronasal system: an update. *Prog Neurobiol* 70:245-318.
- Mitchell PJ, Wang C, Tjian R. 1987. Positive and negative regulation of transcription in vitro: enhancer-binding protein AP-2 is inhibited by SV40 T antigen. *Cell* 50:847-861.
- Mitchell PJ, Timmons PM, Hebert JM, Rigby PW, Tjian R. 1991. Transcription factor AP-2 is expressed in neural crest cell lineages during mouse embryogenesis. *Genes Dev* 5:105-119.
- Mohibullah N, Donner A, Ippolito JA, Williams T. 1999. SELEX and missing phosphate contact analyses reveal flexibility within the AP-2(alpha) protein: DNA binding complex. *Nucleic Acids Res* 27:2760-2769.
- Monge I, Mitchell PJ. 1998. DAP-2, the Drosophila homolog of transcription factor AP-2. *Mech Dev* 76:191-195.
- Moser M, Imhof A, Pscherer A, Bauer R, Amselgruber W, Sinowatz F, Hofstädter F, Schüle R, Buettner R. 1995. Cloning and characterization of a second AP-2 transcription factor: AP-2 beta. *Development* 121:2779-2788.
- Moser M, Rüschoff J, Buettner R. 1997a. Comparative analysis of AP-2 alpha and AP-2 beta gene expression during murine embryogenesis. *Dev Dyn* 208:115-124.
- Moser M, Pscherer A, Roth C, Becker J, Mücher G, Zerres K, Dixkens C, Weis J, Guay-Woodford L, Buettner R, Fässler R. 1997b. Enhanced apoptotic cell death of renal epithelial cells in mice lacking

- transcription factor AP-2beta. *Genes Dev* 11:1938–1948.
- Moser M, Dahmen S, Kluge R, Grone H, Dahmen J, Kunz D, Schorle H, Buettner R. 2003. Terminal renal failure in mice lacking transcription factor AP-2 beta. *Lab Invest* 83:571–578.
- Nottoli T, Hagopian-Donaldson S, Zhang J, Perkins A, Williams T. 1998. AP-2-null cells disrupt morphogenesis of the eye, face, and limbs in chimeric mice. *Proc Natl Acad Sci U S A* 95:13714–13719.
- Oulad-Abdelghani M, Bouillet P, Chazaud C, Dolle P, Chambon P. 1996. AP-2.2: a novel AP-2-related transcription factor induced by retinoic acid during differentiation of P19 embryonal carcinoma cells. *Exp Cell Res* 225:338–344.
- Satoda M, Pierpont ME, Diaz GA, Borne-meier RA, Gelb BD. 1999. Char syndrome, an inherited disorder with patent ductus arteriosus, maps to chromosome 6p12-p21. *Circulation* 99:3036–3042.
- Satoda M, Zhao F, Diaz GA, Burn J, Goodship J, Davidson HR, Pierpont ME, Gelb BD. 2000. Mutations in TFAP2B cause Char syndrome, a familial form of patent ductus arteriosus. *Nat Genet* 25:42–46.
- Schorle H, Meier P, Buchert M, Jaenisch R, Mitchell PJ. 1996. Transcription factor AP-2 essential for cranial closure and craniofacial development. *Nature* 381:235–241.
- Shen H, Wilke T, Ashique AM, Narvey M, Zerucha T, Savino E, Williams T, Richman JM. 1997. Chicken transcription factor AP-2: cloning, expression and its role in outgrowth of facial prominences and limb buds. *Dev Biol* 188:248–266.
- Snape AM, Winning RS, Sargent TD. 1991. Transcription factor AP-2 is tissue-specific in *Xenopus* and is closely related or identical to keratin transcription factor 1 (KTF-1). *Development* 113:283–293.
- Wankhade S, Yu Y, Weinberg J, Tainsky MA, Kannan P. 2000. Characterization of the activation domains of AP-2 family transcription factors. *J Biol Chem* 275:29701–29708.
- Werling U, Schorle H. 2002. Transcription factor gene AP-2 gamma essential for early murine development. *Mol Cell Biol* 22:3149–3156.
- Wilkinson DG, editor. 1993. *In situ hybridization*. Oxford: Oxford University Press. p 75–83.
- Williams T, Tjian R. 1991a. Analysis of the DNA-binding and activation properties of the human transcription factor AP-2. *Genes Dev* 5:670–682.
- Williams T, Tjian R. 1991b. Characterization of a dimerization motif in AP-2 and its function in heterologous DNA-binding proteins. *Science* 251:1067–1071.
- Winning RS, Shea LJ, Marcus SJ, Sargent TD. 1991. Developmental regulation of transcription factor AP-2 during *Xenopus laevis* embryogenesis. *Nucleic Acids Res* 19:3709–3014.
- Zhang J, Hagopian-Donaldson S, Serbedzija G, Elsemore J, Plehn-Dujowich D, McMahon AP, Flavell RA, Williams T. 1996. Neural tube, skeletal and body wall defects in mice lacking transcription factor AP-2. *Nature* 381:238–241.
- Zhao F, Satoda M, Licht JD, Hayashizaki Y, Gelb BD. 2001. Cloning and characterization of a novel mouse AP-2 transcription factor, AP-2delta, with unique DNA binding and transactivation properties. *J Biol Chem* 276:40755–40760.
- Zhao F, Lufkin T, Gelb BD. 2003. Expression of Tfap2d, the gene encoding the transcription factor AP-2 delta, during mouse embryogenesis. *Gene Expr Patterns* 3:213–217.
- Zufall F, Kelliher KR, Leinders-Zufall T. 2002. Pheromone detection by mammalian vomeronasal neurons. *Microsc Res Tech* 58:251–260.

Manuscript I

Comparative expression analysis of the murine Palladin isoforms

Hao-Ven Wang and Markus Moser*

Max-Planck-Institute of Biochemistry, Department of Molecular Medicine, D-82152
Martinsried (Germany)

Running title: Expression analyses of the palladin gene

* Corresponding author:

moser@biochem.mpg.de

Abstract

Palladin is a recently identified phosphoprotein that interacts with a number of actin-associated proteins and thereby fulfils a crucial function as a molecular scaffold in organizing and stabilizing the actin cytoskeleton. Multiple palladin isoforms exist due to different promoter usage and alternative splicing giving rise to at least four major products: a 200 kDa isoform, a 140 kDa isoform and two isoforms with a size of 90-92 kDa. Here, we describe the expression of these isoforms during mouse development and adult tissues by RT-PCR and *in situ* hybridizations. The 200 kDa isoform is predominantly expressed in developing heart and skeletal muscle. The 140 kDa isoform is expressed in various mesenchymal tissues, and also represents the major isoform of the brain. The 90-92 kDa isoforms are almost ubiquitously expressed with highest levels in smooth muscle-rich tissues. Immunohistochemical and immunofluorescence staining with an anti-200 kDa isoform-specific antiserum localizes the large isoform to the Z-discs of cardiac and skeletal muscle cells. Interestingly, the expression of this isoform is initiated and increasing during *in vitro* differentiation and fusion of C2C12 myoblasts suggesting that the the 200 kDa palladin isoform may play a scaffolding role during sarcomeric organization.

Introduction

The precise dynamic organization of the actin cytoskeleton is crucial for almost all cellular processes; in particular cellular morphogenesis, cell motility and cell contractility depend on the coordinative action of various actin-binding proteins that regulate the assembly and disassembly of actin-fibers and the actin-network. Palladin is an actin-associated phosphoprotein that has been shown to fulfil an essential role in maintaining cell morphology and cytoskeletal organization in different cell types. This is achieved by Palladin's multi-domain structure which is supposed to act as a molecular scaffold that recruits multiple actin associated proteins such as α -actinin, VASP, ezrin, profilin, Lasp-1, Esp8 and F-actin itself (Mykkänen et al., 2001; Boukhelifa et al., 2004; Rönty et al., 2004; Goicoechea et al., 2006; Boukhelifa et al., 2006; Rachlin and Otey, 2006; Dixon et al., 2008). In addition, palladin interacts with a number of proteins, which are involved in actin organization such as Abl/Arg kinase binding protein (ArgBP2), lipoma preferred partner (LPP) and SPIN90 (Rönty et al., 2005; Jin et al., 2007; Rönty et al., 2007).

Recent database searches revealed a much more complex genomic organization of the palladin gene than originally thought. The palladin gene structure is highly conserved between mouse and man and spans ~400kb on mouse and human chromosomes 8B3.3 and 4q32.3, respectively. At least three different promoters drive the expression of three major forms that are classified as the 200 kDa, the 140 kDa and the doublet isoforms of 90 to 92 kDa. From each isoform alternative splicing events results in further less well characterized products (reviewed in Otey et al. 2005). The three major isoforms contain three C-terminal immunoglobulin-like domains of the IgCAM (immunoglobulin domain Cell Adhesion Molecule subfamily) class that mediate the binding to ezrin and F-actin (Mykkänen et al., 2001; Dixon et

al., 2008). Depending on the isoform up to three proline-rich regions are N-terminal to the IgCAM domains and mediate the interaction with profilin and Mena/VASP family proteins (Boukhelifa et al., 2004). The short 90 to 92 kDa isoforms are thought to be expressed ubiquitously in chicken, mouse and human tissues (reference?). The 140 kDa isoform is transcribed from an alternative promoter located in the middle of the gene and contains a fourth IgCAM domain and a proline-rich sequence that extends the N-terminus of the 90-92 kDa isoform. Recently, a two hybrid screen identified the actin binding protein Lasp-1 as a novel interactor of the 140 kDa isoform (Rachlin and Otey, 2006). This isoform is mainly expressed during development in a variety of tissues including kidney, spleen, gastro-intestinal tract and skeletal muscle, and to a much lesser extent in adult tissues (Parast and Otey, 2000). Finally, the longest, 200 kDa isoform is transcribed from the most 5' promoter and appends an approximately 1kb long exon onto the 140 kDa transcript. Translation of the additional coding sequence adds a fifth IgCAM domain. Expression of the 200 kDa isoform has been detected in the developing heart of chicken and mouse (Parast and Otey, 2000).

Palladin belongs to the palladin/myotilin/myopalladin family that have multiple IgCAM domains in their C-terminal region in common. The two other members, myotilin and myopalladin, are both expressed in striated muscle and heart and predominantly localize to the Z-disc (Salmikangas 1999, Bang et al., 2001). Both proteins bind α -actinin and are thought to play an essential role in sarcomeric organization (Salmikangas et al., 1999; Bang et al., 2001). In line with this speculation is the observation that single missense mutations in the N-terminus of myotilin cause two distinct inherited muscular disorders called limb-girdle muscular dystrophy 1 A (Hauser et al., 2000) and myofibrillar myopathy (Selcen and Engel., 2004). Both show ultrastructural changes of sarcomeres.

The function of palladin as an actin organizing protein was first analysed in a variety of different cell lines by antisense experiments and siRNA knockdown approaches resulting in a dramatic loss of the F-actin distribution (Parast and Otey, 2000; Rachlin and Otey, 2006). Overexpression of palladin leads to more robust actin-fibers suggesting that palladin is required for the organization and stabilization of the actin cytoskeleton. Inactivation of all palladin isoforms in mouse results in an embryonic lethal phenotype caused by an exencephaly and body wall closure defects. Palladin-deficient embryonic fibroblasts revealed disturbed stress fiber formation, impaired cell attachment to extracellular matrix (ECM) components and reduced cell motility (Luo et al., 2005).

Here we present a comparative expression analysis of the major palladin isoforms during murine embryogenesis and in adult tissues. With the help of an antiserum specific for the 200kDa isoform and an EGFP-fusion protein construct we addressed its cellular localization and showed that the largest palladin isoform is dynamically expressed during myofibrillogenesis.

MATERIALS AND METHODS

RT-PCR

Total RNA (2 µg) was used for first strand cDNA synthesis according to the protocol of the manufacturer using SuperScriptIII polymerase (Invitrogen) and random hexamer primers. Specific cDNA fragments were amplified using the following primers: Exon2 sense: CATCCAGAACTGAGGAGCC; Exon3 sense: TGCTGCCTGTGCATTTTCCC; Exon5 antisense; AGCTTTCGCTGTCAGAGTCC; Exon12 sense: AGGAGCCCTCGACACCCAC; Exon13 sense: CAGATGGGACTTTTCCGCTC; Exon14 antisense: ACTTGGTTCTGCAGCTGCTG.

Whole mount and radioactive *in situ* hybridization

Digoxigenin- or ³³P-UTP-labelled sense and anti-sense riboprobes were generated by *in vitro* transcription from linearized vectors containing 200 kDa and 140 kDa specific or Exon18-19 cDNA fragments. Whole-mount *in situ* hybridization was performed essentially as described (Wilkinson, 1993). For radioactive *in situ* hybridization, paraffin sections from mouse embryos at different embryonic stages were dewaxed, rehydrated and hybridized as previously described (Moser et al., 1995).

Antiserum production

A palladin 200 kDa specific peptide (TSSHDSFYDSLSDVQE; aa) located in exon 2 of the palladin gene (see figure 1) was coupled to Imject Maleimide Activated mKLNH (Pierce) and used to immunize rabbits.

Western Blotting

Both cells and tissues from embryos or adult C57BL/6 mice were homogenized in modified RIPA buffer (50 mM Tris-HCl pH7.4, 150 mM NaCl, 5mM EDTA, 0.1% SDS, 1% Triton X-100, 1% Na-deoxycholate) and in the presence of protease (Roche) and phosphatase inhibitors (Sigma). Equal amounts of total protein (20 µg) were separated by SDS-PAGE under reducing condition and transferred to PVDF membranes (Millipore). Immunoblots were developed using the ECL detection system (Amersham). Palladin 200 kDa isoform specific antiserum (1:10k), rabbit anti-MyoD (1:150, Santa Cruz), rabbit anti-myogenin (1:150, Santa Cruz) antibodies were used together with the appropriate secondary antibody (1:10k, Biorad).

Constructs

Several palladin cDNAs were PCR amplified using the IMAGE cDNA clone BC_027364 and mouse whole embryo cDNA at E15.5 and cloned into the pEGFP-N1 vector (Clontech). Final constructs were confirmed by sequencing.

Immunostaining

Paraffin sections were dewaxed, rehydrated and endogenous peroxidase was blocked by incubating the slides for 20 min in 2.5 ml H₂O₂/75 ml methanol. Blocking was performed for one hour in 10% goat serum/1% BSA/phosphate-buffered saline (PBS) and the palladin 200 kDa isoform specific antibody (1:500) was incubated at 4°C over night. Sections were incubated with a 1:200 dilution of biotinylated anti-rabbit secondary antibody for one hour and transferred to ABC solution (Vector Laboratories) for an additional 30 min. Secondary antibody was detected with diaminobenzidine (DAB). Counterstaining of the sections was performed with methylene green and sections were mounted with Entellan.

Immunohistochemistry

Mouse myoblast cells (C2C12) were grown on 0.2% gelatin (Merck) coated glass cover slips, fixed with 4% PFA/3% sucrose/PBS, permeabilized with 0.25% Triton X-100 in PBS for 10 min, blocked in PBS containing 3% BSA and 5% goat serum for one hour. Cells were immunostained for palladin 200 kDa specific antiserum (1: 800), and co-stained with α -actinin (monoclonal antibodies from Sigma) visualize Z-discs. Alexa488 and Cy3-conjugated secondary antibodies were purchased from Molecular Probes. Stained cells were mounted in Elvanol and pictures were taken with a Leica DMRA2 microscope and a Hamamatsu camera.

Transfections

NIH3T3 cells and primary cardiomyocytes were transfected with EGFP-palladin 200 kDa isoform cDNA construct using Lipofectamine 2000 (Invitrogen) following the manufacturer's instructions.

Isolation and culture of neonatal mouse cardiomyocytes

Cardiomyocytes were isolated from hearts of P1 newborn mice treated with enzyme solution (0.4 mg/ml collagenase (Worthington, Freehold, NJ) and 1 mg/ml pancreatin (Sigma, St. Louis, MO) in ADS buffer (116 mM NaCl, 0.8 mM NaH₂PO₄, 1 g/l glucose, 5.4 mM KCl, 0.8 mM MgSO₄ and 20 mM 2,3-butanedione monoxime in 20 mM HEPES, pH 7.35) for 10 min at 37°C. Fresh enzyme solution (0.3 ml/heart) was added and tissue was incubated for 8 min. The supernatant containing dispersed cardiac cells was transferred to a new tube containing 1 ml FCS (per heart) and centrifuged at low speed (80xg, 6 min), resuspended in 2 ml FCS and kept at 37 °C. The remaining tissue fragments were incubated with fresh enzyme solution (0.3 ml/

heart) as above for additional 5 times. Cell suspensions were pooled and centrifuged at low speed (80xg, 6 min without brake) and resuspended in 4 ml ADS buffer.

Cells were seeded on glass coverslips coated with fibronectin (10 µg/ml) at a cell density of 3.0×10^5 cells/35-mm culture dish in plating medium (67% DMEM, 17% medium M199, 10% horse serum, 5% FCS, 1% Pen/Strep and 4 mM glutamine (Invitrogen)). Cells were incubated at 37°C in a 5% CO₂ humidified incubator. The next day the plating medium was replaced with maintenance medium (75% DMEM, 23.5% medium M199, 0.5% horse serum, 1% Pen/Strep, 4 mM glutamine and 0.1mM phenylephrine).

Isolation and differentiation of primary myoblasts

Primary myoblasts were isolated as described by Rando and Blau (1994). Briefly, hindlimbs were dissected from 1 to 2-day-old mice, placed in PBS, minced with a razor blade and enzymatically dissociated with a mixture of collagenase II (0.1%, Worthington, Freehold, NJ) and dispase (grade II, 2.4U/ml, Roche). The slurry, maintained at 37°C for 30-45 min, was triturated every 15 min with a 5-ml plastic pipette. After centrifugation at 350xg for 10 min, the pellet was resuspended in DMEM containing 20% FCS, 2 mM Glutamin, 1% Pen/Strep (all Invitrogen) and preplated on non-coated tissue culture dishes for 20 min for the attachment of fibroblasts to the dish surface. Non-adherent cells were then transferred into 0.2% gelatine-coated 6-well-plates (about 2 limbs for 1 well). Differentiation was induced with 5% horse serum (Invitrogen) in DMEM for 2-4 days. A myotube was defined as having three or more nuclei.

RESULTS AND DISCUSSION

Genomic organization of the murine palladin gene and expression of palladin isoforms during mouse development and in adult tissues

In order to analyse the expression of individual palladin isoforms during embryonic development and in adult tissues, specific RT-PCR reactions were performed using primers shown in Fig 1 and RNA from whole embryos at embryonic day (E) 7.5 to E18.5 (Fig. 2A). The 200, 140 and both 90-92 kDa isoforms were expressed throughout embryogenesis. However, whereas the 200 kDa and 90-92 kDa isoform B increased from E7.5 until E10.5 and slightly decreased thereafter, the two other isoforms remained almost constant.

The same primers were used to analyse the expression profile of the palladin isoforms in various adult tissues (Fig. 2B). The 200kDa isoform was dominantly expressed in heart and skeletal muscle but much less abundant in several other tissues. In contrast, the 140kDa isoform was expressed in multiple organs and represents the dominant isoform of the brain. The 90-92 isoform A revealed an even wider distribution with absent expression in heart and low expression levels in brain, spleen, skin and testis. Finally, the 90-92 isoform B again was more restricted to tissues rich in smooth muscle cells such as bladder, uterus, small intestine and colon, but is also expressed in liver, kidney and spleen and most prominent in lung. In summary, both small isoforms are dominantöy exppressed in smooth muscle cell.-containing tissues and lung when compared to the two larger isoforms.

Recently a 50kDa palladin isoform was reported to be expressed in mouse embryonic fibroblasts (Luo et al., 2005). We screened the same embryonic and adult tissues for this isoform using the primers shown in Fig 1. However, no specific

product was detected suggesting that this isoform is expressed either at very low levels or only in certain cell types not included in the tissues analyzed.

Tissue specific expression of the 200 kDa and 140 kDa palladin isoforms during embryonic development

To determine the distribution of the individual palladin transcripts during mouse development, we performed whole mount *in situ* hybridizations (ISH) on embryos (E8.5 -11.5) (Fig. 3) and radioactive ISHs on mouse embryo (E12 – E15) sections (Fig. 4) from different developmental stages.

Specific probes for the 200 kDa and 140 kDa isoforms were generated by amplifying the first exons of both variants (see also figure 1 for location of the probes). These were then subsequently subcloned into pBluescript to derive sense and antisense transcripts. In line with the RT-PCR analyses, whole mount ISHs on E8.5 to E11.5 embryos revealed that the 200kDa isoform was strongly expressed in heart. At later stages this isoform was expressed in the ventricles and the atria of the heart. The 200 kDa isoform was first expressed in anterior somites at E9.5 and gave rise to a characteristic double striped signal in the myotome of E10.5 and E11.5 embryos, which most likely represents differentiating myoblasts. In contrast, the 140 kDa isoform revealed a much broader expression pattern and was detected in the anterior neural plate and brain of E8.5 and E9.5 embryos. In addition, the 140 kDa isoform was expressed in somites in a posterior to anterior descending gradient with highest expression levels in epithelial somites. The 140kDa isoform was also expressed in the presomitic mesoderm. Interestingly, the amount of the 140 kDa isoform decreased during the differentiation of the somites into dermo-myotome and sclerotome. At E10.5 and E11.5 the 140 kDa isoform was also found in the facial mesenchyme with strong expression in the branchial arches. Migrating myoblasts of

the epaxial and hypaxial myotome of which the latter invade the limb bud mesenchyme were also positive for the 140 kDa isoform.

We then tried to generate specific probes for the short isoforms (90-92 kDa A and B and the 50 kDa isoform). Unfortunately the 5' exons of the short isoforms were too short and had a high GC content (~70) and could therefore not be used as specific probes for *in situ* hybridizations. To include these isoforms in our ISHs we used a cDNA probe covering exons 18 and 19 (E18-19 probe). By using this probe both long transcripts were also detected, revealing the characteristic staining pattern within the heart, facial mesenchyme, limbs and somites. However, this probe revealed an ubiquitous palladin expression indicating that the short isoforms are expressed throughout all tissues, as suggested by the RT-PCR studies..

In parallel, radioactive *in situ* hybridizations on sections of mouse embryos confirmed the restricted expression pattern of the 200 kDa isoform in the developing heart and skeletal muscle system at E12 and E14 (Fig. 4A, D). Parallel sections hybridized with a 140kDa specific probe showed expression in mesenchymal tissues like the facial mesenchyme, the dermis and the kidney mesenchyme. Weaker signals were detected in the brain, skeletal muscle like the tongue, around the bronchi of the lung, in cartilage and the perichondrium (Fig. 4B, F-K). The E18-19 probe, which detects all palladin isoforms, gave signal in the whole embryo (Fig. 4C and E), confirming that the palladin gene is ubiquitously expressed, although the individual isoforms have a specific expression pattern.

Control hybridizations with the sense probes revealed any signals in the whole mount or in the radioactive *in situ* hybridizations (data not shown).

Altogether these data indicate that the 200 kDa isoform is mainly confined to heart and skeletal muscle cells, the 140 kDa isoform expression is much broader with high

expression levels in mesenchymal tissues and the smaller isoforms are ubiquitously expressed.

Palladin 200 kDa isoform localizes to the Z-discs of cardiac and skeletal muscle cells

To date, the subcellular localization of the largest murine palladin isoform has not been addressed. To discriminate between the 200kDa palladin isoform from the more widely expressed shorter forms we generated a rabbit polyclonal antiserum against an N-terminal peptide localized within exon2 of the palladin gene (see material and methods). Specificity and cross-reactivity of the 200 kDa isoform antiserum are shown in protein lysates from NIH3T3 cells transfected with different EGFP-tagged palladin isoforms (Fig. 5A, B). The specificity of the 200 kDa isoform antiserum was also confirmed by immunohistochemical staining on paraffin sections from mouse embryos showing again the 200 kDa isoform expression in heart and skeletal muscle (Fig. 5D). Furthermore, we generated a second rabbit polyclonal antiserum against a peptide localized in exon 11, which is only present in the 200 and 140 kDa isoforms. Western-Blot analyses revealed that this antiserum specifically binds to these isoforms and it also detects the endogenous 140 kDa isoform expressed in NIH3T3 cells (Fig. 5C).

To investigate the subcellular localization of the 200 kDa isoform in striated muscle tissues, primary cardiomyocytes and myoblasts from mouse embryos were isolated and either transfected with an expression construct encoding for the EGFP-tagged 200 kDa isoform or we used the 200 kDa isoform specific antiserum for immunofluorescence stainings. Both transfected primary cardiomyocytes as well as fused primary myoblasts revealed colocalization of the 200 kDa isoform with α -actinin in a characteristic striped pattern representing the sarcomeric Z-discs (Fig. 5E).

The 200kDa isoform of palladin is induced during myoblast differentiation

C2C12 cells represent a valuable model to study myoblast differentiation and fusion *in vitro*. To address the role of the two large palladin isoforms during myotube differentiation, C2C12 cells were grown for 1, 3 and 6 days in differentiation medium and the levels of the two palladin isoforms were determined by RT-PCR and Western-blot analyses. The differentiation of myoblast into myotubes were confirmed by the change in cell morphology, extent of cell fusion and molecularly by the expression of two myogenic transcription factors, myoD and myogenin. They show a reciprocal expression behaviour during myoblast differentiation, with high MyoD levels in undifferentiated myoblasts which then decreases during the differentiation process, and low myogenin in myoblasts, which becomes up-regulated during myotube formation.

Interestingly, the large 200 kDa isoform of palladin, which is almost undetectable in undifferentiated C2C12 myoblasts, became significantly expressed during the differentiation process (Fig. 6A). In line with this observation, the 200 kDa isoform protein level also increased during differentiation suggesting that the 200kDa isoform is specifically synthesized during the formation of the highly ordered contractile unit in striated muscle cells, the sarcomere (Fig. 6B). mRNA encoding the 140kDa isoform was present at almost constant levels during myoblast differentiation, while levels of the 140kDa polypeptide declined (Fig. 6 A,B).

Our data reveal that the different palladin isoforms are expressed in a tissue specific pattern during development and in adult organs. Only the 90-92 kDa isoform B seems to be almost ubiquitously expressed. The largest, 200 kDa isoform is mainly expressed in striated muscle. Interestingly, this isoform becomes expressed during the differentiation of myoblasts to myotubes and the formation of myofibrils. The 140

kDa isoform is expressed in mesenchymal cells and also in migrating myoblasts during development. During muscle differentiation the transition from a myoblast, which contains stress-fiber-like structures, to fused myotubes that have formed the contractile units critically depends on an ordered expression of striated muscle specific proteins, which become precisely positioned within the sarcomere. Based on palladin's multidomain structure and function as an actin-binding scaffolding protein the 200 kDa isoform might be crucial for the correct assembly of sarcomeric proteins.

ACKNOWLEDGEMENTS

We thank Melanie Ried for excellent technical assistance. The work was supported by the DFG and the Max Planck Society.

REFERENCES

- Bang, M.L., R.E. Mudry, A.S. McElhinny, K. Trombitás, A.J. Geach, R. Yamasaki, H. Sorimachi, H. Granzier, C.C. Gregorio and S. Labeit. 2001. Myopalladin, a novel 145-kilodalton sarcomeric protein with multiple roles in Z-disc and I-band protein assemblies. *J. Cell Biol.* 153: 413-427.
- Boukhelifa, M., M.M. Parast, J.E. Bear, F.B. Gertler and C.A. Otey. 2004. Palladin is a novel binding partner for Ena/VASP family members. *Cell Motil. Cytoskeleton.* 58: 17-29.
- Boukhelifa M., M. Moza, T. Johansson, A. Rachlin, M. Parast, S. Huttelmaier, P. Roy, B.M. Jockusch, O. Carpen, R. Karlsson and C.A. Otey. 2006. The proline-rich protein palladin is a binding partner for profilin. *FEBS J.* 273: 26-33.
- Dixon, R.D.S., D.K. Arneman, A.S. Rachlin, N. Sundaresan, M. Joseph Costello, S.L. Campbell and C.A. Otey. 2008. Palladin is an actin crosslinking protein that uses immunoglobulin-like domains to bind filamentous actin. *J. Biol. Chem.* In press.
- Epstein, H. F., and D. A. Fischman. 1991. Molecular analysis of protein assembly in muscle development. *Science.* 251: 1039-1044
- Goicoechea, S., D. Arneman, A. Disanza, R. Garcia-Mata, G. Scita, and C.A. Otey. 2006. Palladin binds to Eps8 and enhances the formation of dorsal ruffles and podosomes in vascular smooth muscle cells. *J. Cell Sci.* 119: 3316-3324.
- Jin, L., M.J. Kern, C.A. Otey, B.R. Wamhoff and A.V. Somlyo. 2007. Angiotensin II, focal adhesion kinase, and PRX1 enhance smooth muscle expression of lipoma preferred partner (LPP) and its newly identified binding partner palladin to promote cell migration. *Circ. Res.* 100: 817-825.
- Luo, H., X. Liu, F. Wang, Q. Huang, S. Shen, L. Wang, G. Xu, X. Sun, H. Kong, M. Gu, S. Chen, Z. Chen and Z. Wang. 2005. Disruption of palladin results in neural tube closure defects in mice. *Mol. Cell. Neurosci.* 29: 507-515.

Moser, M., A. Imhof, A. Pscherer, R. Bauer, W. Amselgruber, F. Sinowatz, F. Hofstädter, R. Schüle R, and R. Buettner. 1995. Cloning and characterization of a second AP-2 transcription factor: AP-2 beta. *Development*. 121: 2779-2788.

Moza, M., L. Mologni, R. Trokovic, G. Faulkner, J. Partanen and O. Carpen. 2007. Targeted deletion of the muscular dystrophy gene myotilin does not perturb muscle structure or function in mice. *Mol. Cell. Biol.* 27: 244-252.

Mykkänen, O.M., M. Grönholm, M. Rönty, M. Lalowski, P. Salmikangas, H. Suila and O. Carpen. 2001. Characterization of human palladin, a microfilament-associated protein. *Mol. Biol. Cell.* 12: 3060-3073.

Otey, C.A., A. Rachlin, M. Moza, D. Arneman and O. Carpen. 2005. The palladin/myotilin/myopalladin family of actin-associated scaffolds. *Int. Rev. Cytol.* 246: 31-58.

Parast, M.M. and C.A. Otey. 2000. Characterization of palladin, a novel protein localized to stress fibers and cell adhesions. *J. Cell Biol.* 150: 643-656.

Rachlin, A.S. and C.A. Otey. 2006. Identification of palladin isoforms and characterization of an isoform-specific interaction between Lasp-1 and palladin. *J. Cell Sci.* 119: 995-1004.

Pogue-Geile, K.L., R. Chen, M.P. Bronner, T. Crnogorac-Jurcevic, K.W. Moyes, S. Downen, C.A. Otey, D.A. Crispin, R.D. George, D.C. Whitcomb and T.A. Brentnall. 2006. Palladin mutation causes familial pancreatic cancer and suggests a new cancer mechanism. *PLoS Med.* 3: e516.

Rando, T.A., and H.M. Blau. 1994. Primary mouse myoblast purification, characterization, and transplantation for cell-mediated gene therapy. *J. Cell Biol.* 125: 1275-1287.

Rönty, M., A. Taivainen, M. Moza, C.A. Otey and O. Carpen. 2004. Molecular analysis of the interaction between palladin and alpha-actinin. *FEBS Lett.* 566: 30-34.

Rönty, M., A. Taivainen, M. Moza, G.D. Kruh, E. Ehler and O. Carpen. 2005. Involvement of palladin and alpha-actinin in targeting of the Abl/Arg kinase adaptor ArgBP2 to the actin cytoskeleton. *Exp. Cell Res.* 310: 88-98.

Rönty, M., A. Taivainen, L. Heiska, C.A. Otey, E. Ehler, W.K. Song and O. Carpen. 2007. Palladin interacts with SH3 domains of SPIN90 and Src and is required for Src-induced cytoskeletal remodeling. *Exp. Cell Res.* 313: 257525-257585.

Salaria, S.N., P. Illei, R. Sharma, K.M. Walter, A.P. Klein, J.R. Eshleman, A. Maitra, R. Schulick, J. Winter, M.M. Ouellette, M. Goggins and R. Hruban. 2007. Palladin is overexpressed in the non-neoplastic stroma of infiltrating ductal adenocarcinomas of the pancreas, but is only rarely overexpressed in neoplastic cells. *Cancer Biol. Ther.* 6: 324-328.

Salmikangas, P., O. M. Mykkänen, M. Grönholm, L. Heiska, J. Kere, and O. Carpen. 1999. Myotilin, a novel sarcomeric protein with two Ig-like domains, is encoded by a candidate gene for limb-girdle muscular dystrophy. *Hum. Mol. Genet.* 8: 1329-1336.

Shiffman, D., S.G. Ellis, C.M. Rowland, M.J. Malloy, M.M. Luke, O.A. Iakoubova, C.R. Pullinger, J. Cassano, B.E. Aouizerat, R.G. Fenwick, R.E. Reitz, J.J. Catanese, D.U. Leong, C. Zellner, J.J. Sninsky, E.J. Topol, J.J. Devlin and J.P. Kane. 2005. Identification of four gene variants associated with myocardial infarction. *Am. J. Hum. Genet.* 77: 596-605.

Wilkinson, D. G., editor. 1993. *In situ hybridization*. Oxford: Oxford University Press. p 75-83.

Zogopoulos, G., H. Rothenmund, A. Eppel, C. Ash, M.R. Akbari, D. Hedley, S.A. Narod and S. Gallinger. 2007. The P239S palladin variant does not account for a significant fraction of hereditary or early onset pancreas cancer. *Hum. Genet.* 121: 635-637.

FIGURE LEGENDS

Figure 1. Schematic presentation of the murine palladin gene structure and various transcripts. Closed boxes show translated regions of the different splice variants. Arrows indicate the localization of the primer pairs that have been used for RT-PCR reactions. The stars in exon 2 and 11 show the peptide regions which were chosen to generate the 200 kDa specific and 200/140 kDa isoform antisera. The cDNA regions used as probes for the ISHs are shown as grey boxes below the transcripts.

Figure 2. Expression of the different palladin isoforms during mouse development and in adult tissues. RT-PCR analyses with specific primer pairs for the individual palladin isoforms from total RNA extracted from whole embryos at different embryonic stages (A) and from various adult tissues (B). GAPDH was used as the control.

Figure 3. Whole mount *in situ* hybridization on E8.5, E9.5, E10.5 and E11.5 mouse embryos with palladin isoform specific probes. Embryos were hybridized with the 200 kDa specific probe (A), the 140 kDa specific probe (B) and a pan-palladin probe that detects all isoforms (C).

Figure 4. Radioactive *in situ* hybridization of mouse embryo sections with the 200 kDa (A, D), the 140 kDa (B, F-H) and pan-palladin (C, E) cDNA probes. A to C show sagittal sections from whole E12 embryos. D to H show magnifications from sagittal sections of E14 embryos. I to K show bright field images of dark field pictures F to H. Whereas the 200 kDa isoform is only expressed in heart and skeletal muscle (A,D), the 140 kDa isoform is more widely expressed (B) particularly in mesenchymal cells of the facial mesenchyme (F), around the bronchi of the lung (G) and the kidney. The pan-palladin probe reveals an ubiquitous expression pattern (E). fm, facial mesenchyme; kd, kidney; lu, lung.

Figure 5. Characterization of polyclonal palladin antisera and subcellular localization of the palladin 200 kDa isoform to the Z-discs of cardiomyocytes and fused myoblasts. Western blots from NIH3T3 cell lysates transfected with 200 kDa isoform-, 140 kDa isoform-, 90-92 kDa isoform-, 50 kDa isoform- EGFP or EGFP only

constructs were incubated with anti-GFP antibody (A), with anti-200 kDa isoform antiserum (B) and the 200/140 kDa isoform antiserum. (D) Immunohistochemical staining of a 12.5 embryo sagittal section with the anti-200 kDa isoform antiserum reveals strong expression in skeletal muscle and heart. (E) Localization of the 200 kDa palladin isoform to the Z-discs of primary cardiomyocytes, which have been transfected with an EGFP-200-kDa isoform expression construct and costained for α -actinin. Below, fused primary myoblasts were stained with the 200 kDa specific antiserum showing colocalization with α -actinin to the Z-discs of the sarcomeres.

Figure 6. Expression of the 200 and 140 kDa palladin isoforms during *in vitro* myogenesis of C2C12 cells. (A) RT-PCRs from total RNA isolated from C2C12 cells that have been cultured in differentiation medium für 0, 1, 3 and 6 days. PCR was performed with specific primer pairs for the 200 and 140 kDa isoforms and the myogenic differentiation markers MyoD and Myogenin. GAPDH was used as control. (B) In parallel, protein lysates were isolated from the same samples and Western blot analyses were performed and probed with the 200 and 140 kDa isoform antisera, and MyoD and Myogenin antibodies. Actin was used as loading control.

Figure 1

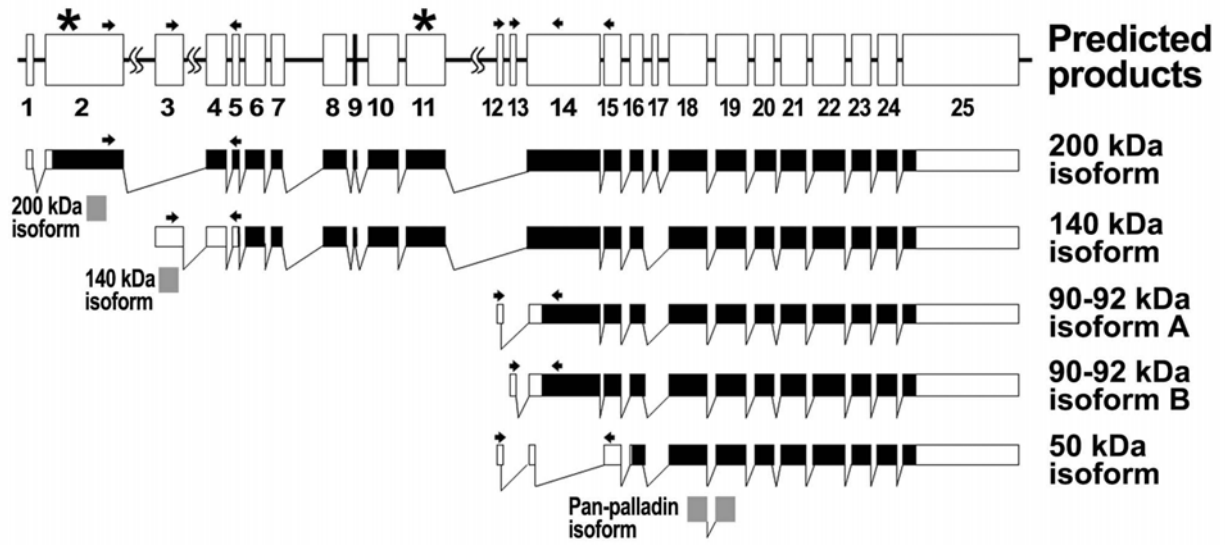


Figure 3

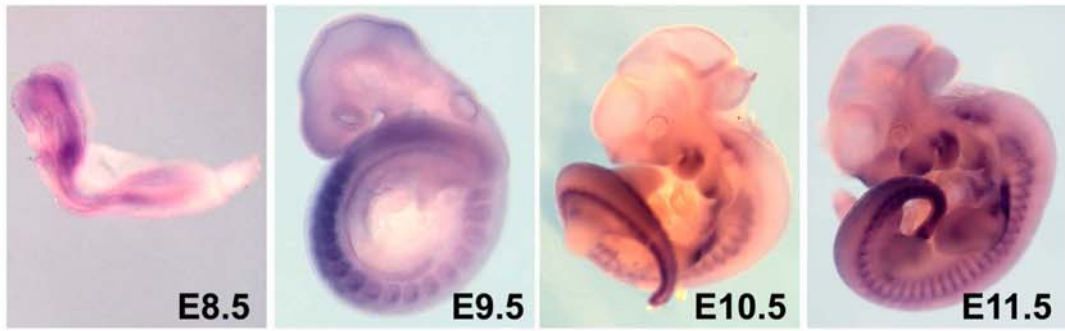
A

200 kDa isoform



B

140 kDa isoform



C

pan-palladin



Figure 4

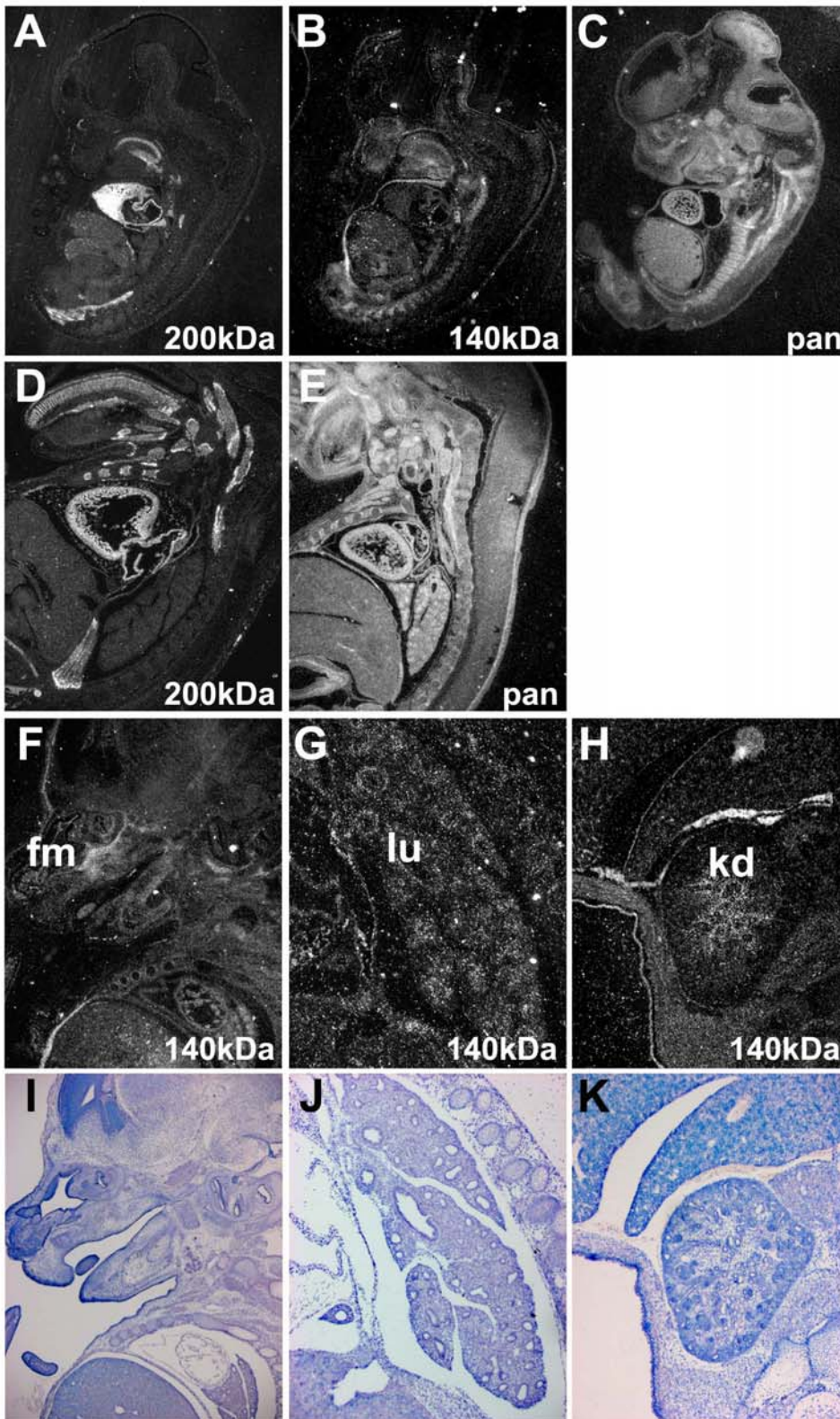
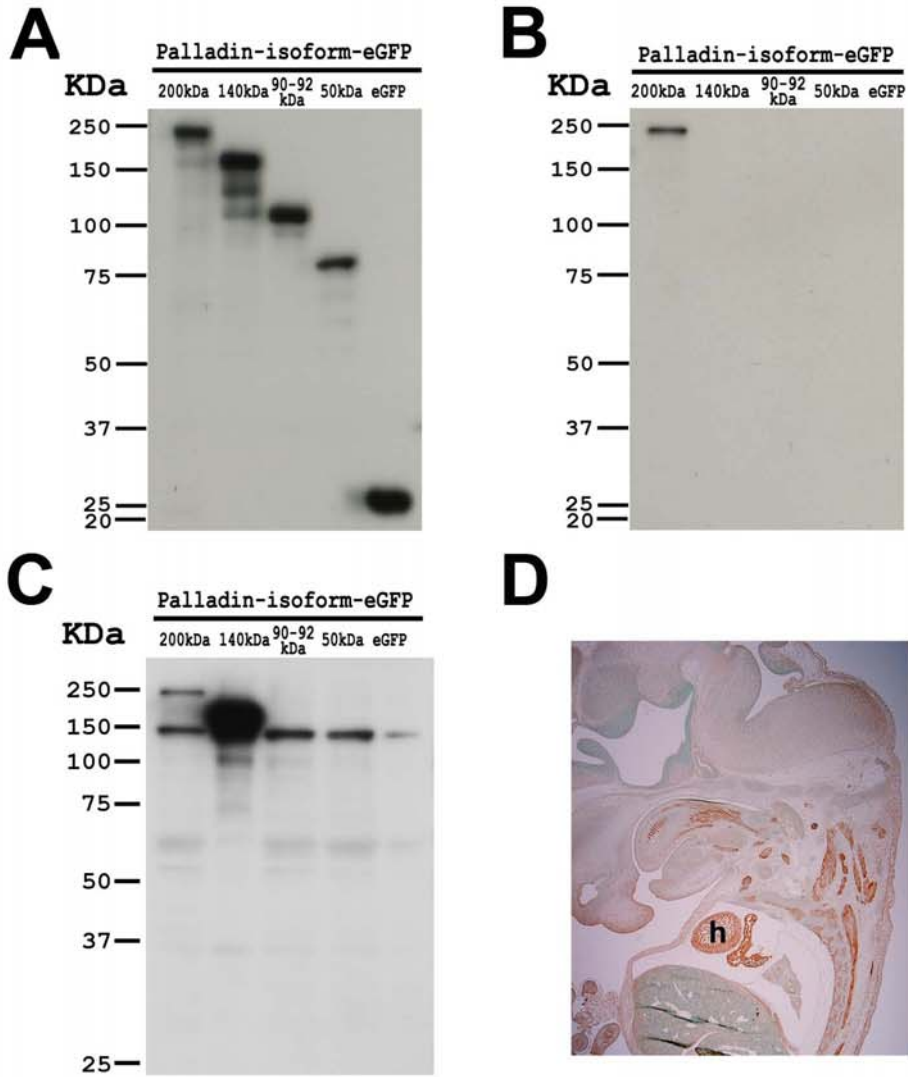


Figure 5



E

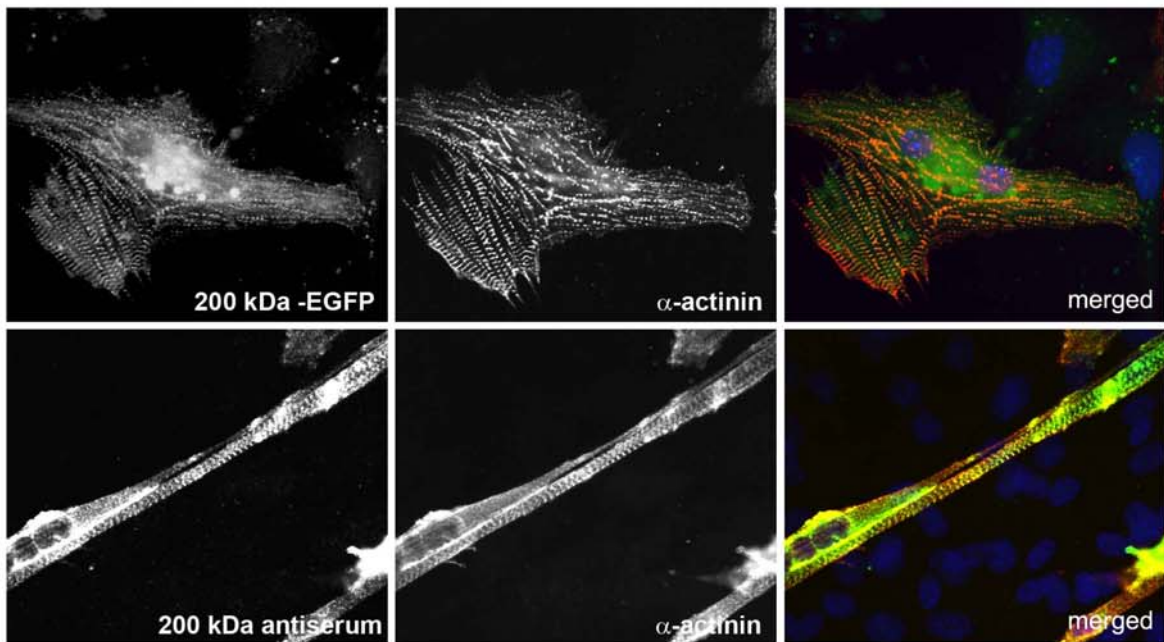
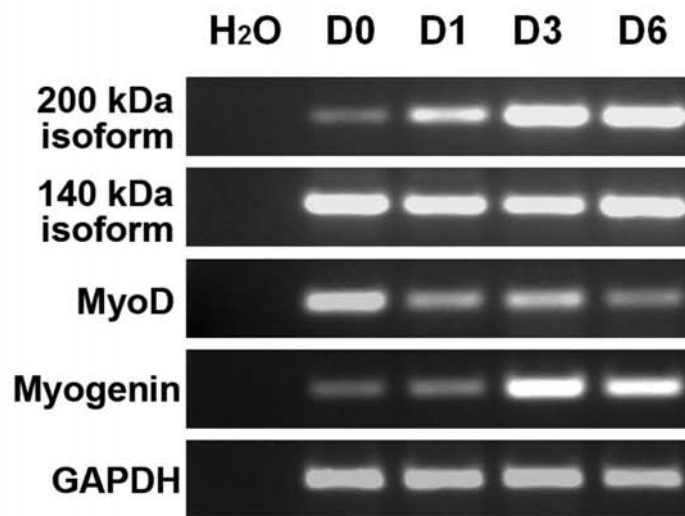


Figure 6

A



B

